



Carnarvon Distributed Energy Resource (DER) Trials

Technical Report #2
Carnarvon Distributed Energy Resource Trials

Version 3

May 2021

*Owned by the
people of WA*

MU Murdoch
University

HORIZON
POWER

Acknowledgement of Country

We acknowledge and pay our respect to Aboriginal and Torres Strait Islander peoples as the First Peoples of Australia.

We are privileged to share their lands, throughout 2.3 million square kilometres of regional and remote Western Australia and Perth, where our administration centre is based, and we honour and pay respect to the past, present and emerging Traditional Owners and Custodians of these lands.

We acknowledge Aboriginal and Torres Strait Islander peoples continued cultural and spiritual connection to the seas, rivers and the lands on which we operate on. We acknowledge their ancestors who have walked this land and travelled the seas and their unique place in our nation's historical, cultural and linguistic history.

We would like to offer particular acknowledgement to the Inggarda peoples of Carnarvon, on who's land this research took place, along with the Whadjuk Nyoongar peoples of Perth on who land the document was compiled and published.

Horizon Power uses the term Aboriginal and Torres Strait Islander (and Aboriginal on future references) instead of Indigenous. Therefore, within all Horizon Power documents the term Aboriginal, is inclusive of Torres Strait Islanders who live in Western Australia.



Corresponding Author: David Edwards (david.edwards@horizonpower.com.au)

Disclaimer: This project received funding from the Australian Renewable Energy Agency (ARENA) as part of ARENA's Advancing Renewables Program. The views expressed herein are not necessarily the views of the Australian Government, and the Australian Government does not accept responsibility for any information or advice contained herein.

While every care had been taken in preparing this report, Murdoch University gives no guarantees in respect to this report. The reader uses this report at their own risk.

Report prepared by:	Report reviewed by (Horizon Power):
Section 3: Md Shoeb ¹ , Simon Glenister ¹ , Gloria Rupf ¹	Principal Contact: David Edwards (david.edwards@horizonpower.com.au)
Section 4: Md Shoeb ¹ , Martina Calais ¹ , Simon Glenister ¹	David Stephens ²
Section 5: Shane Overington ²	Luke Jones ²
Section 6: Suleman Ashraf ²	Peter Howe ²
Section 7: David Edwards ² , Pierce Trinkl ²	Pierce Trinkl ²
Section 8: Pierce Trinkl ²	Shane Overington ²
Section 9: Simon Glenister ¹ , Martina Calais ¹ , Gloria Rupf ¹ , Remember Samu ¹ , David Edwards ²	
Section 10: Bijan Nouri ³ , Niklas Blum ³ , Stefan Wilbert ³ , Remember Samu ¹ , Dean Laslett ¹	
Section 11: Martina Calais ¹ , Md Shoeb ¹ , Simon Glenister ¹ , David Stephens ² , Gloria Rupf ¹	
Murdoch University Project management: Martina Calais ¹ , Parisa Bahri ¹	
¹ Discipline of Engineering and Energy, Murdoch University ² Horizon Power ³ Institute of Solar Research, German Aerospace Centre (DLR)	

Version Record

Version	Date	Description
1	29 November 2020	Initial Draft Report
2	15 April 2021	Draft Report including HP contributions
3	17 May 2021	Final Report

Report at a glance

This report presents the key findings from several studies that were completed as part of the Carnarvon Distributed Energy Resource (DER) Trials, a collaboration between Horizon Power and Murdoch University, covering topics such as aggregated unmasked load, minimum system load, the effect of PV generation and cloud events on voltages in LV networks and spinning reserve requirements, incorporating short-term solar forecasting and feed-in management in spinning reserve strategies and all sky imager nowcasting systems. It complements the project's first publication, Technical Report #1 (Moghbel et al. 2019), and should be read in the context of the details outlined in that report.

This report:

- Presents the study on the unmasking of the load for a subset of the Carnarvon load using the project's unique data set, namely the Wattwatcher data, which recorded net load and PV and battery generation at the premises of the trial participants.
- Provides the results of an analysis completed by Murdoch University of SCADA data to determine the minimum load seen by the Mungullah Power Station in Carnarvon during the analysis period 2017-2020.
- Discusses the effect of PV power generation (and cloud events) on LV network voltage based on a study of the voltages on two LV networks in Carnarvon. High voltage events may be exacerbated due to the measurement of the voltages analysed in this study not being at the point of supply (i.e. it is not a Horizon Power network voltage), but a voltage measured within the customer's switchboard, which is downstream of a lead-in cable.
- Explores the potential of applying advanced analytics to customer advanced meter infrastructure (AMI) data (network meters) to identify single-phase PV systems and their contribution to high voltage excursions so that some single-phase PV systems could be moved to other network phases in order to reduce peak voltage events, which can cause inverter trips.
- Presents the procedure and results of an audit of approximately 135 inverters from residential and commercial PV systems in Carnarvon, which was carried out by the Horizon Power project team to check for compliance with Horizon Power's technical requirements. The audit was used to help determine if inverter settings were playing a role in the unexpected behaviour of legacy PV systems in the town observed during the trials.
- Summarises the experiments and observations from the Carnarvon DER Trials. The trials tested various aspects of battery/PV systems installed in 2018/2019, which have Reposit boxes, to determine the adequacy of DER, in a broader sense, to provide ancillary services in addition to supplying power when DER penetration increases or in an islanded microgrid mode. Experiments carried out during the trials covered pre-requisite functions, basic control of an individual node and basic control and administration of VPPs.
- Explores the value proposition for customer connected batteries and how a win-win outcome could be created for both the customer and Horizon Power by testing the effectiveness of Time of Use (ToU) tariffs in managing a battery system connected behind the customer meter over time on a nominated trial participant (a primary producer business) PV/Battery DER system.
- Investigates the use of spinning reserve control strategies to manage increased PV penetration in Carnarvon and accommodate for changes in PV generation due to cloud shading of distributed PV through PowerFactory simulation studies of the Mungullah Power Station.
- Presents a potential spinning reserve strategy using PV feed-in management and short-term solar forecasting, which is contrasted in its operation against the existing spinning reserve strategy by using a hypothetical cloud event scenario.

- Describes an example skycamera based forecasting system, the WobaS system, which provides insights into forecast uncertainties that can then be used to model PV power. The performance of the WobaS system for Carnarvon was estimated based on the experience with five existing systems in Germany, Portugal and Spain.
- Outlines Horizon Power's existing approaches to calculating network hosting capacity and suggests a hosting capacity determination approach based on the findings from the trials and the literature.

The findings and outcomes are summarised below:

- The study of the aggregated unmasked load showed that fluctuations seen in the net load between 7:30 and 16:30 are largely due to cloud shade induced PV generation fluctuations and the largest unmasked load for the load subset occurred mainly in the summer months and around the middle of the day, indicating that consumers may proactively be using PV generated power when it is available.
- The minimum system load in Carnarvon from the SCADA data analysis was found to occur on 8th June 2019 at 14:09 and appeared not to be significantly impacted by PV generation. The next two lowest load minimums had very similar characteristics and load levels with one of these in August 2019, a time by which more PV hosting capacity had been released.
- The voltages studied on two LV networks in Carnarvon were found to vary with the PV output power following cloud events. Some sites were more prone to reaching higher voltages often compared to others. Inverter trips were observed during periods of higher voltages. These observations are aligned with the findings presented in the previous technical report on the project (Moghbel et al. 2019). Based on the finding from the first report, Horizon Power is analysing the application of power quality response modes and phase balancing to mitigate voltage rise issues as well as having put in place an inverter settings audit on the respective network.
- A constrained k-means algorithm was found to provide a high accuracy for phase identification, enabling the balancing of DER in the network and thereby improving the outlook for hosting capacity by reducing the peak voltage events that can cause inverter trips.
- Results from the inverter audit indicate there is a problem with the installation of inverters in Horizon Power's system, particularly with inverter settings and compliance with future Feed-in Management (FiM) readiness. Out of the 135 inverters that were audited, only 2 could be confirmed as compliant. A combination of installers being unaware of Horizon Power's technical requirements and a lack of accountability for non-compliant installations are identified as potential causes to the low rate of compliance.
- Response time, ramp rates and how accurately the system achieves the desired setting or setpoint were found to be recurring themes in a number of the experiments involving VPPs and are important considerations from a system control point of view. Of importance was that the VPPs behave in the desired manner, which is that the net export power adjusts to a Reposit node setpoint within 5 minutes. Experiments on VPP Configuration and Control and the Feed in Management (Export Limit) demonstrated the Reposit product as an attractive solution to these DER issues from the prosumer and network operator perspective.
- An optimised outcome that benefits both the customer and Horizon Power can be achieved through the application of the ToU tariff structure for managing a battery system. In the experiment that tested the effectiveness of the tariff structure, it was found that the ToU tariff with a smart DER control device could save the customer \$836 per year or 36% of their annual electricity bill compared to just a the ToU tariff with DER but no smart control device., Horizon Power also benefited from reduced power and energy consumption during the afternoon/evening peak.

- The simulations of the Mungullah Power Station demonstrated that the frequency regulation capability of the Power Station is not affected by PV cloud shading induced power ramping, provided reserve capacity is available and reverse power flow is avoided. However, under very high penetration scenarios and with the 3-minute start time of the gas generators at Mungullah Power Station, the power-ramp rate causes a shortfall in available time to start the next gas engine generator. The estimated installed PV capacity thresholds where this will occur are provided.
- The example spinning reserve strategy using PV feed-in management and short-term solar forecasting and its application to the hypothetical scenario is envisaged to have the following benefits:
 - Pre-emptive ramping of managed PV and knowledge of future available PV output with a lead time prior to cloud events allows for adjustment of the spinning reserve during cloud events while ensuring that generator loading remains at desirable levels.
 - An accurate prediction of a sustained clear weather period allows for the operation of the power station with decreased spinning reserve, which may result in significant fuel savings and operational benefits (reduced runtime of expensive generators).
- Forecasting uncertainties are expected to be lower in Carnarvon than at the WobaS test sites due to its closer proximity to the equator, resulting in higher average solar elevation angles and thereby a higher nowcasting accuracy, as well as it being much less cloudy than the other sites. Specific recommendations for the placement of skycameras in Carnarvon for the inclusion of a WobaS system into power system control have been provided.
- To achieve very high levels of distributed renewable energy generation in remote networks, local issues and adverse effects at distribution network levels become increasingly important to address. Therefore, to determine hosting capacity in remote networks, an approach is required which includes the LV distribution network perspective and considers adverse impacts at the local level as well as at the system level. A stochastic approach to determine the PV hosting capacity of an LV network is suggested, which would need to be repeated for other LV networks, the impact of these hosting capacities then studied at the HV feeder level and system level to determine the remote system's hosting capacity.

1 Executive Summary

This report presents the key findings from several studies that were completed as part of the Carnarvon Distributed Energy Resource (DER) Trials. It complements the project's first publication, Technical Report #1 (Moghbel et al. 2019)¹, and should be read in the context of the details outlined in that report. Since the initial studies of the Carnarvon DER trials, work on this project continued in a number of areas. This report is concerned with the following studies, and key findings are summarised below.

1.1 Aggregated unmasked load using Wattwatcher data from trial participants

The project's unique data set, which recorded net load and PV generation at the premises of the trial participants allowed for the unveiling of true customer load (which is masked by the PV generation) for a subset of the Carnarvon load. The study showed that fluctuations seen in the net load between 7:30 and 16:30 are largely due to cloud shade induced PV generation fluctuations. Also, the largest unmasked load for this load subset occurred mainly in the summer months and around the middle of the day. This may reflect these particular consumers proactively using PV generated power when it is available.

1.2 Minimum system load in Carnarvon

Murdoch University analysed high voltage (HV) feeder data to determine the minimum system load seen by the Mungullah Power Station during the analysis period 2017-2020 (from 7:30 to 16:30 for each day). The minimum system load in Carnarvon was found to occur on 8th June 2019 at 14:09. This appeared to be not significantly impacted by PV generation due to the PV capacity being only 1MW in association with the misalignment in time between minimum load and maximum irradiance. The next two lowest load minimums had very similar characteristics and load levels, with one of these being in August 2019, a time by which more PV hosting capacity had been released.

1.3 Effect of PV generation and cloud events on the voltages in selected LV networks

The voltages on two LV networks in Carnarvon were investigated to analyse the effect of PV power generation (and cloud events) on the LV network voltage. Voltages varied with the PV output power variation following cloud events. Some sites were more prone to reaching higher voltages often compared to others. Inverter trips were observed during periods of higher voltages. These observations are aligned with the findings presented in the previous technical report on the project (Moghbel et al. 2019), where a review of load and PV generation balancing across phases and investigation of the inverter settings were recommended. Horizon Power is already analysing the application of power quality response modes and phase balancing to mitigate voltage rise issues. A more comprehensive inverter settings audit on the respective network is also in place.

¹ <https://arena.gov.au/knowledge-bank/horizon-power-carnarvon-der-trials-technical-report/>

1.4 DER connection phase identification

In response to the inverter trips that were observed during periods of high voltage in the LV network voltage research conducted by Murdoch University, the Horizon Power project team started to explore the potential of applying advanced analytics to customer meter data in order to identify single phase solar PV systems that would benefit from being re-allocated to other network phases that are less congested with fewer high voltage excursions. A sample of 30 days of synchronised 1-minute interval data from 2600 meters across the town of Carnarvon was collected for the study. The collected data was analysed using constrained k-means clustering to develop a process to identify single-phase PV systems on the network and their impact on system voltage at times of peak solar insolation. The constrained k-means algorithm was found to achieve phase identification with high accuracy. Overall, the results from this study have shown that phase identification enables the balancing of DER in the network, improving the outlook for hosting capacity by reducing the peak voltage events that can cause inverter trips.

1.5 Carnarvon inverter audit

An audit of approximately 135 inverters from residential and commercial PV systems in Carnarvon was carried out by the Horizon Power project team to check for compliance with Horizon Power's technical requirements. The audit was prompted by Murdoch University's findings of some inverters tripping multiple times a day and, after close inspection of the Wattwatcher data of the trial participants, the Horizon Power project team concluding that many of the legacy PV systems in the town were not behaving as expected. The audit was used to help determine if inverter settings were playing a role in the dysfunctional operation. Results from the inverter audit indicate there is a problem with the installation of inverters in Horizon Power's system, particularly with inverter settings and FiM compliance. Out of the 135 inverters that were audited, only 2 could be confirmed as compliant. A combination of installers being unaware of Horizon Power's technical requirements and a lack of accountability for non-compliant installations are identified as potential causes to the low rate of compliance.

1.6 Visibility & control of Solar PV

The Carnarvon Trials used battery/PV systems installed in 2018/2019, which have Reposit boxes² that facilitate communications with and control of these new systems by Horizon Power. Trials 1 and 2 tested various aspects of these systems to determine the adequacy of DER, in a broader sense, to provide ancillary services in addition to supplying power when DER penetration increases or in an islanded microgrid mode. The trials included experiments on pre-requisite functions, basic control of an individual node and basic control and administration of VPPs. Tests on the basic functionalities of the Reposit systems examined the acquisition of data, quality of the data and the time taken for the data to appear, in particular into the Core Services database but also the Reposit cloud and Wattwatcher cloud services. Response time, ramp rates and how accurately the system achieves the desired setting or setpoint are recurring themes in a number of the experiments involving VPPs and are important considerations from a system control point of view. Of importance was that VPPs behave in the desired manner, which is the net export power adjusted to a Reposit node setpoint within 5 minutes. The basic operation of DER control was also tested through a series of experiments on direct battery control via battery dispatch. Experiments on VPP Configuration and Control and the Feed in Management (Export Limit) demonstrated the Reposit product as an attractive solution to DER issues from the prosumer and network operator perspective.

² A Reposit box is a DER controller, which allows Horizon Power to monitor and control their DER systems through aggregation into a VPP established in the Reposit cloud platform.

1.7 Tariffs and energy storage control

The value proposition for customer connected batteries and how a win-win outcome could be created for both the customer and Horizon Power was explored through another experiment. A PV/Battery DER system of a trial participant (a primary producer business) was nominated for the experiment to test the effectiveness of Time of Use (ToU) tariffs in managing a battery system connected behind the customer meter over time. It sought to investigate the value of optimised battery operation for customers who are not in a position to significantly change their consumption behaviour. Therefore, the trial participant was not asked to change their consumption behaviour in any way but was aware that their Reposit box was optimising their battery function. This experiment found that an optimised outcome that benefited the customer and Horizon Power could be achieved through the application of the ToU tariff structure. The customer benefited from a lower electricity bill (assuming they were actually on the nominated ToU tariff), whilst Horizon Power benefited from reduced power and energy consumption during the afternoon/evening peak.

1.8 Effects of cloud events on spinning reserve requirements

Spinning reserve control strategies can be used to manage increased PV penetration in Carnarvon and accommodate for changes in PV generation due to cloud shading of distributed PV systems. The relevant background on the generation and operating philosophy for the Mungullah Power Station and a description of the existing spinning reserve strategy are provided in this report. PowerFactory simulation studies are presented, which investigated the impact of cloud events on the system performance to identify limiting factors on the design of an effective and reliable spinning reserve control strategy. The simulations demonstrated that the frequency regulation capability of the Mungullah Power Station is not affected by PV cloud shading induced power ramping as long as reserve capacity is available, and reverse power flow is avoided. However, with the 3-minute start time of the gas generators, under very high penetration scenarios, the power ramp-rate will be problematic, causing a shortfall in available time to start the next gas engine generator. The estimated installed PV capacity thresholds where this will occur are provided.

1.9 Example spinning reserve strategy based on short-term solar forecasting and feed-in management

A potential spinning reserve strategy using PV feed-in management and short-term solar forecasting is presented, which is contrasted in its operation against the existing spinning reserve strategy by using a hypothetical cloud event scenario. The application of the strategy under this scenario highlights the following benefits of using a solar forecasting system in combination with PV feed-in management:

- Proactive ramping of managed PV and knowledge of future available PV output prior to cloud events with a lead time that is greater than the start time of generators, allowing for adjustment of the spinning reserve during cloud events while ensuring that generator loading remains at desirable levels.
- Accurate prediction of a sustained clear weather period, allowing for the operation of a power station with decreased spinning reserve, which can result in significant fuel savings and operational benefits.

The potential strategy is simplified and limited in that it does not consider the impact of batteries, load changes and load forecast uncertainties as well as solar forecast uncertainties. Knowledge of the forecast uncertainty will improve the system control robustness and allow for adjustment of control decisions, if necessary.

1.10 Improved cloud forecasting with an all sky imager based nowcasting system WobaS

An example skycamera based forecasting system, the WobaS³ system is presented to provide insights into forecast uncertainties. WobaS provides the option to predict the plane of array irradiance for each PV installation, or each zone of a PV installation, in the forecast domain separately. With irradiance data specific to the orientation of the PV system, the resulting PV power can be modelled. The performance of the system for Carnarvon was estimated based on the experience with five existing WobaS systems in Germany, Portugal and Spain. Carnarvon is much closer to the equator than the five sites, leading to much higher average solar elevation angles at Carnarvon and therefore a higher nowcasting accuracy. Furthermore, GHI data reveals that Carnarvon is much less cloudy than the WobaS test sites. Therefore, the uncertainties are expected to be lower overall for the WobaS system in Carnarvon than at the previously investigated sites. Specific recommendations for the placement of skycameras in Carnarvon for the inclusion of a WobaS system into power system control have been provided.

1.11 Existing and suggested hosting capacity calculation approaches

Horizon Power's current methodologies to calculate renewable energy hosting capacity have primarily focussed on system-level impacts, i.e. impacts related to spinning reserve and generator loading capability, generator start times and generator step load capabilities. To achieve very high levels of distributed renewable energy generation in remote networks, local issues and adverse effects at distribution network levels become increasingly important to address. The voltage studies performed as part of the Carnarvon DER Trials have confirmed that voltage rise issues exist in some LV networks and will increase as PV penetration rises. Hence, to determine hosting capacity in remote networks, an approach is required which includes the LV distribution network perspective and considers adverse impacts at a local level as well as at the system level. A stochastic approach to determine the PV hosting capacity of an LV network is suggested. The process would need to be repeated for other LV networks. Once all LV networks' hosting capacities are determined, the impact of these hosting capacities need to be studied at the HV feeder level and system level to determine the remote system's hosting capacity. This approach also allows for the examination of methods to increase PV hosting capacity and DER integration.

The studies presented in this report are part of the activities performed under the Carnarvon DER Trials project, which aims to provide Horizon Power with recommendations on strategies to increase PV hosting capacity in Carnarvon and other networks.

³ WobaS stands for "Wolkenkamera basiertes Nowcasting System" (in German: cloud camera based nowcasting system)

Table of Contents

Acknowledgement of Country	2
Corresponding Author	3
Report at a glance	4
1 Executive Summary.....	7
1.1 Aggregated unmasked load using Wattwatcher data from trial participants.....	7
1.2 Minimum system load in Carnarvon	7
1.3 Effect of PV generation and cloud events on the voltages in selected LV networks	7
1.4 DER connection phase identification.....	8
1.5 Carnarvon inverter audit.....	8
1.6 Visibility & control of Solar PV	8
1.7 Tariffs and energy storage control	9
1.8 Effects of cloud events on spinning reserve requirements	9
1.9 Example spinning reserve strategy based on short-term solar forecasting and feed-in management.....	9
1.10 Improved cloud forecasting with an all sky imager based nowcasting system WobaS	10
1.11 Existing and suggested hosting capacity calculation approaches.....	10
Table of Contents	11
List of Figures	14
List of Tables.....	18
List of Abbreviations.....	19
2 Introduction.....	20
2.1 Project overview	20
2.2 DER Hosting capacity.....	21
2.2.1 Generation and power system hosting capacity limitations.....	21
2.2.2 Network hosting capacity limitations	22
2.2.3 Hosting capacity at Horizon Power	22
2.3 Report purpose and structure.....	23
3 Studies into aggregated Wattwatcher load data and minimum system load	26
3.1 Aggregated Wattwatcher load data	26
3.2 Carnarvon minimum load	28

4	Effect of PV generation and cloud events on the voltages in selected LV networks.....	30
4.1	Cloudy day.....	30
4.2	Clear sky day.....	33
5	DER connection phase identification	36
5.1	Algorithm motivation	36
5.2	Data preparation.....	36
5.3	Clustering results.....	37
5.4	Aggregate comparison	39
5.5	Field inspection.....	40
5.6	Improving hosting capacity.....	43
6	Carnarvon inverter audit	47
6.1	Inverter audit methodology.....	47
6.2	Audit results summary	49
7	Visibility & control of Solar PV	53
7.1	Overview of the Carnarvon Trials 1 and 2 experiments.....	53
7.2	Summaries and observations of the Carnarvon Trials 1 and 2 experiments.....	55
8	Tariffs and energy storage control	62
8.1	Validated learnings.....	62
8.2	Change in DER behaviour.....	63
8.3	Utility benefit Time of Use tariff	66
8.4	Customer benefit Time of Use tariff	68
8.5	Further experiments	69
9	Effects of cloud events on spinning reserve requirements	70
9.1	Existing spinning reserve strategy	70
9.2	Impact of cloud events on the system performance.....	71
9.2.1	Background and simulation descriptions	72
9.2.2	Simulation results	74

9.3	A Short-term Solar Forecasting and Feed-in Management based spinning reserve strategy.....	80
9.3.1	Sky camera-based forecast system integration into power station control systems	81
9.3.2	Potential benefits of a spinning reserve strategy using short-term solar forecasting with feed-in management	82
10	All-sky imager based nowcasting system WobaS.....	86
10.1	Introduction to the WobaS system.....	86
10.2	General accuracy information for the WobaS System	88
10.3	Accuracy estimation for Carnarvon	90
10.4	Modelling aggregated PV generation from all-sky-imager based irradiance forecasts	91
10.5	System configuration for Carnarvon.....	92
11	Hosting capacity calculation approaches	93
11.1	Horizon Power’s existing approaches to calculating hosting capacity	93
11.1.1	Calculation of power system hosting capacity	93
11.1.2	Calculation of local network hosting capacity	94
11.2	Suggested hosting capacity calculation approach	94
12	Recommendations	98
13	Summary	101
14	References	104
15	Appendices	107
15.1	Appendix 1.....	107
15.1.1	Calculations for the unmasked load of a customer and the aggregated unmasked load for customers with WWs	107
15.1.2	Aggregated unmasked load, normalised aggregated PV and the aggregated net load plots	107
15.2	Appendix 2	110
15.3	Appendix 3	113
15.4	Appendix 4	125
15.4.1	Predictive Analytics Model Forecasting – Carnarvon DER Trials	125
15.4.2	Findings.....	127
15.4.3	Key findings/changes required to improve accuracy	127
15.4.4	Conclusions.....	129

List of Figures

Figure 1.	Horizon Power’s hosting capacity development timeline	22
Figure 2.	Maximum fluctuation factor for PV output and unmasked load	26
Figure 3.	Time of the day when maximum load occurred for customers during the time of day analysed (7:30 to 16:30)	27
Figure 4.	Time of the year when the maximum load occurred for the customers during the analysis period (November 2018 to March 2020, during the co time of day considered (7:30 to 16:30))	27
Figure 5.	Express A and B load data for the three lowest load days 8 th June, 24 th August and 9 th June 2019	28
Figure 6.	Irradiance for each of the low load days 8 th June, 24 th August and 9 th June 2019.	29
Figure 7.	Global horizontal irradiance on 22nd August 2019	30
Figure 8.	Range of voltages at different sites of Network-A on 22nd August 2019 (7.30 to 16.30)	31
Figure 9.	Voltage, PV output and net power of Site A4 on 22nd August 2019 (7:30 to 16:30)	32
Figure 10.	A zoomed view of Figure 9 showing the variation of voltage with PV output and net power	32
Figure 11.	Voltage at the sites of Network-B on 22nd August 2019 (7:30 am to 4:30 pm)	32
Figure 12.	GHI on 31 st January 2020	33
Figure 13.	Ranges of voltage at different sites of Network-A on 31 st January 2020	33
Figure 14.	Voltage, PV output and net power of Site A2 on 31 st January 2020	34
Figure 15.	Voltage, PV output and net power of Site A4 on 31 st January 2020	34
Figure 16.	A zoomed view of Figure 15 showing the voltage variation with PV output and net power	35
Figure 17.	Voltages at the sites of Network-B on 31 st January 2020	35
Figure 18.	Principal Component representation of meter-phase data for two sample periods	37
Figure 19.	Clusters resulting from the algorithm for three sample periods in June 2020	38
Figure 20.	Gibson Street Feeder Phase A SCADA measured apparent power (SCADA A in orange), MID aggregated apparent power from algorithm assigned phases (MID A in blue) and apparent power from original phase labels (MID A OPL in grey)	39
Figure 21.	Gibson Street Feeder Phase B SCADA measured apparent power (SCADA B in orange), MID aggregated apparent power from algorithm assigned phases (MID C in blue) and apparent power from original phase labels (MID C OPL in grey)	40
Figure 22.	Gibson Street Feeder Phase C SCADA measured apparent power (SCADA C in orange), MID aggregated apparent power from algorithm assigned phases (MID B in blue) and from original phase labels (MID B OPL in grey)	40

Figure 23. Algorithm assigned phase compared with field recorded phase labels. SCADA measured apparent power (orange) and MID aggregated apparent power (blue).....	42
Figure 24. Comparison of voltages for meters on Phase B with meter number 8 from Table 2. Meters 1, 2 and 3 are labelled for the purpose of this figure and are unrelated to the meter numbers of Table 2.	42
Figure 25. Max voltage heat map and current (bars) for properties connected to Phase A of the Gibson Street Feeder.....	43
Figure 26. Max voltage heat map and current (bars) for properties connected to Phase B of the Gibson Street Feeder.....	44
Figure 27. Max voltage heat map and current (bars) for properties connected to Phase C of the Gibson Street Feeder.....	44
Figure 28. Max voltage heat map and current (bars) for properties connected to Phase C of the Gibson Street Feeder.....	46
Figure 29. Feed-In Management (FiM) requirements checklist	48
Figure 30. DMCS – Repost control architecture. (a) DMCS stack with the sections contained within the red border having been built, completed and used in the Carnarvon DER trials. (b) DMCS stack in the overall control scheme.	54
Figure 31. Typical day before ToU	63
Figure 32. Typical day after ToU.....	64
Figure 33. Compensating for cloud cover.....	65
Figure 34. Graphical consumption comparison.....	67
Figure 35. Graphical average maximum load comparison.....	68
Figure 36. PV power change and Ramp-Rate (RR) versus time duration of the change in PV power generation (Glenister et al. 2019b)	73
Figure 37. Voltage at the MGP 22kV B bus bar, CRN B2 bus bar and MGP 11kV Board B. Load increase due to a 3.4MW, 2.4MW and 1.2MW decrease in PV output power over 300 seconds corresponding to 11.4MW, 6MW and 3MW of installed PV capacity, load initially minimum. Reactive power absorption by the network decreased due to inverter Volt-VAr systems backing off, causing the voltage to rise	75
Figure 38. Frequency response of gas engine generators to the load ramps. Load ramps are shown in Figure 60 (Appendix).....	76
Figure 39. Load increase due to a 4.7MW decrease in PV output power over 300 seconds, assuming 11.4MW of installed PV capacity, load initially minimum. The total load and one gas generator load are shown. Reactive power decreased and spinning reserve dropped from 1.75MW to 0 in 132 seconds.....	77
Figure 40. Frequency response to load increases due to cloud shading of PV for 3, 6 and 11.4MW of PV capacity.....	78

Figure 41. Frequency response to load decreases due to cloud unshading of PV for 3, 6 and 11.4MW of PV capacity.....	79
Figure 42. A hypothetical cloud event scenario and the existing spinning reserve strategy operation.....	83
Figure 43. The hypothetical cloud event scenario and the application of an example spinning reserve strategy using a short-term solar forecasting system in combination with PV feed-in management and generation control.....	83
Figure 44. (Left) Mobotix all-sky imager at Murdoch University; (Right) all-sky image at Murdoch University	86
Figure 45. Cloud models and topographical map around CIEMAT’s PSA with spatial DNI information.....	87
Figure 46. MAD for DNI at the 5 sites for different DNI variability classes (from Nouri et al., 2020).....	89
Figure 47. Overall MAD and RMSD for DNI at the 5 sites (from Nouri et al., 2020).....	89
Figure 48. GHI and DNI error metrics for the ASI system at PSA (24.09.2019 to 28.11.2019). The error metrics are derived from a spatially averaged irradiance nowcast over an area of 1 km ² and the averaged signal from 8 reference stations distributed within this area. Bias refers to the average deviation.....	90
Figure 49. Colour-coded GHI plot with hour of the day on the y-axis and time within the year on x-axis for Carnarvon (upper plot, 2019) and PSA (lower plot, 2010).....	91
Figure 50. Example positions of two ASIs to cover Carnarvon’s PV systems.....	92
Figure 51. Flowchart of a stochastic approach to determine the PV hosting capacity of an LV network.....	96
Figure 52. PV generation, net load and unmasked load for all WW systems on 22/08/2019	108
Figure 53. An expanded view of Figure 52 around the time of the largest change in PV generation on 22/08/2019.....	108
Figure 54. a) Express feeders A and B net load for Carnarvon on 22nd August 2019 over the same time period as in Figure 3 of Glenister et al. (2020). (b) An expanded view, showing the power changes between 14:50 and 14:59	109
Figure 55. Voltage, PV output and net power for Site A2 on 22nd August 2019	110
Figure 56. Voltage, PV output and net power for Site A8 on 22nd August 2019	110
Figure 57. Voltage, PV output and net power for Site A8 on 31 st January 2020	111
Figure 58. PV output and battery power for Network-B sites on 31 st January 2020	111
Figure 59. Net power for Network-B sites on 31 st January 2020	112
Figure 60. “Carnarvon Generation Model – Nov 2017” PowerFactory model online diagram.....	113
Figure 61. Gas engine generator load ramps used to test performance of the gas engine generators. The right y axis is 3.5 – 5.3MW for the 5 th curve only and easy comparison between the 3 rd and 5 th power ramps. The 4 th curve shows the per generator ramp corresponding to the total power ramp in the 5 th ramp.....	114

Figure 62. Diesel engine generator load ramps used to test performance of the diesel engine generators	115
Figure 63. Diesel engine generators frequency response to load ramping. The load ramps are shown in Figure 62.....	116
Figure 64. Real power and reactive power changes corresponding to the voltage changes shown in Figure 37. The 11.4MW PV scenario net load power increase stops at 7MW to prevent overloading of the generators	117
Figure 65. Real power and reactive power changes corresponding to the voltage changes shown in Figure 37. The 11.4MW PV scenario net load power increase stops at 7MW to prevent overloading of the generators.....	118
Figure 66. Voltage on the Mungullah 11kV Board B HV bus bar during the power changes.....	119
Figure 67. Load increase due to a 1.2MW decrease in PV over 300 seconds. 3MW of installed PV capacity, initial minimum load, total load and one gas generator load are shown. Reactive power decreases also.....	120
Figure 68. Load increase due to a 2.4MW decrease in PV over 300s. 6MW of installed PV capacity, initial minimum load, total load and one gas generator load are shown. Reactive power decreases also.....	121
Figure 69. Load decrease due to PV output increase for 3MW of PV. 850 + j300 kVA increase in PV.....	122
Figure 70. Load decrease due to PV output increase for 6MW of PV. 1.7 + j0.6 MVA increase in PV.....	123
Figure 71. Load decrease due to PV increase for 11.4MW of PV. 4.7 + j2MVA increase in PV	124
Figure 72. 7-day ahead predictions of the Carnarvon residual demand for the period 24 th September – 1 st October 2016	126
Figure 73. Carnarvon PV Generation and Irradiance based on 7-day cloud cover predictions for the period 27 th August – 3 rd September 2016.....	126
Figure 74. Prediction of PV generation from the predictive models for the period of 2 nd – 7 th August 2016	128
Figure 75. Day-ahead forecasts from IBM Deep Thunder and PV Generation for the period of 12 th – 20 th July 2016	128

List of Tables

Table 1. Summary of Clustering Results.....	38
Table 2. Field Recorded Phases compared against Algorithm Assigned Phases.....	41
Table 3. Maximum voltages near meter number 1 with high maximum voltage on Phase A to be shifted to Phase C.....	45
Table 4. Maximum voltages comparison for meter number 9 shifted from Phase C to Phase A.....	46
Table 5. Horizon Power technical requirements inverter settings.....	47
Table 6. Classification of results.....	49
Table 7. Results summary.....	50
Table 8. Detailed audit results including failed and incomplete systems.....	51
Table 9. Safety issues.....	52
Table 10. Carnarvon trials covering the basic functionality of the Reposit control systems and data acquisition systems.....	55
Table 11. Carnarvon trials covering basic control of DER energy storage and VPPs including primary inverter control for network support.....	58
Table 12. Time of Use Tariff.....	62
Table 13. Consumption comparison.....	66
Table 14. Average maximum load comparison.....	66
Table 15. Comparison of customer annual cost of energy.....	69
Table 16. Spinning reserve “Load increasing” operation examples in Carnarvon (“X” indicates “running”).....	70
Table 17. Spinning reserve “load decreasing” operation examples in Carnarvon (“X” indicates “running”).....	71
Table 18. RMS PowerFactory simulations performed.....	71
Table 19. Criteria used to assess PowerFactory RMS simulations.....	72
Table 20. Derived factors from previous work on this project (S. Glenister et al. 2019b) used to scale power ramps for PowerFactory RMS simulations.....	72
Table 21. Reactive power estimation factors used for the PowerFactory simulations.....	74
Table 22. Scenarios for various PV penetrations and cloud induced power changes based on experience from WW data.....	75
Table 23. Problematic installed PV capacities for starting gas engine generators.....	80
Table 24. Scenario assumptions.....	82
Table 25. Description of DNI variability classes.....	88
Table 26. HV feeder loads for the minimum load scenario in the “Carnarvon Generation Model – Nov 2017”.....	121
Table 27. Summary of the predictive models of the selected subset of LV feeders at Carnarvon.....	125

List of Abbreviations

AMI	Advanced Metering Infrastructure
API	Application Programming Interface
ASI	All-sky Imagers
BaU	Business as Usual
CNN	Convolutional Neural Network
CRN	Carnarvon
CSL	Clear Sky Library
DER	Distributed Energy Resources
DHI	Diffuse Horizontal Irradiance
DMCS	DER Management and Control System
DNI	Direct Normal Irradiance
EG	Embedded Generation
FIM	Feed-in Management
GHI	Global Horizontal Irradiance
HV	High Voltage
IEEE	Institute of Electrical and Electronics Engineers
L	Latency
LV	Low Voltage
MAD	Mean Absolute Deviations
MAPE	Mean Absolute Percentage Error
MID	Meter Instantaneous Data
MPS	Mungullah Power Station
MW	Mega Watt
PCC	Point of Common Coupling
PELS	Pre-emptive Load Shedding (in Spanish: Solar Platform of Almería)
POA	Plane of Array
PSA	Plataforma Solar de Almeria
PV	Photovoltaic
RMSD	Root Mean Square Deviations
RR	Ramp Rates
SCADA	Supervisory Control and Data Acquisition
SWIS	Southwest Interconnected System
ToU	Time of Use
VPP	Virtual Power Plant
WA	Western Australia
WobaS	Wolkenkamera basiertes Nowcasting System (in German: cloud camera based nowcasting system)
WW	Wattwatcher

2 Introduction

2.1 Project overview

Horizon Power has, over the last three years, conducted a series of technology trials in the town of Carnarvon in the Gascoyne – Mid West region of Western Australia (WA), to explore economically efficient options for microgrid operation. The trials have examined the management of high penetration levels of Distributed Energy Resources (DER); cloud-based aggregation of DER into Virtual Power Plants; the use of advanced data analytics to improve DER management, and, the use of mobile apps that provide customers with data on which they can make informed decisions.

Carnarvon, situated on the mouth of the Gascoyne River 900 km north of Perth, has a population of approx. 5,500. Horizon Power commissioned a new 13MW gas-fired (with diesel peaking) Power Station, named Mungullah, in 2014. Ownership of the power station offers control system access, integration and optimisation options that would not be possible with an independent power producer operating under a power purchase agreement. With an economic base of predominantly primary producers, Carnarvon experienced rapid uptake of solar photovoltaic (PV) systems from 2008 to 2011 with higher than average system sizes, typically 10-30kW, used to offset cool room and water pumping power purchases.

The distribution system has a high feeder and transformer loading of solar PV and requires sufficient spinning reserve to cover the variability in renewable energy generation caused by coastal weather patterns. Carnarvon was the first regional WA town to start pushing the boundaries of Horizon Power's solar PV hosting capacity in 2011. The town's population has always held great enthusiasm for solar PV with >350 customer connected systems as well as two commercial solar farms operated by Solex (45kW), which was the first privately owned commercial solar farm in Australia, and EMC (300kW).

The Carnarvon DER trials, which commenced in late 2017 and include a team of researchers from the Engineering and Energy Discipline at Murdoch University, aim to resolve the technical, operational and transitional barriers to a high penetration DER business future. By conducting a series of technology trials and experiments over three years involving the monitoring and control of solar PV and energy storage, we aim to answer questions such as: Have we fully explored the operational risks associated with a DER control system? Can we employ controls to manage DER in a microgrid to support Horizon Power's future projections of high penetration DER? Can such a DER management solution monitor and control energy storage to reduce peak demand or peak export? And, can the use of such a control solution be used to increase DER hosting capacity and penetration of renewable energy into the network?

The project hypothesis is that, in the future, the same level of visibility and control that we have had over centralised power stations in the last few decades can be gained over distributed energy generation, and the contribution from DER can be managed to increase hosting capacity and achieve reliable and robust microgrid operation. The Carnarvon DER trials, aim to experimentally understand how to manage DER in a microgrid environment, how DER orchestration can be used to remediate power quality issues and how a system operator can effectively exchange DER value with customers. Key to the management of microgrids with high penetration DER is gaining an understanding of the impact of weather patterns on renewable energy generation and customer load, particularly cloud events, and how that renewable energy generation variability impacts the way the power system is operating.

2.2 DER Hosting capacity

As a direct result of Government incentives and the falling cost of solar PV systems, Horizon Power has experienced a rapid rise in the connection of DER to its networks, predominantly PV generation. As a result, Horizon Power sees significant solar PV generated energy levels being exported back into its networks. There is a limit to the amount of DER that can be installed on networks, particularly small islanded systems, before the quality of supply and reliability limits are exceeded. This limit, called Hosting Capacity, may be defined as the amount of DER that the power system can support, or host, at any point in the power system. Hosting Capacity may be expressed at the power system level, or at the local network level.

A number of issues affect hosting capacity in terms of both generation and the network, including:

- Generator Spinning Reserve and maximum/minimum loading capability;
- Generator start times;
- Generator step load capability;
- System voltage profiles;
- System frequency and voltage stability;
- Voltage regulation;
- Network loading capability;
- Fault level and protection requirements; and
- Network Power quality, including harmonics, and voltage flicker.

Ultimately there is a finite technical limit to the amount of PV that can be connected to a network without some form of intervention to ensure power quality and reliability.

2.2.1 Generation and power system hosting capacity limitations

Safe and reliable power system operation requires that the system has, at any given time, sufficient capacity available to cover fluctuations in system load. For an electrical system to function, there must be a balance between load demand and energy generated. The scheduling of generation sets to help maintain this balance is based on experience and forecasting. It ensures that enough sets are available to provide sufficient additional or spare capacity to cover the predicted load changes at any given time. This spare capacity is known as Operational Reserve and includes the spinning reserve available from the rotary or spinning generators, plus reserve capacity available from inverter-based generation.

The variable nature of solar generation is such that when a cloud event or system disturbance occurs, the energy output of many solar PV systems can drop sharply, and this manifests itself as a rapid transfer of load away from the PV generation and onto Horizon Power's generation equipment. This rapid transfer of load has the ability to affect the operation of smaller power stations on islanded systems. The ability of the power system to meet this sudden increase in load is dependent on the characteristics of the generator sets and how many are online at the time of the event. Similarly, when the cloud event finishes, the sometimes rapid reappearance of the sun manifests itself as a spike in PV system production and a sudden excess of energy flowing into the network. If insufficient Operational Reserve and step load capability are available in the system to cover the fluctuations in renewable energy generation, generators will overload, resulting in power system instability and outages. Sufficient Operational Reserve can be provided by keeping additional generation online, but this comes with both an operational and environmental cost.

Another problem experienced by utilities in relation to DER is reverse power conditions at substations and power stations due to an excess of generation at times of light load and high DER output. If generator minimums are compromised, this can result in maintenance issues and generator trips.

Details on the current method applied by Horizon Power to calculate the overall Total Hosting Capacity for its power systems are given in Section 11.1.1.

2.2.2 Network hosting capacity limitations

Network hosting capacity varies from location to location within the network and considers the effect of DER on thermal ratings, voltage regulation, fault levels, protection systems and power quality. It can be determined for any node in a distribution network and defined as the maximum capacity of DER that can be added to the particular node without causing the network to operate outside its reliability and quality of supply conditions when the contributions of all DERs connected to the network are considered.

The current approach used by Horizon Power to calculate Local Network Hosting Capacity is outlined in Section 11.2.

2.2.3 Hosting capacity at Horizon Power

Hosting capacity limits were first introduced at Horizon Power in 2009. These limits were primarily driven by power generation constraints and have been reviewed regularly since then as power systems have changed and evolved (see Figure 1).

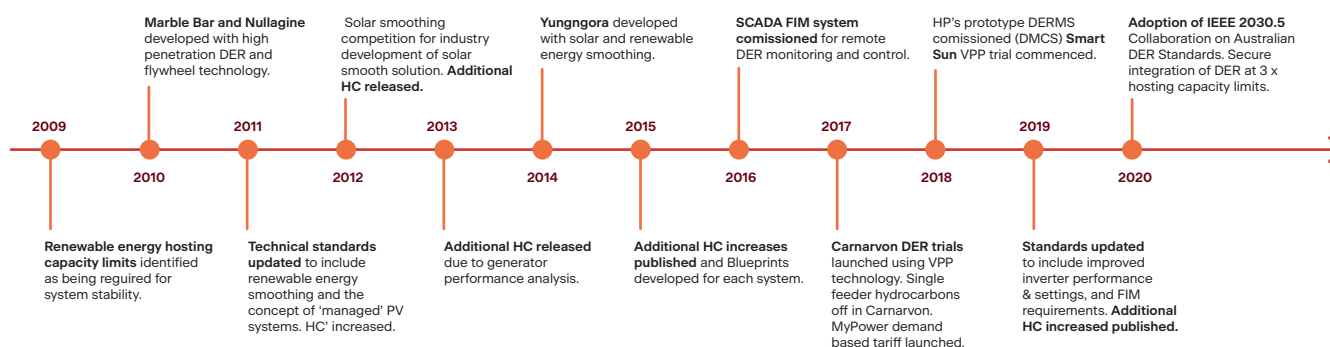


Figure 1. Horizon Power's hosting capacity development timeline.

By 2011, due to the popular demand for solar PV, many of Horizon Power's systems had reached their available Hosting Capacity. At that point in time, Horizon Power introduced a new suite of technical requirements that allow for increased amounts of renewable energy generation with the use of a concept known as renewable energy smoothing. Renewable energy smoothing involves some customers installing a portion of energy storage with their PV system to cover the fluctuations in the output of their own PV system and to act as a shock absorber for the system. Horizon Power adopted a flexible approach in defining the technical standards, which has seen some innovative approaches in customers managing their loads or utilising sky cameras to forecast solar variability. The adoption of renewable energy smoothing saw a significant increase in hosting capacity.

In 2013, Horizon Power updated its hosting capacity calculations to expand on the concept of renewable fluctuation factors, which take into account diversity between PV installations and expected output fluctuations for individual PV systems. The hosting capacity calculations were also updated to include an allowance for short term generator overload capability and a time-based risk assessment of the available

operational reserve. These changes resulted in increased hosting capacity across the majority of systems.

By 2016, Horizon Power commissioned its SCADA Feed-in Management system for remote control and monitoring of the output of larger commercial DER systems. This has assisted in mitigating the effects of excess DER generation on the system at times of light load and has, in turn, increased hosting capacity.

Between 2017 and 2019, Horizon Power intensified its research efforts, embarking on DER trials in Broome, Carnarvon and Onslow to improve its understanding of the performance of systems with high levels of DER and to test a number of DER management platforms.

In 2019, Horizon Power updated its calculations and released a significant amount of hosting capacity across its systems, by incorporating:

- a range of learnings from the Broome, Carnarvon and Onslow trials, such as updated data on renewable energy fluctuation factors and performance of energy storage and DER control systems;
- the latest system data such as equipment parameters, load characteristics, power system control philosophies and data on operational reserve levels;
- updated inverter settings for improved resilience;
- dynamic modelling of power system stability; and
- consideration of power station generator start-up times and energy storage time constants.

Many of these updates to calculation methodologies have been undertaken in collaboration with industry and academic institutions.

The Carnarvon DER trials carried out with our research partner Murdoch University are one of these collaborations. An overview of the research activities from this collaboration are contained in this report.

2.3 Report purpose and structure

This report complements the project's first publication, Technical Report #1 (Moghbel et al. 2019)⁴, and should be read in the context of the details outlined in that report. Information about PV fluctuation factor, PV diversity factor, voltage rise observations, data collection and analysis detailed in Technical Report #1 support the contents of this report.

Since that first report, work on the Carnarvon DER trials continued in a number of areas, including:

- Wattwatcher data collected during the project provided a unique view of the unmasked load in contrast to the net load for the customers participating in the trials. The analysis of this data is presented in this report. Furthermore, the minimum load seen by the Mungullah Power Station is a critical parameter with respect to generator loading and spinning reserve. Findings from an investigation into minimum load days are also reported.
- The voltage analysis presented in Technical Report #1 (Moghbel et al. 2019) has been expanded to support a closer investigation into voltage variations at specific sites on two LV networks for sample cloudy and clear days.
- The Wattwatcher data was also used to observe the worst cases of power fluctuations in the PV generation. Analysis of the spatial diversity and the amount of PV generation in Carnarvon was used to develop a method to estimate the PV generation fluctuation at different levels of penetration in Carnarvon.

⁴ <https://arena.gov.au/knowledge-bank/horizon-power-carnarvon-der-trials-technical-report/>

The method uses a mathematical approach based on a Wavelet transform function which utilises irradiance data from a single pyranometer or power output data from a single PV system, PV power capacities, distances between PV systems and cloud speed information (Glenister, S., et al. 2020). This enabled modelling of changes to PV power output due to cloud movements of unmonitored and future PV systems in Carnarvon and allowed explicitly for estimations of worst-case ramp events in PV generation. This work provided the necessary inputs for the simulation studies investigating the impact of cloud events on system performance, which are presented in this report.

- Following on from the research by Murdoch University in the early stages of the trials, which identified mass inverter trip events, Horizon Power commenced two pieces of work to investigate options to improve customer DER operation. The first was the application of advanced analytics to customer meter data to identify single phase solar PV systems that would benefit from being re-allocated to a less congested phase, i.e. phases with lesser high voltage excursions. The second was an audit of inverter systems in the town to ascertain compliance with Horizon Power's DER connection technical requirements, which have required specific inverter settings since 2010.
- Horizon Power performed a series of experiments, which tested various aspects of battery/PV systems with Reposit boxes installed in Carnarvon in 2018/2019. These experiments tested various aspects of these systems to determine the adequacy of DER, in a broader sense, to provide ancillary services in addition to supplying power when DER penetration increases or in an islanded microgrid mode. The experiments covered, for example, basic control and administration functions of Virtual Power Plants (VPPs), and provided valuable insights into performance characteristics of feed-in management systems such as latency of VPP control. Findings from this work, along with a review of short-term solar forecasting system capabilities, led to the development of an example spinning reserve strategy using solar forecasting with feed-in management. The strategy is described in this report and assessed using a hypothetical cloud event and PV penetration scenario for Carnarvon.
- The value proposition for customer connected batteries and how a win-win outcome could be created for both the customer and Horizon power was explored through another experiment. The PV/Battery DER system of a trial participant (a primary producer business) was nominated for the experiment to test the effectiveness of Time of Use (ToU) tariffs in managing a battery system connected behind the customer meter over time. It sought to investigate the value of optimised battery operation for customers who are not in a position to significantly change their consumption behaviour. The outcome from this experiment has highlighted the potential opportunities with managing battery systems through the application of ToU tariffs, which can be further investigated through trials with multiple properties.
- Collaboration between Murdoch University and researchers from the Institute of Solar Research from the German Aerospace Centre enabled further insights into the requirements, capabilities and forecast uncertainties of an example skycamera based forecasting system, the WobaS system. A description of the system and an estimation of its performance for Carnarvon, based on the experience with five existing WobaS systems in Germany, Portugal and Spain, is provided in this report.
- Drawing on the findings from the trials as well as literature to suggest a hosting capacity determination approach, which allows for the examination of methods to increase PV hosting capacity and DER integration.

The studies and investigations mentioned above and presented in this report are based on the weather-energy-related dataset collected during the Carnarvon DER Trials. The project uses a unique monitoring infrastructure comprising of a variety of data acquisition systems. SCADA, Wattwatcher and environmental parameter data are recorded, creating a coincident data set with records at 5-second intervals. The data collection and approach has been described in more detail in the Technical Report #1 (Moghbel et al. 2019).

The report is structured as follows:

- Section 3 analyses aggregated and unmasked load and reports on the investigation into minimum net load seen by the Mungullah power station (using feeder data) in Carnarvon.
- Section 4 presents voltage study results based on Wattwatcher data with a particular focus on the effects of cloud events on the voltage at various points in the system.
- Section 5 describes the use of data analytics and advanced meter data to determine DER connection phase identification.
- Section 6 outlines the Carnarvon inverter settings audit carried out across the town.
- Section 7 discusses achieving visibility and control of DER using the Reposit Power Virtual Power Plant technology
- Section 8 explores the application of ToU tariffs to control customer energy storage.
- Section 9 contains simulation study results investigating the impact of cloud events on system performance. This section also provides descriptions of the existing spinning reserve strategy and an example strategy for increased PV penetration using solar forecasting with feed-in management to deal with cloud events.
- Section 10 introduces the WobaS system as an example of a skycamera based solar forecasting system and provides an estimation of the system's performance for Carnarvon.
- Section 11 presents a suggested hosting capacity calculation approach.
- Section 12 describes the key recommendations for managing different aspects of DER.
- Section 13 provides a summary of the report, along with concluding remarks.
- Section 14 contains references to the material used in this report, and finally,
- Section 15 provides further information in appendices.

3 Studies into aggregated Wattwatcher load data and minimum system load

3.1 Aggregated Wattwatcher load data

The output of PV systems mask the true load of the network, and therefore the network only sees the net load of any customer. In order to understand the actual load profile, it is important to unmask the true load. To calculate the unmasked load⁵, data on the PV generation and net power export/import by the customers along with the charging and discharging power of batteries is required. This data is available for customers with Wattwatchers (WWs), which can be used to help provide a true picture of a subset of the Carnarvon load (with WWs) in contrast to the net load. Details on the calculations for the unmasked load for the customer and the aggregated unmasked load of the customers with WWs is given in Appendix 1 (Glenister et al. 2020).

Figure 2 shows the PV and unmasked load fluctuation factor for a time interval ranging from 30 seconds to 5 minutes (similar to the PV fluctuation factor analysis presented in Moghbel et al. (2019)). The calculation is carried out for the analysis period from November 2018 to March 2020, and only for daylight hours from 7:30 to 16:30. The magnitude of the unmasked load fluctuation factor is lower than the PV fluctuation with a small positive slope over the interval range.

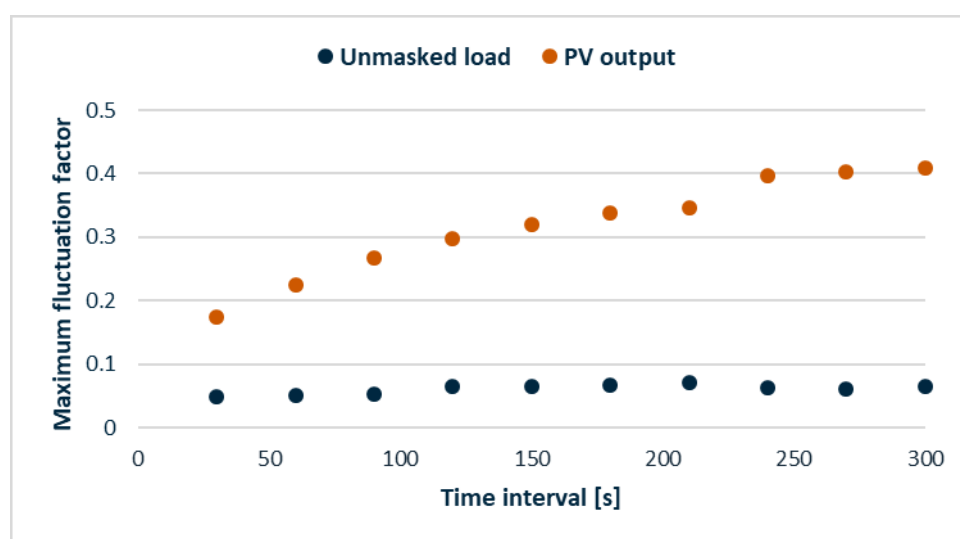


Figure 2. Maximum fluctuation factor for PV output and unmasked load.

The aggregated unmasked load was found to be relatively constant, while the net load exhibited an inverted solar profile (see Figure 51, which shows plots of the PV generation, net load and unmasked load for all WW systems on 22nd August 2019, in Appendix 1). Furthermore, it is evident from Figure 2 as well as Figure 51 and Figure 52 in Appendix 1, that the fluctuation of the net load is dominated by the fluctuation of the PV generation for this subset of the Carnarvon network.

⁵ The load, which is seen by the network when there is no PV output, i.e. the actual consumption of the customers. Battery charging is not considered as customer load.

Figure 3 shows the time of the day when maximum unmasked load occurred for customers. It shows that for most customers, the maximum load took place during noon. Figure 4 shows the distribution of maximum unmasked load over the months of the year. It is evident that the maximum loads have occurred mainly in the summer months of December, January and February. Figure 4 suggests that the cooling demands are mainly contributing to the maximum unmasked load during the time of the day considered (7:30 to 16:30), which is expected from a predominantly residential load.

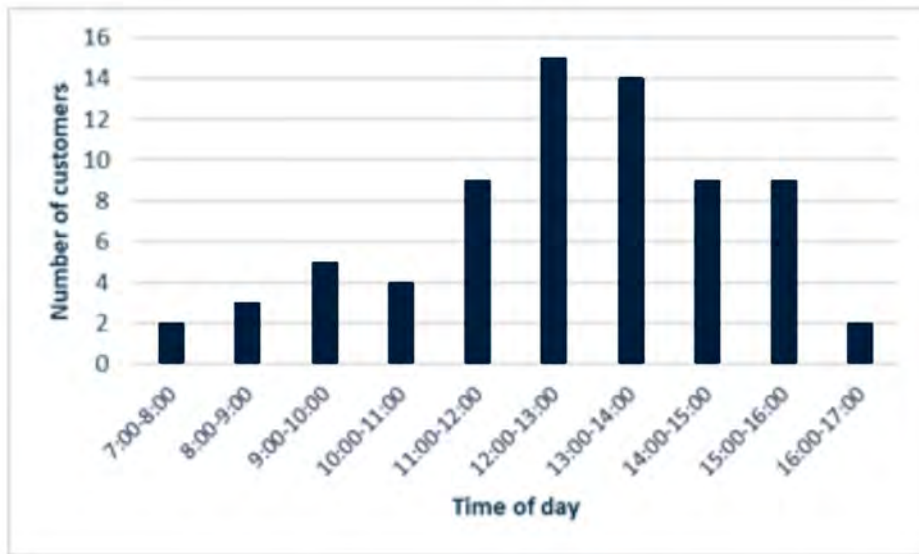


Figure 3. Time of the day when maximum load occurred for customers during the time of day analysed (7:30 to 16:30).

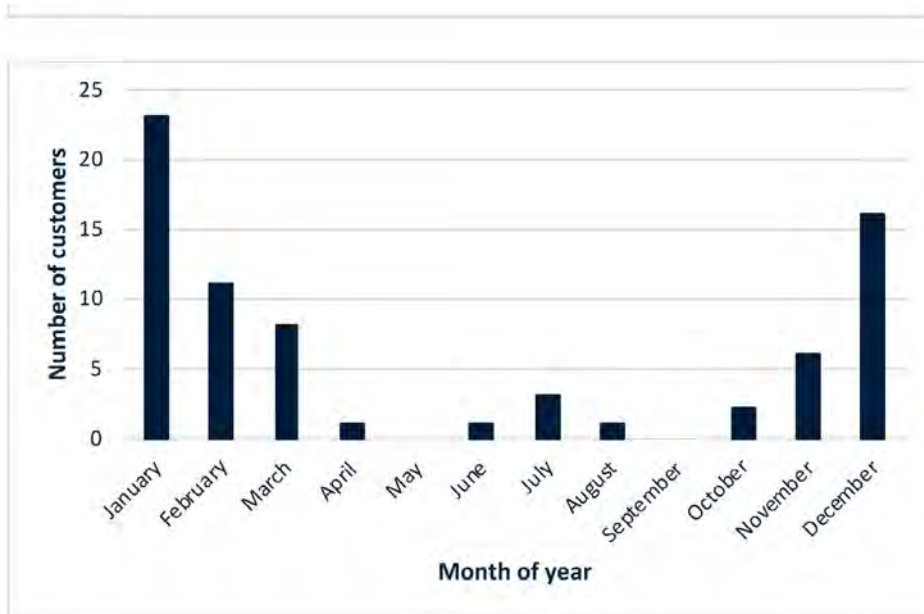


Figure 4. Time of the year when the maximum load occurred for the customers during the analysis period (November 2018 to March 2020, during the co time of day considered (7:30 to 16:30)).

3.2 Carnarvon minimum load

One potential issue is the net load seen by the Mungullah Power Station (the gas/diesel power station supplying Carnarvon). With the increasing penetration of PV, the net load can be pushed to ever lower levels. The peak PV generation generally does not coincide with peak load demand, which can cause the load levels of the fossil fuel based generators to drop well below 50% loading around midday on some days. Exacerbating this is that a lower level of spinning reserve in line with the lower load cannot be safely assumed during these periods because of the potential for cloud induced power decline of the PV resource. Therefore, an investigation into the minimum load seen by the Mungullah power station was required. The data provided was from the SCADA monitoring system on the express A and B feeders. These feeders operate at 22kV and are 5.5km in length from the Mungullah power station to the Iles Road HV switchboard. This HV switchboard is the origin of the six 22kV distribution lines that supply Carnarvon town and surrounds. These express feeders are the corridor through which the total Carnarvon non-PV generation flows.

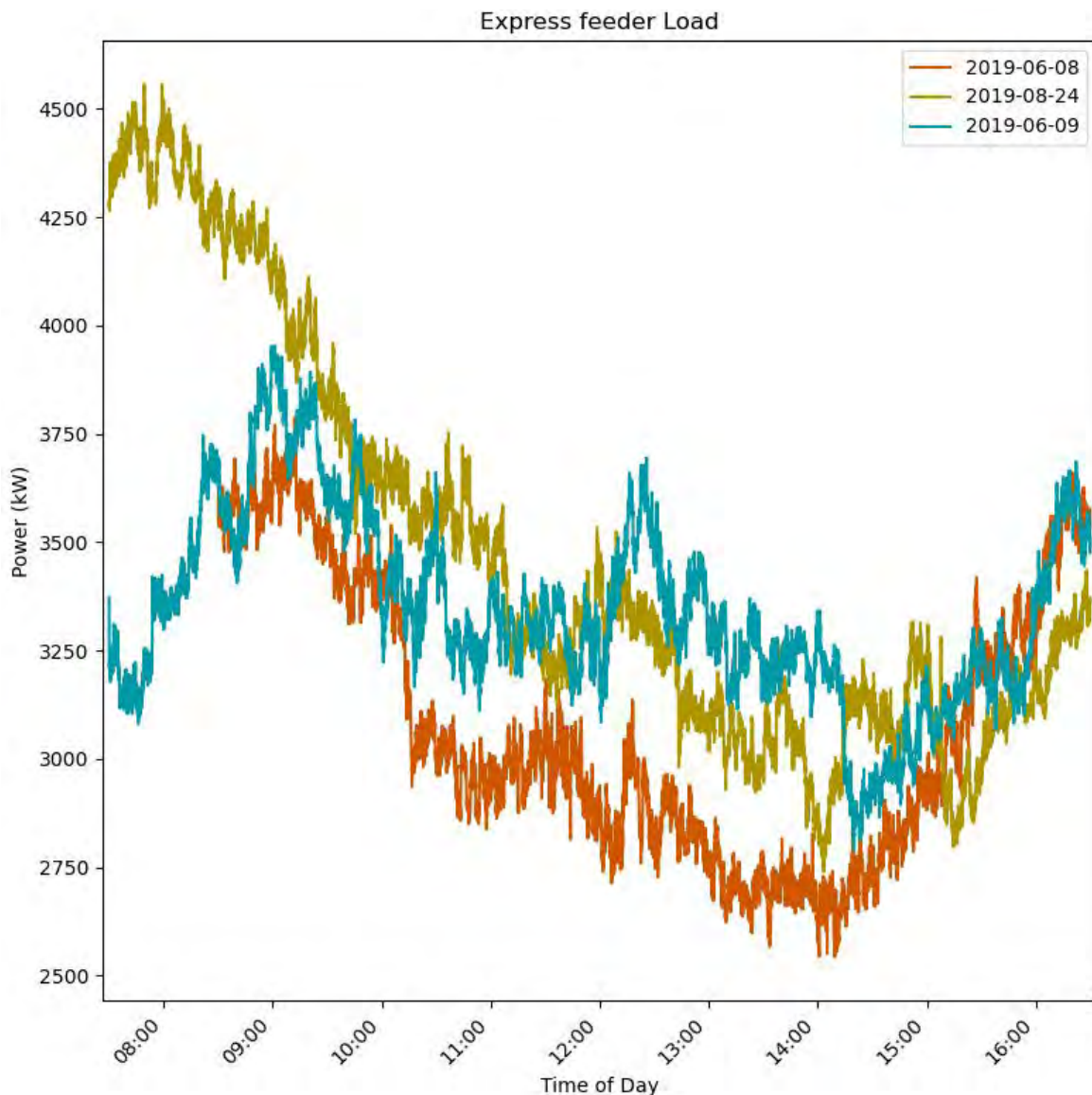


Figure 5. Express A and B load data for the three lowest load days 8th June, 24th August and 9th June 2019.

This SCADA data was made available as part of the Carnarvon DER trials project and covered the period 2017 – 2020. On 1st July 2019, 10MW of PV hosting capacity was made available for new distributed PV systems to be installed across all Horizon Power’s networks. Within six months of this date, the amount of installed PV capacity in Carnarvon went from about 1MW to 3MW; however, the majority of the data for the express feeders pre-dates this PV increase.

Figure 5 shows the time series for the three lowest load days found in this SCADA data. The minimum load was 2.54MW on 8th June 2019 at 14:09. The next two days with the lowest load ranking behind 8th June were 24th August 2019 (2.74MW) and 9th June 2019 (2.79MW). All three days had minimum loads below 3MW and the time of day in all three cases is around 14:00 (14:09, 14:03 and 14:20, respectively). Both June 8th and 9th were partially cloudy days, and 24th August was a clear day, as shown in Figure 6.

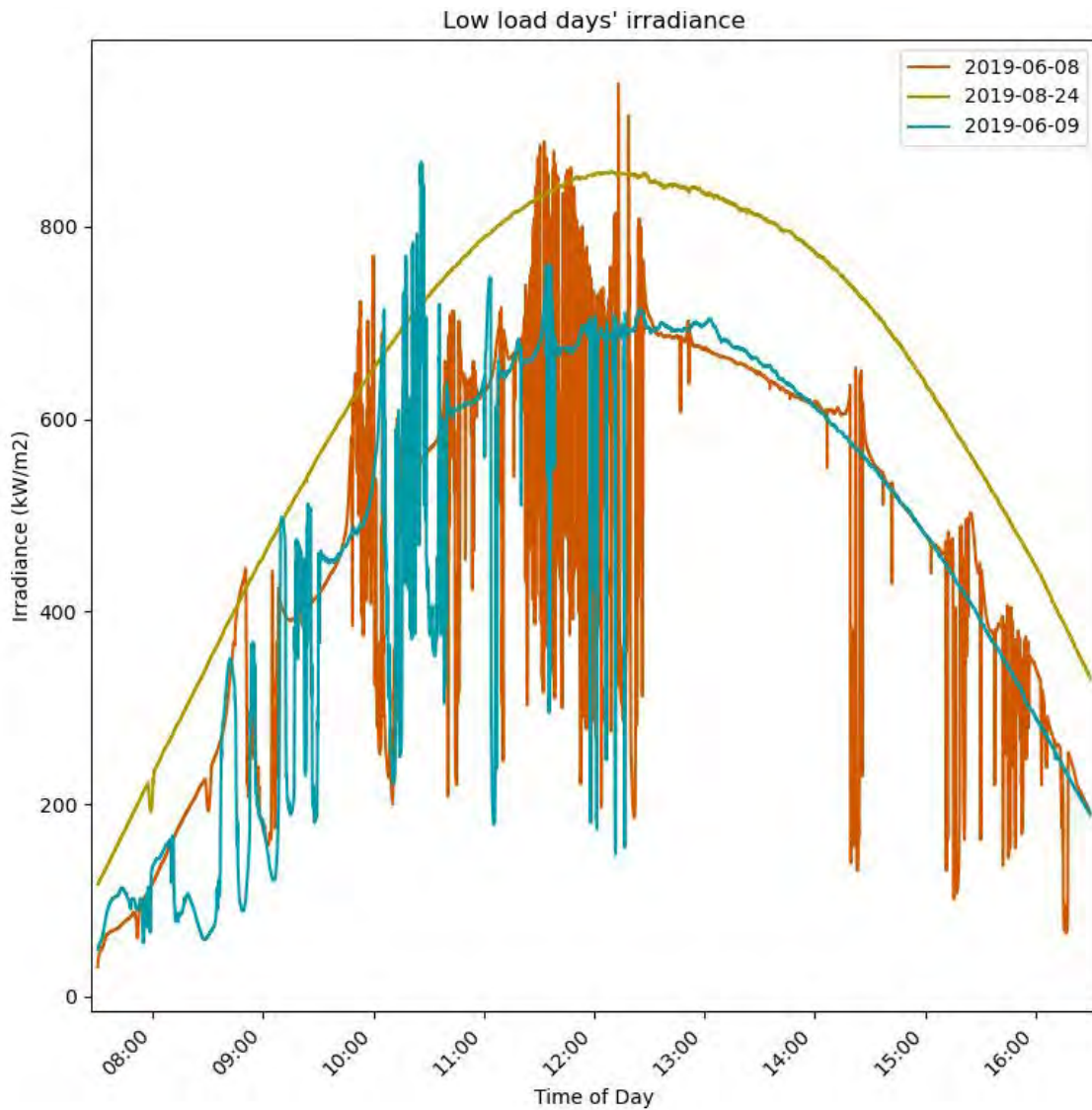


Figure 6. Irradiance for each of the low load days 8th June, 24th August and 9th June 2019.

The actual minimum load numbers (2.54, 2.74 and 2.79MW) are somewhat artificial, in the sense that the load signal from the SCADA system fluctuates over time. To get a better sense of the minimum load, the time series in Figure 5 shows the load over time-of-day. It does not appear that the net load seen by the Mungullah

power station was significantly affected by the PV generation since the amount of PV capacity was only 1MW for the June period and not significantly higher by August 2019. Also, the time-series data followed a similar pattern for all three days, reaching minimum power at around 14:00 and increasing beyond that time. While the minimum load occurred during a period of high PV generation, the minimum load period does not align with the peak PV generation period as can be seen from a comparison of the load data in Figure 5 and the irradiance data in Figure 6.

4 Effect of PV generation and cloud events on the voltages in selected LV networks

The voltages on two LV networks were investigated to analyse the effect of PV power generation (and cloud events) on the LV network voltage. The two chosen networks, Network-A and Network-B were selected based on the data availability (i.e., number of systems with WWs and PV system information). Also, these two networks were found to be among the networks presenting higher over-voltage events in the previous analysis. Phase voltage data of the Nett WWs (closest to the LV network) were analysed along with the PV power generation at the selected sites. Specific sites were chosen because of the large voltage ranges observed in the data for these sites. For the analysis, a day with high PV output fluctuation (due to cloud events) and a day with low PV fluctuations were chosen. Of the two networks, Network-A had a high penetration of PV (about 150kW), and Network-B had a moderate level of PV penetration (about 30kW). Both networks use overhead distribution lines at 415V (line-line).

4.1 Cloudy day

Figure 7 shows the global horizontal irradiance (GHI) on 22nd August 2019, the selected cloudy day.

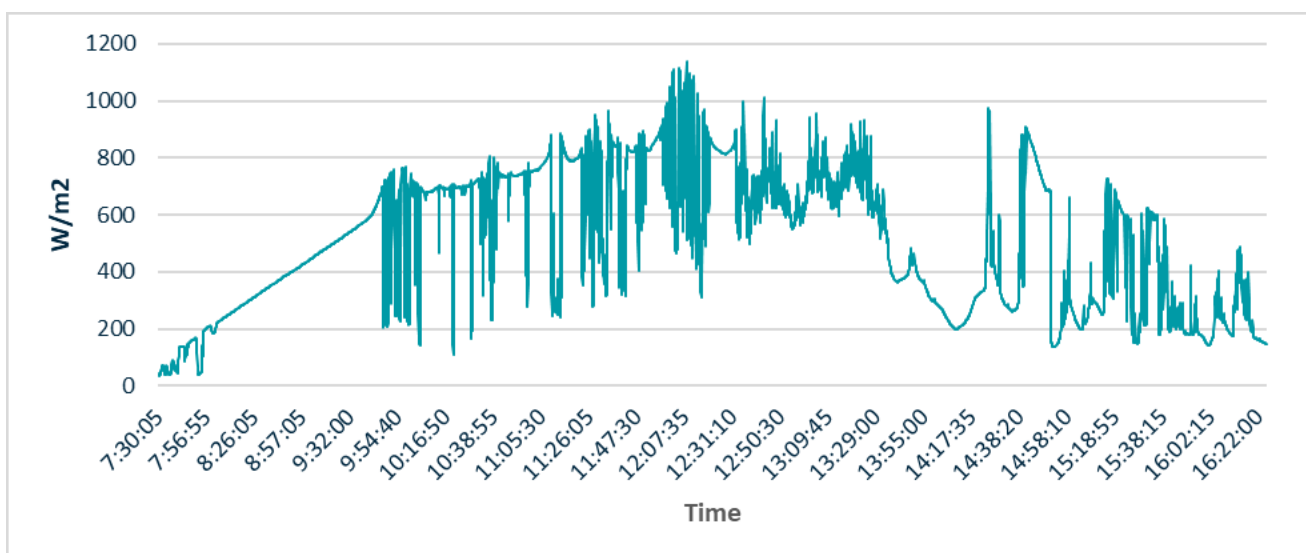


Figure 7. Global horizontal irradiance on 22nd August 2019.

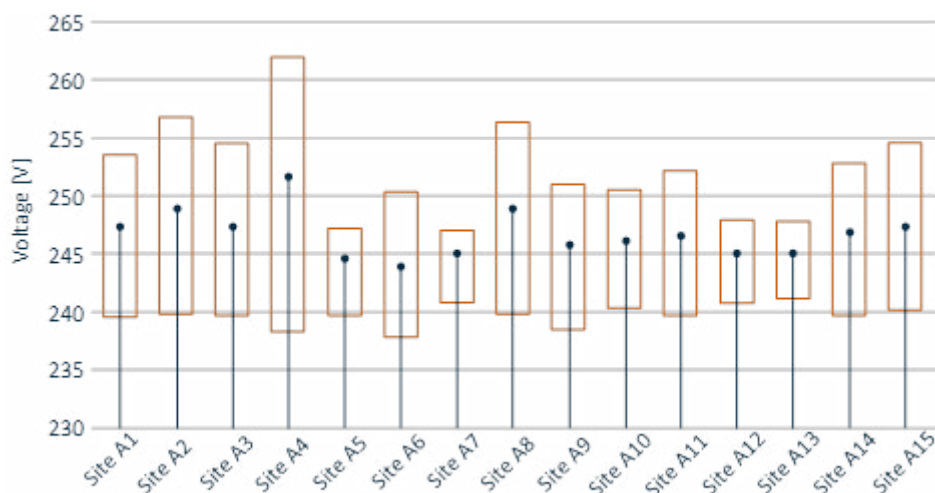


Figure 8. Range of voltages at different sites of Network-A on 22nd August 2019 (7.30 to 16.30).

In Network-A, 15 sites with PV systems (out of a total of 21 sites with PV systems) were considered based on the data availability. The ranges of voltage variation over the day (from 7.30 am to 4.30 pm) on 22nd August 2019 are presented in Figure 8, which shows that the voltages for most of the sites were above the nominal voltage (i.e., 240V) on that day. Site A2 and A8 went above 255V, and Site A4 went beyond 260V, in some instances. These sites also experienced a wider voltage range. On the other hand, some sites experienced a very consistent voltage (i.e., narrow range), such as Site A5, A7, A12 and A13. It is to be noted that sites A5 and A7 are located close to (i.e. less than 100 meters from) the transformer while Site A2, A4 and A8 are at the end of the network branches (located more than 600 meters from the transformer). Site A2, A4 and A8 were used to further investigate the variation of the voltage during this day. The time series of phase voltage, PV output power and net power consumption of Site A2, A4 and A8 are shown in Figure 55, Figure 9 and Figure 56, respectively. At the beginning of the day when PV generation is low, the voltage tended to move around the nominal value, following load variations. As the PV output started to increase, and the site started to export power (instead of importing), the voltage also rose, as depicted in Figure 9. Once the cloud came into play, resulting in ramp-ups and downs of the PV output, the net power of the site also changed. It can be seen that both load and PV output variations influenced the voltage at the sites. During periods with low load variation, the voltage at a site tended to follow the pattern of the PV generation of the site. Figure 10 zooms into a cloud event when the PV output reduced by about 5kW over one minute, which resulted in a change of 5kW in the net power (export) and a voltage drop from 257 V to 245 V. Comparing Figure 9 against Figure 55 and Figure 56 it can be seen that there are a large number of inverter trips occurring during the day in Figure 9 due to the high voltage at this site.

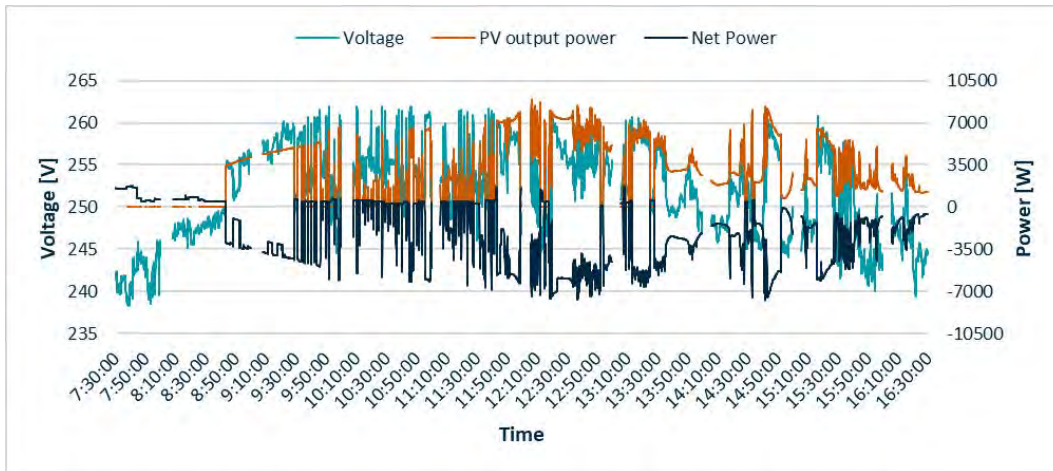


Figure 9. Voltage, PV output and net power of Site A4 on 22nd August 2019 (7:30 to 16:30).

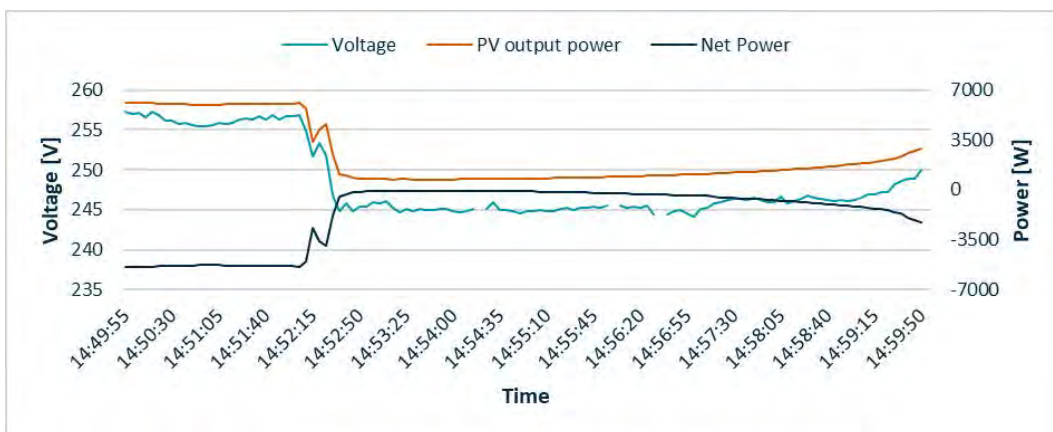


Figure 10. A zoomed view of Figure 9 showing the variation of voltage with PV output and net power.

In Network-B, four sites with PV systems were considered for the analysis. Figure 11 shows the voltages observed over the day for those four sites. The voltages varied with PV output, but within a small range, e.g., Site B2 and B3 varied between 233V and 246V.

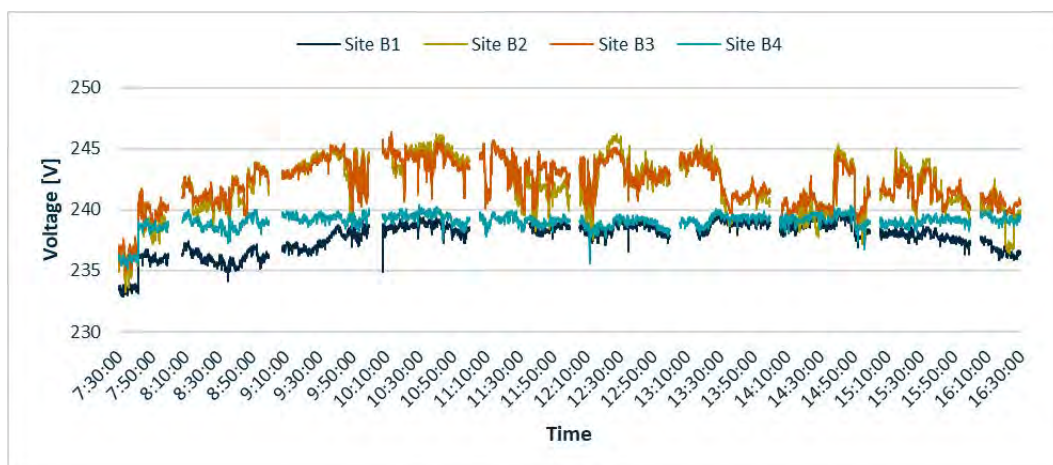


Figure 11. Voltage at the sites of Network-B on 22nd August 2019 (7:30 am to 4:30 pm).

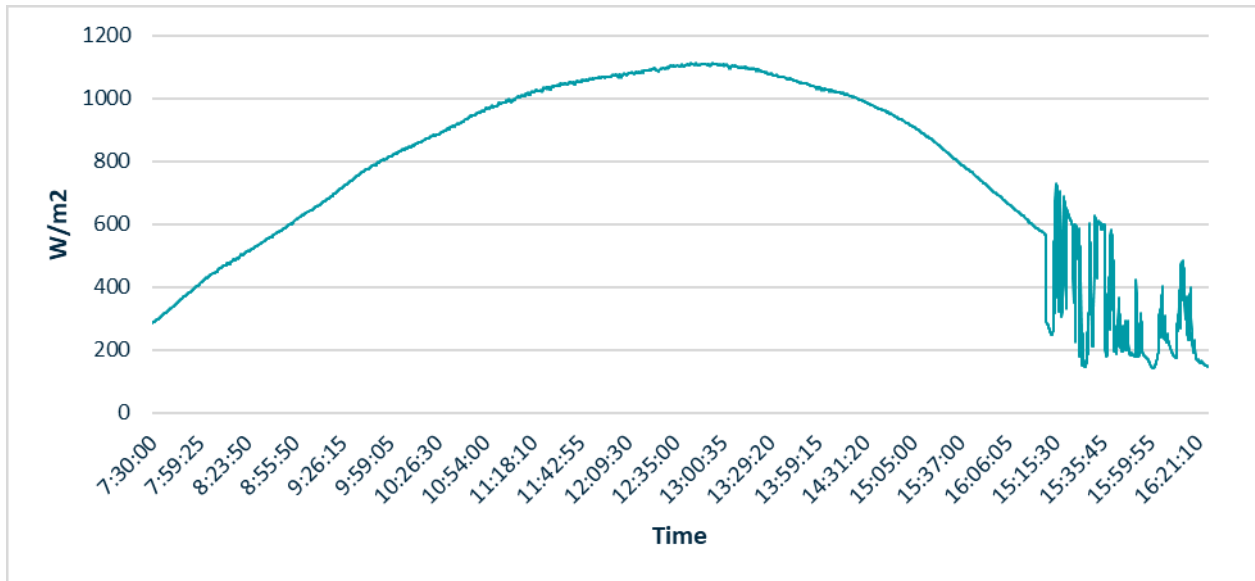


Figure 12. GHI on 31st January 2020.

4.2 Clear sky day

The GHI for 31st January 2020, the selected day with mostly clear sky conditions (some localised cloud shading was recorded for this day in the late afternoon at the irradiance monitoring site) is shown in Figure 12. The ranges of voltage variation over the day (from 7.30 am to 4.30 pm) on 31st January 2020 are presented in Figure 13. Site A4 again had the highest voltage variation on this day while Site A5 and A7 had very consistent voltage with a narrow range of variation, similar to the cloudy day.

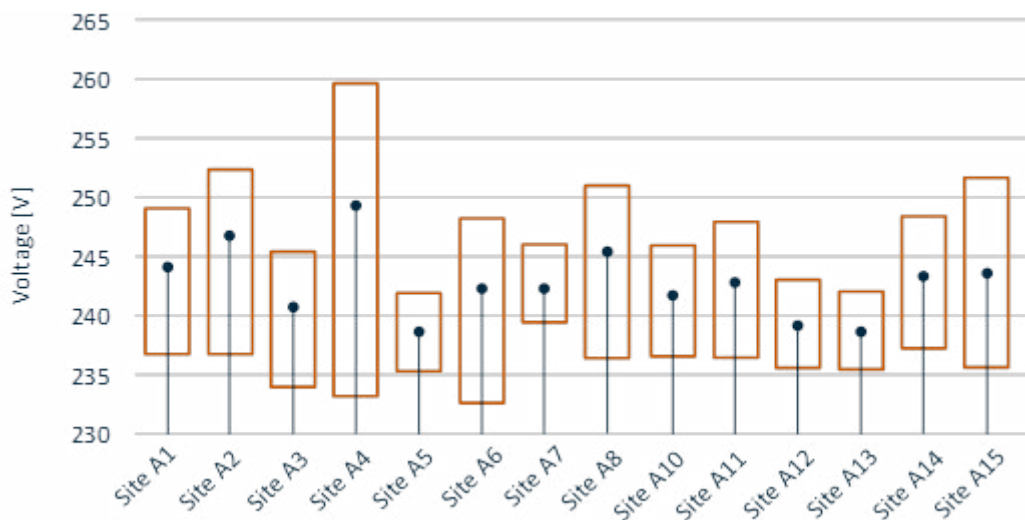


Figure 13. Ranges of voltage at different sites of Network-A on 31st January 2020.

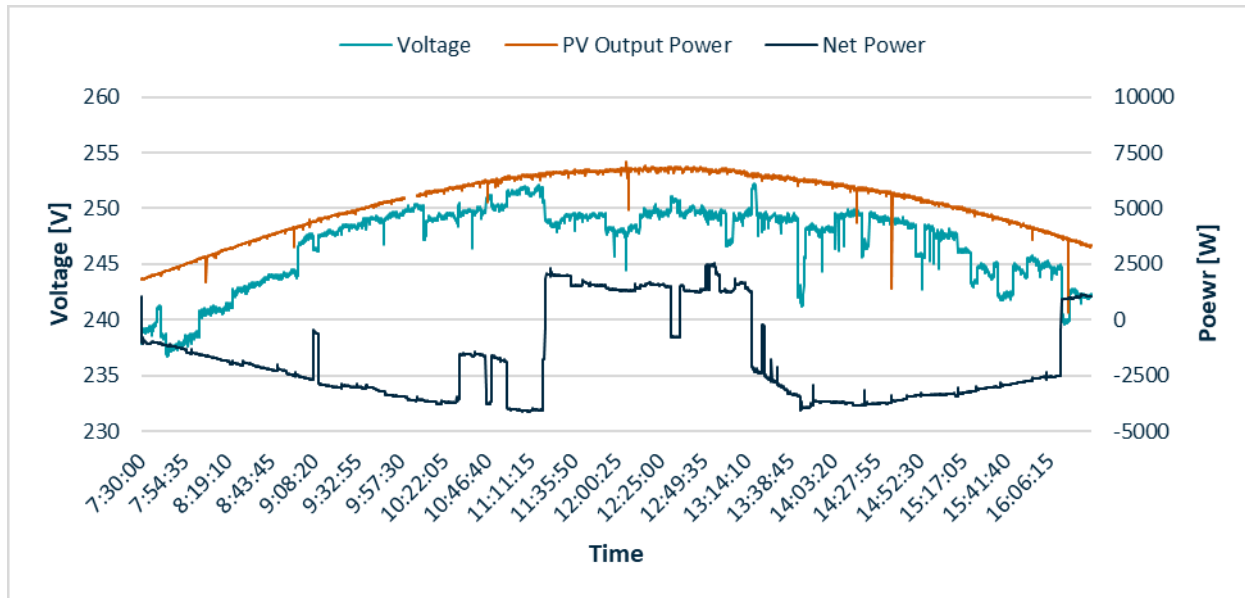


Figure 14. Voltage, PV output and net power of Site A2 on 31st January 2020.

The voltage, PV output and net power consumption of Site A2 are shown in Figure 14. In this case, it is interesting to observe that even though the PV output variation was low, there were some noticeable load changes, which were causing some voltage variation. The voltage variation for Site A4 is shown in Figure 15 where the voltage was generally following the PV output with some variations due to load changes, except during a period with suspected inverter trip events in the middle of the day. Figure 16 shows a zoomed view of such an event. At 11:59 am the inverter tripped, and the voltage dropped to 249V from 258V. Then, at 12:01 the inverter had reconnected, and the voltage went up to 259 V. After 5 minutes of persistent voltage around 258 V, the inverter again tripped, and the voltage dropped to 249 V. About two minutes later, the inverter had again reconnected, and the voltage increased to 257V.

The voltage, PV output and net power consumption of Site A8 are shown in Figure 56 in Appendix 2.

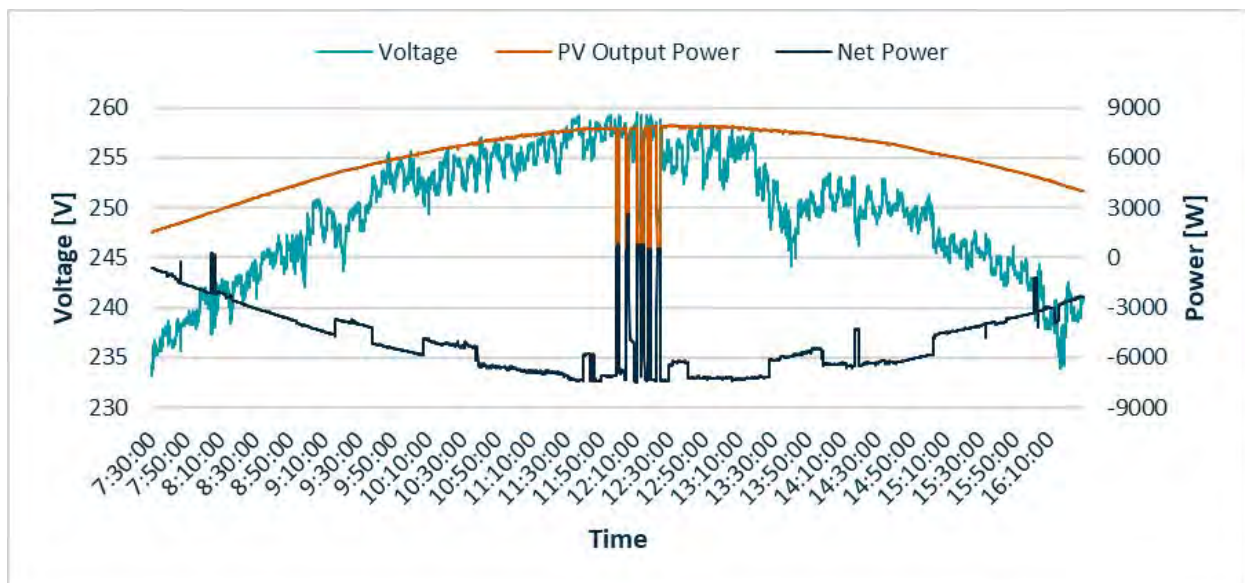


Figure 15. Voltage, PV output and net power of Site A4 on 31st January 2020.

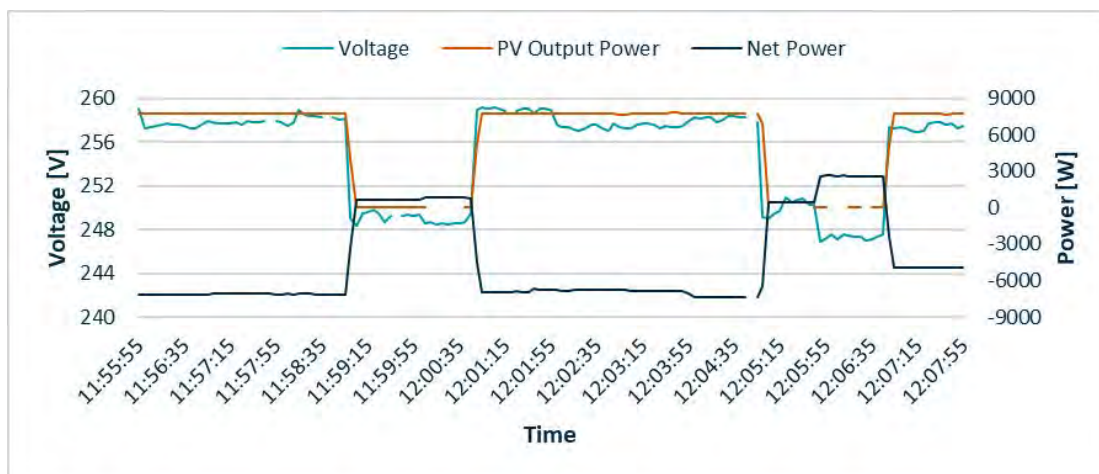


Figure 16. A zoomed view of Figure 15 showing the voltage variation with PV output and net power.



Figure 17. Voltages at the sites of Network-B on 31st January 2020.

The voltages of the selected four sites of Network-B are shown in Figure 17. The voltage generally followed the PV output of the system for all the sites. However, there was a rapid voltage increment at 9:00 and the voltage dropped at 13:22. These variations seem to be related to load changes at other sites on this network. Figure 58 and Figure 59 shows the PV output and net power of the four sites of Network-B.

The measurement of the voltages analysed in this study is not at the point of supply (i.e. it is not a Horizon Power network voltage), but a voltage measured within the customer’s switchboard, which is downstream of a lead-in cable that potentially exacerbates high voltage events. These voltages vary with the PV output power following the cloud events. However, the extent of the variation may depend on the simultaneous load variation, network topology, lead-in cable and distance from the transformer. Some sites were more prone to reaching higher voltages often (e.g., Site A4) compared to others. Inverter trips were observed during periods of higher voltages (e.g., higher than 257 V). These observations are aligned with the findings presented in (Moghbel et al. 2019). The adopted measures to mitigate voltage issues need to be selective and based on individual LV network behaviour. A review of load and PV generation balancing across phases and investigation of the inverter settings were recommended in (Moghbel et al. 2019). Horizon Power is already analysing the application of power quality response modes and phase balancing to mitigate voltage rise issues. An inverter settings audit on the respective network is also in place.

5 DER connection phase identification

Following the research by Murdoch University outlined in Section 4, which identified inverter trips caused by voltage rise, the Horizon Power project team started to explore the potential for reducing peak voltage events by physically rebalancing PV distribution systems across the network phases. The hypothesis being that by applying analytics to Advanced Meter Infrastructure (AMI) data to identify single-phase PV systems and their contribution to peak voltage events, some single-phase PV systems could be moved to other network phases to reduce peak voltage events. The project team used the SensorIQ product from Itron to collect synchronised 1-minute meter readings from 2600 meters across the town of Carnarvon. The period for data collection before commencing the phase identification process ranged from April 1, 2020 up to June 30, 2020, however, for reasons discussed in the following section, only 30 days of data (approximately) is required for the analysis. Details on how the data was analysed using constrained k-means clustering to develop a process to identify single-phase PV systems on the network and their impact upon system voltage at times of peak solar insolation are provided in the following section.

5.1 Algorithm motivation

Each meter and its phase or phases must belong to one of three phases in the network; this identifies the problem as a classification problem. In the beginning, the motivation to use the data to solve the phase identification problem came from the understanding that when the network is unloaded, the meters at each property become voltmeters. The meters can measure the voltage of the phase it is connected to, and any neighbouring meter (within proximity) on the same phase will experience a similar voltage or change in voltage. The following discussion provides an overview of the data preparation, the algorithm, the results from this classification and how it can be utilised to improve hosting capacity in the network.

Previously, a k-means clustering algorithm was developed and applied in Denham, Western Australia for phase identification of meters at properties. The k-means algorithm is given the number of groups to classify the data into and iterates over many guesses to determine the best representation of the data with respect to the chosen number of groups. Over time the algorithm begins to converge until it reaches a point where it can no longer make significant improvements to the combinations of groups. In the case of phase identification, the number of groups is set to three (one for each phase of the network), and the data for classification comes from the meter-phases (i.e. voltages). There is a concern, however, that this method neglects the fact that a three-phase meter cannot have two phases that are the same. For this reason, the constrained k-means algorithm is used in this investigation.

The addition of the constraint portion of the algorithm ensures that the three phases of each three-phase meter in the network are never assigned to the same phase. For example, a three-phase meter must have one phase connected to phase A, one to phase B and one to phase C. The difference between the constrained k-means algorithm and the standard k-means algorithm is that every time a classification of a meter-phase occurs, the other phases of that meter are checked to determine if they have already been included in that phase group. By having this comparison as part of the classification process, the algorithm can make a more accurate decision for which phase of the network to assign a meter-phase to.

5.2 Data preparation

The data source for this study is the Meter Instantaneous Data (MID) as recorded from the AMI meters installed at properties in Carnarvon, Western Australia. The MID offers one-minute interval readings of voltage and current for single and three-phase meters connected to one or all the three phases in the

Carnarvon network. The period for data collection was between 1st April 2020 and 30th June 2020. During this time data recording was switched from 15-minute intervals to one-minute intervals and to the best of our knowledge there were no major changes to the network.

This understandably led to large amounts of data that needed to be processed for use in this study. In total there were over 300 million data points belonging to 2,540 meters spread across Carnarvon. A copy of the raw data was stored on S3 in parquet format and was cleaned and stored (again) in CSV files using PySpark with six slave processors, each having four cores and 120Gb of RAM each (24 cores, 720Gb of RAM total). As part of the data cleansing process, the data was checked for missing data measurements and anomalies. Any small gaps were filled (gaps less than 3 minutes were imputed) and any abnormal measurements (average voltage greater than 300V or less than 180V) were removed. In addition, for the sample period considered it was decided to take only night-time data (less load and no PV generation), and the meter must have had at least 90% coverage otherwise there was not sufficient data to mathematically characterise an individual meter-phase.

The voltage deltas (changes) from one interval to the next for each meter-phase over a sample period were used as the input to the algorithm. The data was standardised using Z-Score normalisation to ensure that all variations in the data were represented on the same scale. Taking two principle components of each sample of voltage deltas for each meter-phase, the amount of data was reduced to a two-dimensional representation. This helped with computer processing limitations and visualisation. The classification had to occur in a timely manner and at the end of the classification, scatter plots of the two-dimensional representation of each meter-phase showed which group it was classified into.

Reducing the sample for each meter phase from thousands of voltage delta points over time to two principal components could have led to information loss. This means that the algorithm may not have been able to classify the meter phases. Therefore, several periods of data were examined to determine the potential for classification. Figure 18 displays the principal components of the meter-phase data for two sample periods; each point in the plots represents a meter-phase. The x and y-axis values resulting from the two principal components are dimensionless and serve to represent the differences between the sample data of each meter-phase. The plot on the left in Figure 18 demonstrates a set of meter phase data that may not separate into groups using the algorithm since it appears to be a single cluster. For the plot on the right, the data set exhibits a clear separation into three possible groups suggesting that it will be classified using the algorithm.

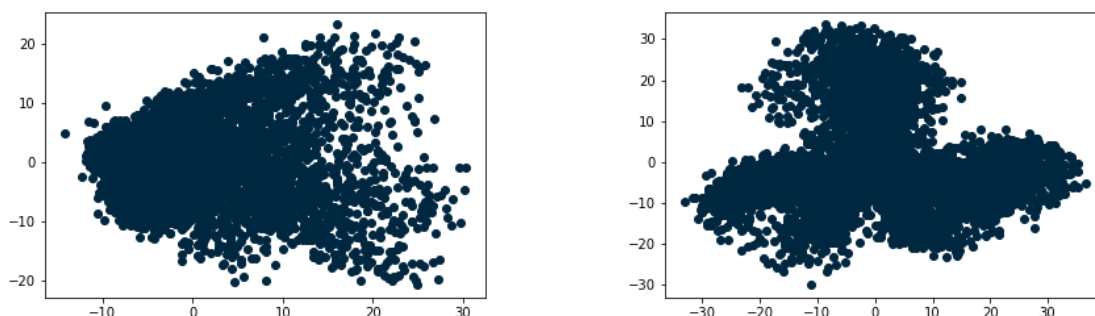


Figure 18. Principal Component representation of meter-phase data for two sample periods.

5.3 Clustering results

Using the above method for investigating each period of data, three sample periods were selected to perform the clustering (grouping) on. These periods were all from June 2020, and each period exhibited a similar shape to that shown in the right hand plot of Figure 18. Figure 19 displays the clustering results from the three sample periods selected from June 2020. Each cluster label (0, 1 and 2) is arbitrarily assigned

identifying points that belong to the same group. The position of each group (Top, Left and Right) represents the three phases A, B and C of the Carnarvon network. Using this information, it was then possible to map the assigned clusters for each sample period to the phase label A, B and C and evaluate the accuracy of the algorithm.

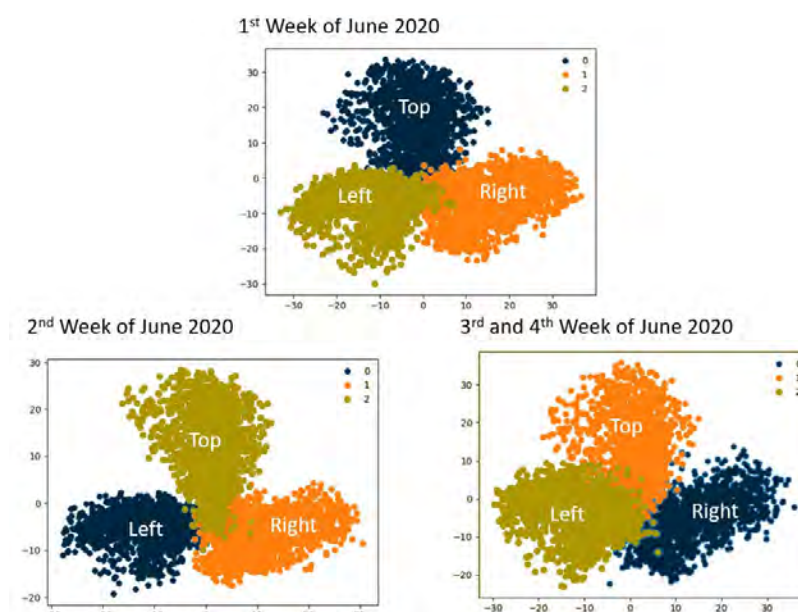


Figure 19. Clusters resulting from the algorithm for three sample periods in June 2020.

Table 1 outlines the overall results for the clustering of the meter-phases in Carnarvon and the results for the Gibson Street Feeder. In Carnarvon, there is obviously a mixture of single and three-phase meters as there are 2,540 meters but 5,514 meter-phases. Of this total number of meter-phases, the three sample periods for June were compared to investigate if the algorithm classified each meter-phase the same for each period (all agreement), for two of the periods (partial agreement) or for none of the periods (disagreement). For the three sample periods and all the meters that have MID in Carnarvon, there is 90.8% agreement. If the partial agreement was included the agreement for the algorithm rose to 99.6% for the whole of Carnarvon. A subset of the classification (using meters on the Gibson Street Feeder only) resulted in 100% agreement. This agreement across the three sample periods in June suggested that the results of the algorithm were consistent and that it is likely that for other sample periods, each meter-phase would be correctly grouped with meter-phases that are on the same phase in the Carnarvon network. It was also possible to compare some aggregates of the Gibson Street Feeder to improve the confidence in the results.

Table 1. Summary of Clustering Results.

	Carnarvon		Gibson Street Feeder	
Total Meters	2,540		36	
Meter-Phases	5,514		80	
All Agreement	5,010	90.8%	76	95%
Partial Agreement	485	8.8%	4	5%
Disagreement	19	0.4%	0	0%
Agreement	5,495	99.6%	80	100%

5.4 Aggregate comparison

The MID aggregated apparent power from the meter-phases was compared to the Gibson Street Feeder transformer per phase apparent power SCADA measurement. This provided a good comparison of the before and after view of the meter-phases on the network and the improvement in phase assignment by using the algorithm. Figure 20, Figure 21 and Figure 22 demonstrate increased correlation between the per phase SCADA measured apparent power and the MID aggregated apparent power resulting from the meter-phases after using the algorithm. The MID aggregate prior to the phase identification algorithm is shown in grey and the MID aggregate after applying the algorithm is shown in blue. One thing to note is that the MID phase labels A, B and C are arbitrary; the algorithm cannot determine if the phase labelled as A for SCADA is the same as the phase labelled A for MID; instead, the signals were matched based on their overall shape and correlation. This is not to say that the algorithm was wrongly classifying the meter-phases, just that the algorithm labelling process is random and does not have knowledge of the SCADA phase labels.

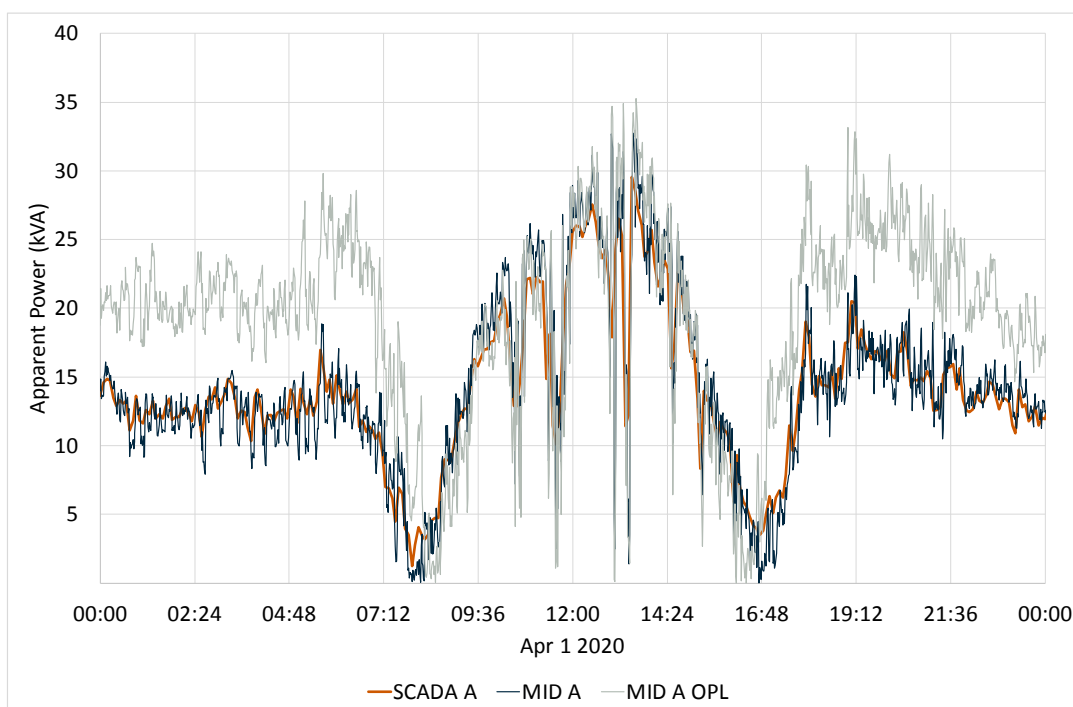


Figure 20. Gibson Street Feeder Phase A SCADA measured apparent power (SCADA A in orange), MID aggregated apparent power from algorithm assigned phases (MID A in blue) and apparent power from original phase labels (MID A OPL in grey).

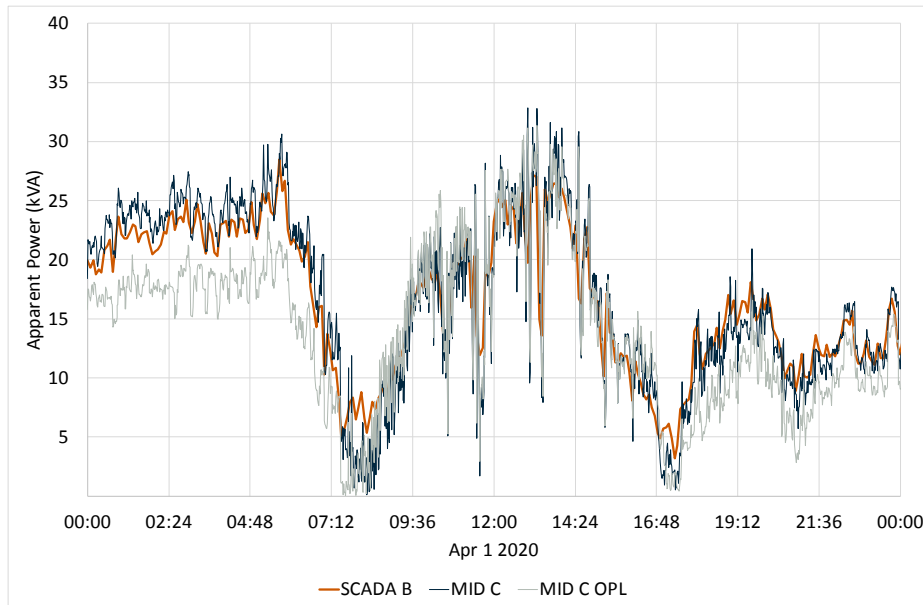


Figure 21. Gibson Street Feeder Phase B SCADA measured apparent power (SCADA B in orange), MID aggregated apparent power from algorithm assigned phases (MID C in blue) and apparent power from original phase labels (MID C OPL in grey).

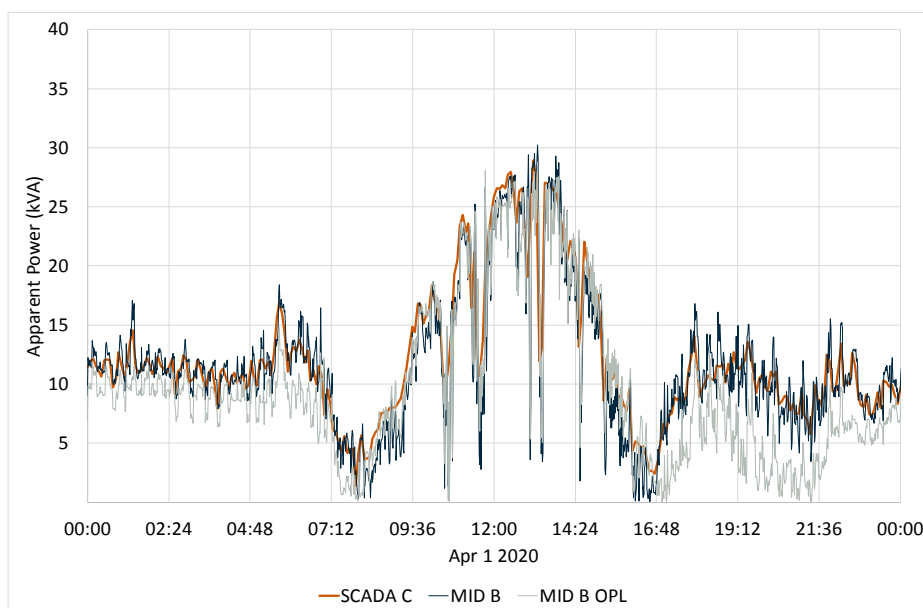


Figure 22. Gibson Street Feeder Phase C SCADA measured apparent power (SCADA C in orange), MID aggregated apparent power from algorithm assigned phases (MID B in blue) and from original phase labels (MID B OPL in grey).

5.5 Field inspection

The results of the phase identification algorithm have been used to determine which phases of the DER connected on the Gibson Street Feeder are ready for balancing across the phases with increased confidence. To check the real-world phases against those arbitrarily assigned by the algorithm, a linesman was sent out to each single-phase meter on the Gibson Street Feeder. This was necessary since the

phase labels of the algorithm, as previously mentioned, were arbitrarily assigned. The algorithm identified which meter-phases are on the same phase though it does not have knowledge of the physical network. The results from this inspection were used to locate the connection of the single-phase meters in the network and thus provided a reference for the phase labels A, B and C of the algorithm. In addition, it presented an opportunity to compare the field inspection results against assignment by the algorithm. Table 2 lists the field inspection phases, the phase label assigned using the algorithm and the original phase label recorded against each meter. The original phase label as listed shows that all meters were arbitrarily recorded as being connected to phase A, which was correct only some of the time. On the other hand, the assigned phase compared to the field inspection phase showed an agreement for 13 out of 14 of the single-phase meters. These results also indicated that Phase A corresponds to Red phase, Phase B to White phase and Phase C to Blue phase.

Table 2. Field Recorded Phases compared against Algorithm Assigned Phases.

Meter Number	Field Phase	Assigned Phase	Original Phase Label
1	Blue	C	A
2	Blue	C	A
3	Blue	C	A
4	Blue	C	A
5	Blue	C	A
6	Blue	C	A
7	Blue	C	A
8	Red	B	A
9	Red	A	A
10	Red	A	A
11	Red	A	A
12	White	B	A
13	White	B	A
14	White	B	A

The property for which the algorithm appeared to be incorrect (meter number 8) was then investigated at the signal level to confirm the result. By changing the phase of the meter in the algorithm assignment, the MID apparent power was aggregated again and compared against the SCADA measured apparent power for both scenarios (algorithm and field inspection). Figure 23 indicates that changing the MID aggregation from the results of the algorithm to the results of the field inspection, resulted in the apparent power significantly differing from the SCADA measured apparent power. A large portion of the Phase B MID aggregated apparent power was shifted to Phase A in the field inspection scenario, suggesting that in this case meter number 8 belonged to Phase B as assigned by the algorithm.

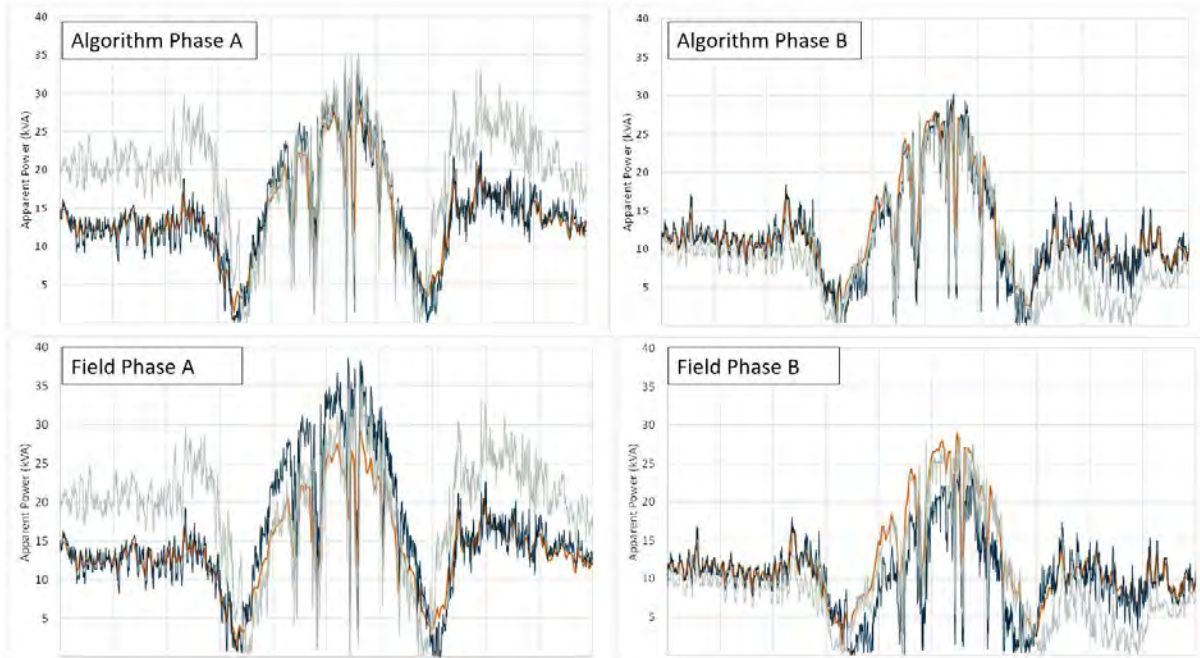


Figure 23. Algorithm assigned phase compared with field recorded phase labels. SCADA measured apparent power (orange) and MID aggregated apparent power (blue).

In addition to the comparison of the per phase apparent power, the meter voltage for the same period could be observed for meter number 8 (Table 2) and compared to other meters on the algorithm assigned phase B, as shown in Figure 24. In Figure 24, the ‘field inspection – Phase A’ diagram compares the voltage signal of meter number 8 against three three-phase meters connected to Phase A, while the ‘algorithm assigned – Phase B’ diagram compares the voltage signal of meter number 8 against the same three-phase meters for Phase B. From these two comparisons, it seems that the voltage signal of meter number 8 had a better correlation with Phase B than with Phase A (Phase B being the result of the algorithm assignment).

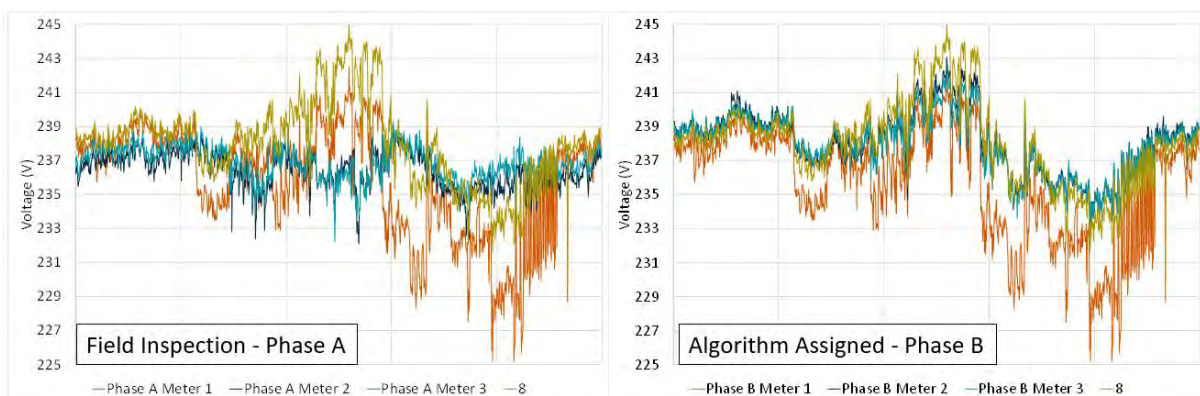


Figure 24. Comparison of voltages for meters on Phase B with meter number 8 from Table 2. Meters 1, 2 and 3 are labelled for the purpose of this figure and are unrelated to the meter numbers of Table 2.

Following up with the linesman in the field it was decided that the connection for meter number 8 would be checked a second time. On re-inspection, the connection for this meter was confirmed as being connected to phase B – white. This means that for this small sample of 14 single-phase meters, the algorithm achieved 100% accuracy.

5.6 Improving hosting capacity

As mentioned, the main goal for the phase identification was to be able to determine how much DER was on each phase as some of the inverters were tripping due to overvoltage. For ease of changing the balance between phases in the network, only single-phase meters with DER were considered. Figure 25, Figure 26 and Figure 27 provide a comparison of maximum voltage and the contributing current from each meter experienced on the spurs connected to the Gibson Street Feeder. For one of the spurs of Phase A there was a much higher voltage that may be attributed to an unmanaged DER injecting a large current into the grid (Figure 25). The property generating this large current had a single-phase meter connected to Phase A only. Given the lower voltage on Phase C for this area of the Gibson Street Feeder, it was suggested that this DER and meter be moved from Phase A to Phase C in an attempt to lower the voltage on Phase A (Figure 25 and Figure 26). In addition, Phase B already had a large current being injected onto the grid within proximity, so it was thought that shifting to Phase B would only shift the problem from Phase A to Phase B (Figure 26). Note that while there was large current injected onto the grid at the property on the right in Figure 25, the voltage of each of the phases in Figure 26 and Figure 27 was not as high.

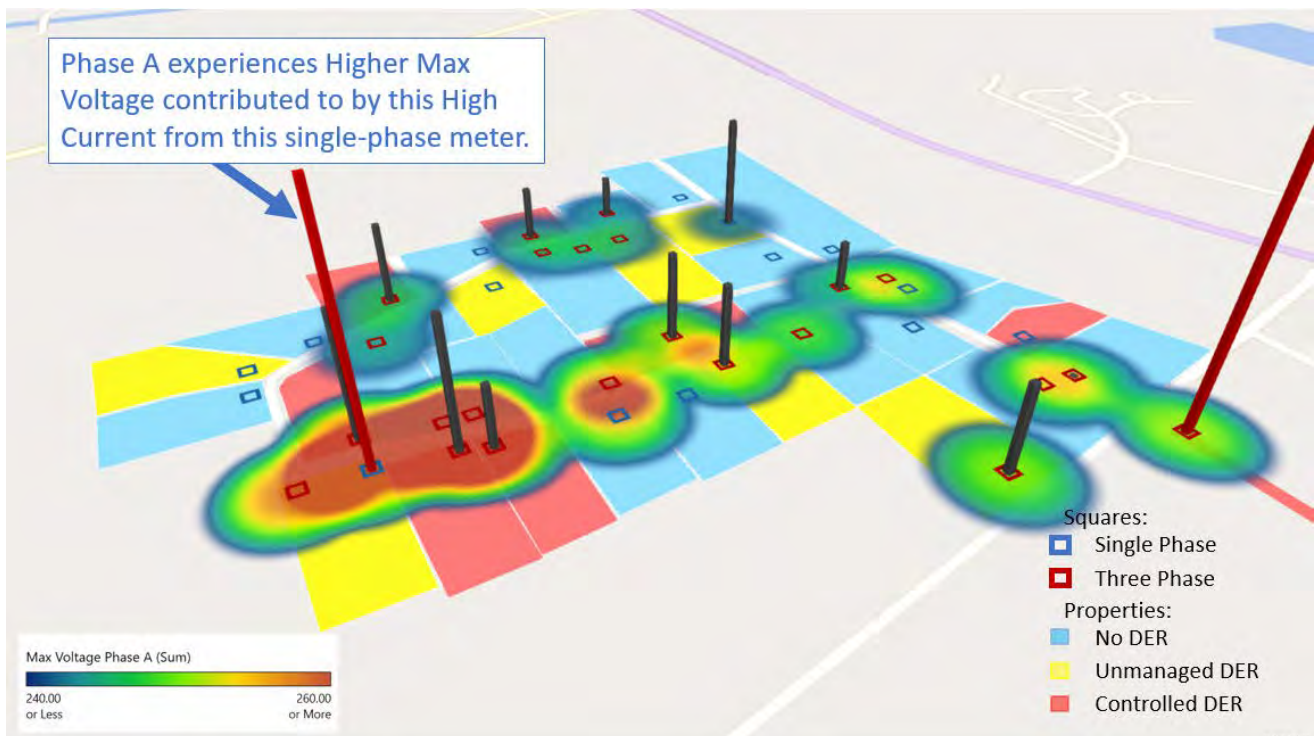


Figure 25. Max voltage heat map and current (bars) for properties connected to Phase A of the Gibson Street Feeder.

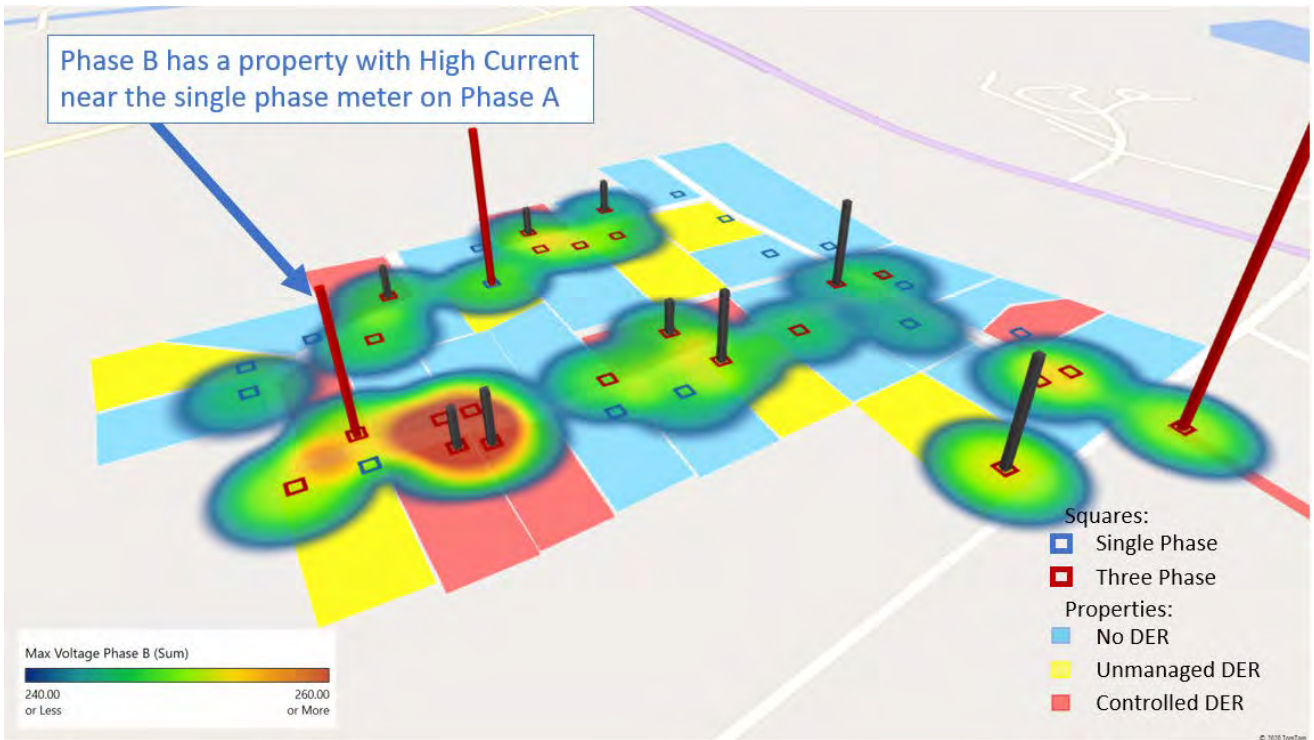


Figure 26. Max voltage heat map and current (bars) for properties connected to Phase B of the Gibson Street Feeder.

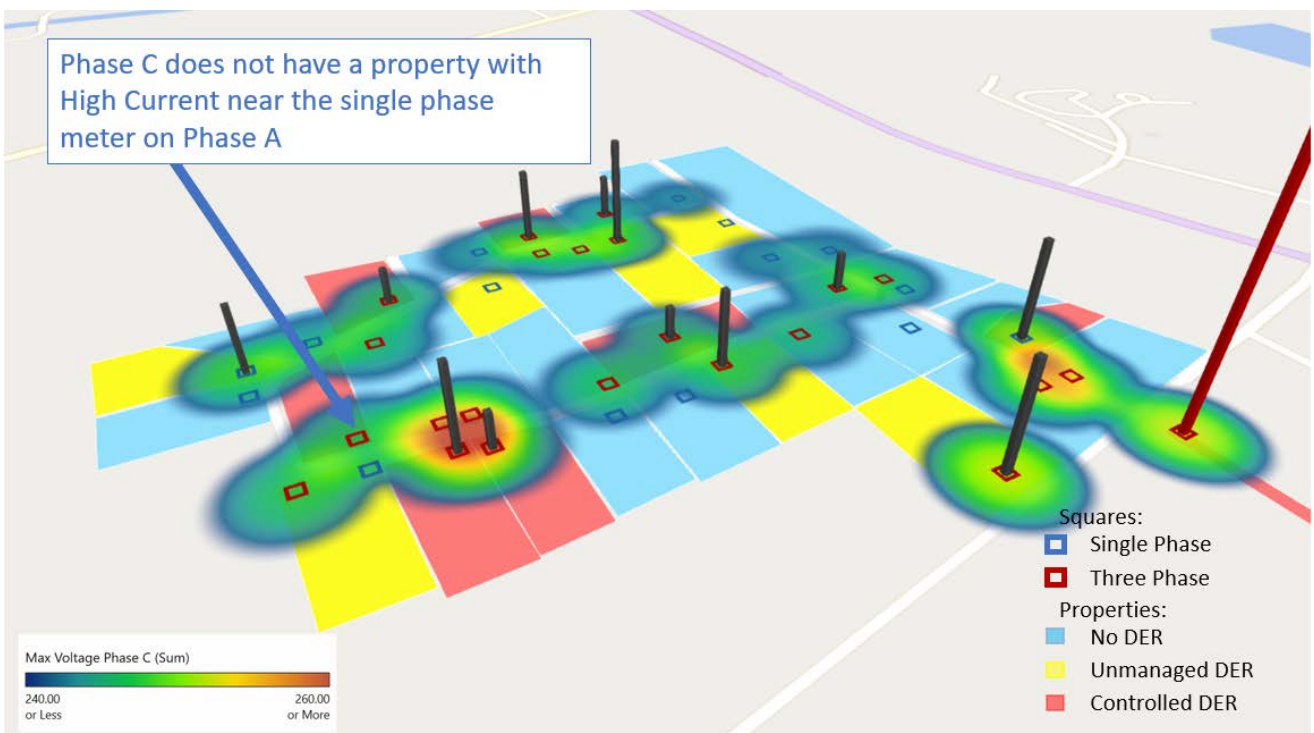


Figure 27. Max voltage heat map and current (bars) for properties connected to Phase C of the Gibson Street Feeder.

Table 3 identifies high maximum voltages of meters within proximity of the high current meter on Phase A prior to the shift (Figure 25) and the resulting voltages after the change to Phase C. The meter numbers are not related to the meter numbers previously used in Table 2, instead, these meter numbers are for reference within Table 3 (and Table 4). The phase change reduced the maximum voltage on Phase A from 259.7 V to 253.3 V, however it increased the maximum voltage on Phase C from 247.5 V to 257 V. This was unexpected given that the maximum voltage on Phase C was 247.5V before the phase change. This exercise also confirmed that it was possible to shift single-phase DERs with high current from one phase to another to lower the voltage on the network.

Table 3. Maximum voltages near meter number 1 with high maximum voltage on Phase A to be shifted to Phase C.

Phase A – Red				Phase C – Blue			
Meter Number	Before	Meter Number	After	Meter Number	Before	Meter Number	After
1	259.7	2	253.3	3	247.5	1	257
2	259.1	3	253.1	5	246.6	5	255.4
3	258.8	5	253	7	246.2	4	255.2
4	258.2	4	252.3	4	246.1	3	255.1
5	257.7	6	252	2	246.1	2	255
6	257.6	7	251.7	8	246	7	254.5
7	256.9	8	249.8	6	245.8	6	254.5

The next single-phase DER and meter to be considered for movement is highlighted in Figure 28, this meter will be referred to as meter number 9. Meter number 9 had a medium to high current and is positioned near a node that connects to the spur for meter number 1 from Table 3. It was hypothesised that this DER could have been contributing to a higher voltage at the node which led to an increase in the voltage at the end of the line on Phase C (near meter number 1). Table 4 outlines the maximum voltages for a period following the shift of DER and meter number 9 from Phase C to Phase A. The maximum voltage for Phase A has remained within range, lowering from 253.3 V to 252.2 V while the Phase C maximum voltage has dropped from 257 V to 254.5 V. Through shifting these DERs and meters between phases, the outlook for reducing overvoltage caused by DER is improved.

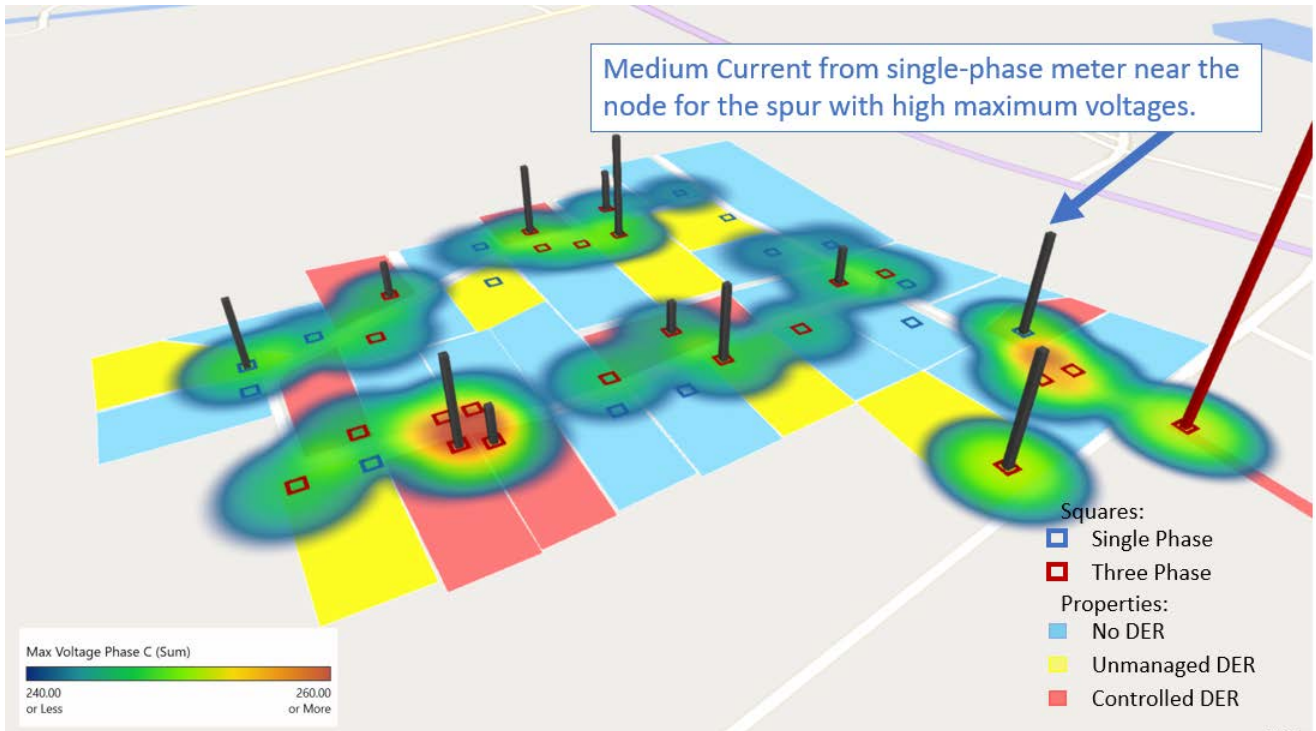


Figure 28. Max voltage heat map and current (bars) for properties connected to Phase C of the Gibson Street Feeder.

Table 4. Maximum voltages comparison for meter number 9 shifted from Phase C to Phase A.

Phase A – Red				Phase C – Blue			
Meter Number	Before	Meter Number	After	Meter Number	Before	Meter Number	After
2	253.3	2	252.2	1	257	10	254.5
3	253.1	3	252.2	5	255.4	11	254.4
5	253	5	251.6	4	255.2	1	253.7
4	252.3	4	251.2	3	255.1	4	252.8
6	252	6	251.1	2	255	3	252.8
7	251.7	7	250.7	7	254.5	5	252.3
8	249.8	9	250.1	6	254.5	2	252.2
12	248.9	8	249.6	9	250.8	6	251.9

6 Carnarvon inverter audit

Due to the nature of Horizon Power networks i.e. isolated and non-interconnected, Horizon Power has a range of prescribed inverter settings that differ from the rest of Western Australia. These settings have been developed over time to ensure that PV systems can operate reliably in the conditions that are often unique to isolated power systems, which experience a wider range of frequency and voltage conditions compared to larger and firmer power systems. Horizon Power's inverter settings are prescribed in the technical requirements that form part of the customer connection agreement. It is the installer's, and by extension, the customer's responsibility to ensure that these settings are programmed into the inverter at the time of installation, and the customer is left with a compliant PV system.

In response to Murdoch University's findings outlined in Section 4, which revealed inverters tripping multiple times a day, and after close inspection of the Wattwatcher data of the trial participants, the project team concluded that many of the legacy PV systems in the town were not behaving as expected. To determine if inverter settings were playing a role in the dysfunctional operation, the Horizon Power project team undertook an audit of residential and commercial PV systems in Carnarvon. Approximately 135 inverters have been audited at the time of writing and checked for compliance with Horizon Power's technical requirements. The process and results of this audit are shown in the following sections and are being used to improve DER connection approval processes.

6.1 Inverter audit methodology

The inverter audit process involved the following three main steps:

1. Identify which standard applies to the inverter under audit in accordance with Horizon Power's superseded technical requirements or the revised technical requirements post-July 2019. Table 5 demonstrates the progression of the technical requirements settings that Horizon Power has implemented with the revision of the AS4777 standard. In addition to the settings requirements, the post-July 2019 requirements need to comply with the Feed-in Management (FiM) requirements, as shown in Figure 29.

Table 5. Horizon Power technical requirements inverter settings.

Settings	Technical Requirements				
	Pre-2015	2015		2019	
	Limit	Limit	Delay	Limit	Delay
Under Frequency (Hz)	46.5	46.5	1s	45	1s
Over Frequency (Hz)	53	53	0s	53	0s
Frequency Reconnect Min (Hz)	x	47.5	60s	47.5	60s
Frequency Reconnect Max (Hz)	x	50.15	60s	50.5	60s
Under Voltage (V)	190	190	1s	180	1s
Sustained Overvoltage (V)	x	255	10 min	258	10 min
Over Voltage 1 (V)	x	x		260	1s
Over Voltage 2 (V)	265	265	0s	265	0s
Voltage Reconnect Min (V)	x	253	60s	216	60s
Voltage Reconnect Max (V)	x	216	60s	253	60s
Ramp Rate	x	Enabled		Enabled	
Volt-Watt Response Mode	x	Enabled		Enabled	
Volt-Var Response Mode	x	X		Enabled	
Hz-Watt Response Mode	x	Enabled		Enabled	

FIM (Class 3, Basic and LV EGI)	
Check	Complies?
Comms enclosure present.	Yes / No
Gateway device is housed in comms enclosure.	Yes / No / NA
Dimensions of enclosure must be approximately H:200mm, W: 200mm, D: 200mm.	Yes / No
Enclosure must be IP24 rated or higher, dependant on local conditions.	Yes / No
Enclosure must be suitably UV rated and non-transparent.	Yes / No
Enclosure must be located in a safe and accessible location near inverter.	Yes / No
Enclosure shall be screw sealed or hinge lockable.	Yes / No
GPO Installed adjacent to comms enclosure and is labelled "SGD Power".	Yes / No
Enclosure is labelled "Inverter Comms".	Yes / No
Enclosure shall be within 1m distance from inverter.	Yes / No
Enclosure shall be positioned more than or equal to 1200 mm from ground level.	Yes / No
<p>Ensure that all communications from the inverter(s) shall be terminated inside, including DRED and MODBUS TCP connections. The installer shall also ensure any AS/NZS 4777 DRED adapters required are installed either inside the inverter or in the enclosure, with final DRED connections terminated inside the box.</p> <p>If the Proponent intends to also connect the inverter directly to their LAN, the Proponent shall ensure this is done only if a suitable additional network port or Wi-Fi connection is available. The primary inverter Ethernet connection must be connected to a terminated socket inside the Inverter Comms enclosure.</p> <p>Where the Proponent installs multiple inverters, all of the communications from each inverter shall be brought back and terminated within the box.</p>	Yes / No

Figure 29. Feed-In Management (FiM) requirements checklist.

2. Complete the relevant checklist for compliance across the following categories:

- Site Safety – checking for safety of the installation
- Site Photos – the inverter name plate details to be confirmed with Horizon Power’s records
- Device Measurements – taken from the inverter to determine whether voltages and power flows are acceptable
- Inverter Settings – used to determine the passive anti-islanding, ramp rates, voltage and frequency response modes for solar and battery inverters
- Feed-in Management compliance – checks for FiM compliance for Class 3, Basic Micro and LV EG systems. The FiM compliance checklist can be located in Figure 29.
- Solar Smoothing Battery – determine battery health

3. Classify each system as having passed, failed or incomplete as shown in Table 6.

Table 6. Classification of results.

Classification of Results		
Passed	Incomplete	Failed
<ul style="list-style-type: none"> All relevant information is provided for the 6 categories, if applicable, and complies with HP standard. 	<ul style="list-style-type: none"> The provided information is compliant; however, there is information missing i.e. setting parameters – voltage/frequency limits, delays etc. Inverter password is unknown by customer or installer and hence no settings were provided. 	<ul style="list-style-type: none"> Information provided does not comply with the Horizon Power standard in force when the system was installed. Safety issues on site. The system does not meet the FiM requirements. Inverters settings not configured at all.

6.2 Audit results summary

As outlined in Table 7, out of the 135 systems, 2 systems passed, 83 systems failed and information received for 50 systems was deemed to be incomplete. Table 8 provides details of the issues that were identified during the audit. The results indicated that inverter grid setting configuration such as incorrect passive anti-islanding and inverter response mode settings were the most common reasons for systems to fail the audit. For the systems installed post-July 2019, 34 did not meet the FiM requirements (see Figure 29). The main requirements from the checklist that are considered essential by Horizon Power are the presence of a GPO, comms enclosure and that the comms to the inverter are appropriate.

The degree to which systems failed to meet Horizon Power’s FiM requirements ranges from zero compliance i.e. the installer did not consider FiM at all, to systems with one or two FiM requirements missing such as a GPO or communications enclosure either missing or not to Horizon Power’s specifications. The systems with zero FiM compliance highlight a larger problem, specifically that installers active in Horizon Power’s service area are not familiar with Horizon Power’s requirements and are installing systems that are non-compliant.

The electricians contracted for the audit were unable to provide the frequency and voltage reconnect parameter delays for a large number of the systems inspected. Horizon Power’s requirements state that the delays should be set to 60s, but they were seldom programmed into the inverters.

Forgotten or lost passwords was an issue frequently identified throughout this audit. The auditors were unable to access 13 inverters because the passwords were not available. They were also unable to access the settings for 23 inverters, with two due to firmware issues, five due to the inverters being faulty and 16 due to the age of the inverter.

One observation made is that some older inverters have been replaced due to age related failure but there is no record of the replacement date. These systems have been installed without FiM but because the replacement date is not on record, Horizon Power cannot determine which of the technical requirements in Table 5 applies to them. If they were installed post-July 2019, then they have failed to meet the FiM requirements.

The settings in some brands of inverters are only accessible by the manufacturer. In addition to lengthening the time taken for obtaining the settings, not all settings were provided by the manufacturer and those that were provided were delivered in a format that made it difficult to compare with Horizon Power's standards.

Overall, the results from the inverter audit indicate there is a problem with the installation of inverters in Horizon Power's system, particularly with inverter settings and FiM compliance.

Table 7. Results summary.

Results Summary	
Pass	2
Fail	83
Incomplete	50
Total	135

Table 8. Detailed audit results including failed and incomplete systems.

Requirement	Number of Inverters			Total			
	Disabled	Missing ⁶	Incorrect				
Under Frequency	0	5	44	49			
Over Frequency	0	3	48	51			
Frequency Reconnect Min	0	19	12	31			
Frequency Reconnect Max	0	18	30	48			
Voltage Reconnect Min	0	16	33	49			
Voltage Reconnect Max	0	16	19	35			
Sustained Overvoltage Parameter	0	9	28	37			
Overvoltage V1	0	2	42	44			
Overvoltage V2	0	6	24	30			
Under Voltage	0	6	16	22			
Voltage – Watt Response Mode	5	22	11	38			
Volt – Var Response mode	8	13	14	35			
Hz – Watt Response Mode	9	25	15	49			
Ramp Rate	5	10	9	24			
Missing/Forgotten Passwords	13						
Inverter left on Manufacturer’s Factory Defaults (no AS4777)	4						
FiM Compliance	GPO		Enclosure	Inverter Comms	Other Requirements	Missing Info	Total
	28		31	29	28	6	34
Settings not possible to retrieve/access	Firmware Issues	Faulty Inverter	Old Inverter		Total		
	2	5	16		23		

⁶ Information was missing from the auditor check list which could by extension mean it was not programmed into the inverter or irretrievable.

Table 9. Safety issues.

Safety Issue	Count
Roof Top Isolator – Facing up the roof (exposed to weather conditions)	4
DC Bus voltage too high (>600V)	1
Inverter exposed to direct sunlight	1
Top Entry into inverter DC isolator	1
Conduit Labelling	3
No Export limiting devices	2

7 Visibility & control of Solar PV

7.1 Overview of the Carnarvon Trials 1 and 2 experiments

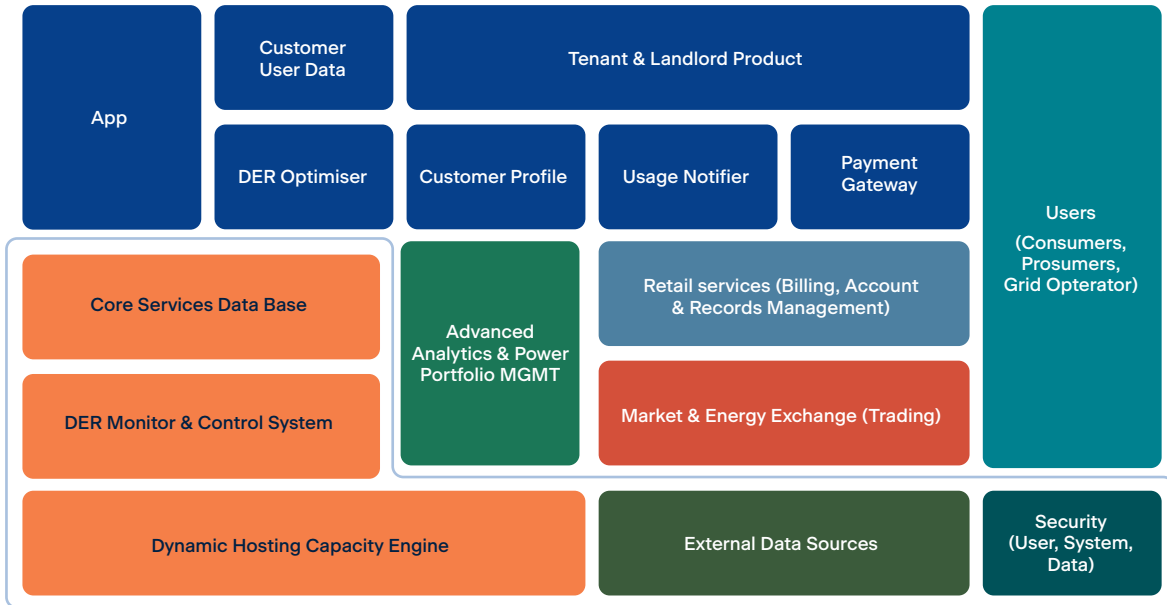
The Carnarvon DER Trials used battery/PV systems installed in 2018/2019, which have Reposit boxes that facilitate communications with and control of these new systems by Horizon Power. Trials 1 and 2 tested various aspects of these systems to determine the adequacy of DER, in a broader sense, to provide ancillary services in addition to supplying power when DER penetration increases or in an islanded microgrid mode. The trials covered pre-requisite functions, basic control of an individual node and basic control and administration of VPPs. Table 10 and Table 11 summarise the experiments that were carried out for Trials 1 and 2.

The Carnarvon trials were designed to test the control of embedded generation (EG) installed in the LV networks around Carnarvon. The trials predominantly focus on the Gibson St microgrid with a high penetration of PV and new PV/battery systems that form a VPP. Part of the trials included a large number of tests involving VPPs. Time to respond (latency (L)), ramp rates (RR) and how accurately does the system achieve the desired setting or setpoint (A) are recurring themes in a number of the tests and are important considerations from a system control point of view.

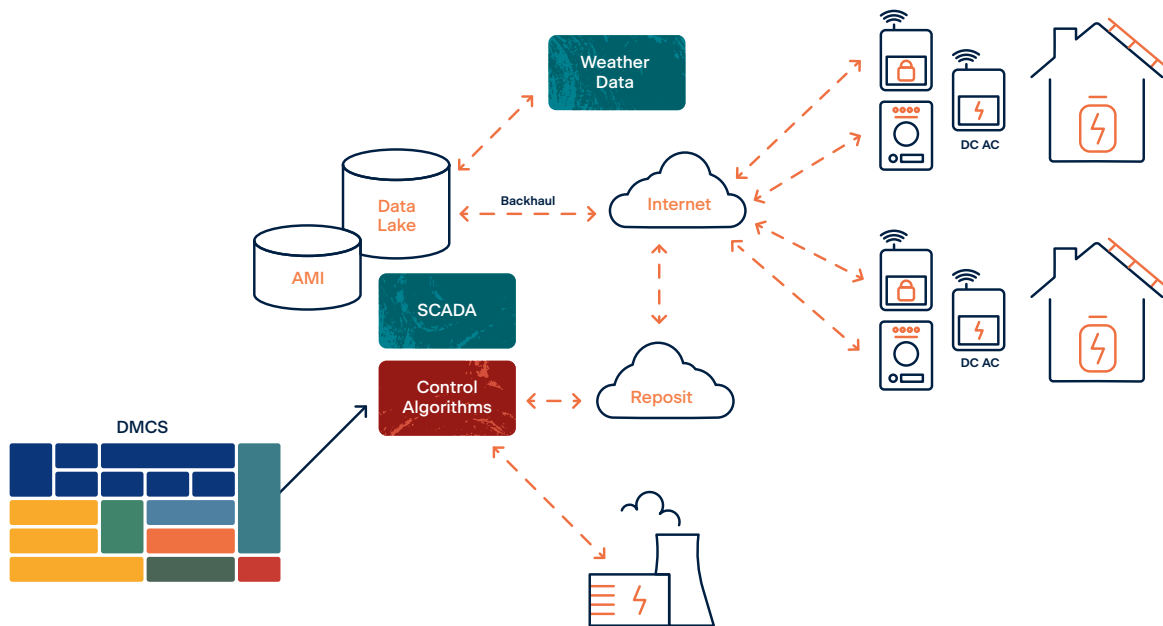
Table 10 describes tests of basic functionalities of the Reposit systems that are the pre-requisite capabilities to facilitate the higher functions enabling control of DER. These tests examined the acquisition and quality of the data and the time taken for the data to appear, particularly into the Core Services database and the Reposit cloud and Wattwatcher cloud services. The Core Services database is where DER Management and Control System (DMCS) ingests data from SCADA and the Reposit API to control VPPs and DER. Figure 30 shows the DMCS architecture, with only the sections contained within the red border built, completed and used in the Carnarvon trials for the Reposit/DMCS control system. Loss of communications and its effect on VPP operation were also examined. Of importance was that the VPP behaves in the desired manner, which is, the net export power adjusts to a Reposit node setpoint within 5 minutes. The last series of experiments in Table 10 looked at the effect of the Reposit system on prosumer internet service data volumes.

Table 11 includes the Trials 1 & 2 experiments that examined the basic operation of DER control. The Battery control series of experiments tested direct control via battery dispatch. This was followed by a series of experiments concerned with VPP configuration and control testing for correct VPP operation. The VPP Configuration and Control test and the Feed-in Management (Export Limit) test go to the Reposit product's core as an attractive solution to DER from the prosumer and network operator perspective.

A further experiment investigated the Reposit's Grid Credit system and whether this can be reliably used to reward customers for ancillary services provided by their DER (such as a behind the meter activity like reducing load during the peak period by discharging a battery). Finally, a series of experiments around primary inverter control functionalities (DER network support) and specifically the Volt-VAr response mode to mitigate voltage rise was also performed.



(a)



(b)

Figure 30. DMCS – Repost control architecture. (a) DMCS stack with the sections contained within the red border having been built, completed and used in the Carnarvon DER trials. (b) DMCS stack in the overall control scheme.

7.2 Summaries and observations of the Carnarvon Trials 1 and 2 experiments

Table 10. Carnarvon trials covering the basic functionality of the Reposit control systems and data acquisition systems.

Experiment	Description	Key Findings	Comments and Observations
Data Visibility (Trinkl 2020a)	A series of experiments ensured the data (V, I, P, Q, S & frequency for all phases) from both WW and Reposit devices is available in the appropriate locations (CS DB, WW & Reposit customer portals) and the amount of missing data is quantified. 10 WW and 10 Reposit participants were randomly chosen for this experiment. The WW and Reposit data should appear correctly timestamped in the Core Services database, and the most recent data should be no more than 6 minutes old. (L) The experiment also verified supplementary data visibility in the CS DB (weather data, sky camera images, AMI data from the Gibson St feeder and SCADA data from the HV feeders in Carnarvon). The experiments were performed over three days (07-09/05/2019) based on data from each data source for at least one week.	<p>Most of the data was gathered and stored correctly in the CS DB, visible in the associated online portals and available from CS DB within 5 minutes. Further findings included:</p> <ul style="list-style-type: none"> • The GHI data from the weather station was corrupted, and there was missing and duplicated weather parameter data. Uncorrupted and missing data could be retrieved from the online portal of the weather station and re-inserted into the CS DB. • On average, 16-17% of the WW data was missing from the downloaded dataset which led to an investigation into the reasons for this; it is suspected that the missing data is associated with a service downtime due to a maintenance event. • On average, 0.1-4.5% of Reposit data was missing with the Battery State of Charge parameter being associated with the highest amount of missing data (7.2-8.1%). 	<p>The series of experiments provides an insight into data quality and visibility of the data sources used for the trials. The findings are limited as the data sets investigated for each source were analysed for periods ranging between one week and one month.</p> <p>The report also suggests a minimum data requirement suitable for DER visibility and Feed-in Management and voltage control as follows:</p> <p>5-minute resolution values of real and reactive power flow (preferably both gross and net generation) and voltage.</p>

Experiment	Description	Key Findings	Comments and Observations
<p>Loss of Communications (Trinkl 2020b)</p>	<p>A series of experiments looked at the loss of communications on a VPP. The response of curtailed PV systems during the loss was checked to ensure the system moves in a controlled manner to the default setting and within 5 minutes. Another aspect of these experiments was whether 14 days of data is logged within the Reposit box and returned once communications are restored. (L, RR & A)</p>	<p>The trial showed that the default setpoints were reached in case of communication loss upstream from the Reposit Box or secure gateway device at the customer property. This was however not the case for all inverters, once onsite communication failure occurred downstream from the Reposit Box to the inverter (e.g. a disconnection of the Ethernet cable between the Reposit Box and the inverter).</p> <p>During the trials, systems responded within the required time of 5 minutes, ramped within the required rate of 16.66% per minute and achieved the setpoint within the required margin of error of 10%. The experiments also confirmed that at least 14 days of data is stored locally when communications are lost to a Reposit box.</p>	<p>The experiment led to the following recommendations with regards to mitigation strategies of communication failure occurrences downstream from the Reposit Box:</p> <ul style="list-style-type: none"> • Mandating the communications cable installation in conduit and ensuring that it is not possible to unplug the communications cable without partially disassembling the system. • Requiring DER systems to be feed-in manageable at all times or otherwise can be disconnected by HP. The VPP dashboard allows for monitoring connectivity between Reposit Boxes and inverters. <p>The downstream loss of communication (between the Reposit Box and inverter) in feed-in managed systems is addressed in new standard requirements under Section 6 DR AS/NZS 4777.2:2020 (Generation control function). For example, if the generation control function is enabled, any loss of signal shall cause the inverter (or multiple inverter combination) to operate at the soft export limit (if activated) within 15s.</p> <p>A smooth ramp-down cannot be guaranteed (as the energy source may cease, i.e. the irradiance may drop during the ramp down). Even though a widespread communication failure is considered unlikely, generally a smooth ramp down is desirable. It is therefore suggested to review the proposed response times in Section 6.1 in DR AS/NZS 4777.2:2020 (15s (soft limit) and 2s (hard limit) respectively) to determine their appropriateness for microgrid operations and whether to include ramp rate limits while the generation control function is enabled and a loss of signal occurs.</p>

Experiment	Description	Key Findings	Comments and Observations
Customer Internet Connection (Trinkl 2020c)	A series of experiments measured the amount of data traffic used by the Reposit box and curtailment signals sent by HP. This is of concern for Horizon Power in light of the fact that a large number of networks are in remote locations where internet services are expensive. Furthermore, the experiment sought to establish if using the customer's internet connection to gain control of DER is a reliable and safe method for communication.	An availability, based on time, of 98% was achieved by analysing connectivity data for all 17 Reposit boxes collected from the time of their installation (this corresponds to an analysis period of approx. 1 month, from April to May 2019). Three instances of an outage of more than 24 hours occurred (38, 102 and 274 hours). Excluding these instances, the average availability was 99%. Average data usage was 321 Mb per month per Reposit Box based on the data collected for one month from 17 Reposit boxes and considered acceptable. As the data usage is evenly distributed over time, the impact on the bandwidth of customers is also considered acceptable.	<p>Upgrading and/or utilising dedicated communication networks (e.g. Silver Springs Network or 4G) are not recommended for enabling control of DER given the acceptable availability and data usage results from these trials. Nevertheless, if widespread outages to customer internet connections occur, guaranteed default setpoint functionality is paramount and needs to be ensured (see above).</p> <p>Reliance on customer's internet connection also poses the risk of reduced availability over time due to other factors such as replacement of modems, disconnection of ethernet cables, and changes to security settings. A longer analysis period than the approximately one-month period used in this experiment allows for a better assessment of the likelihood of these factors affecting the availability of the customer's internet connection. In this context, it should be noted that the fallback setpoint ensures that reverse power flow can be avoided (see "Loss of Communications" experiment above) when the internet connection is lost. The fallback setpoint is chosen so that the PV system will ramp down to zero net export, which still allows customers to meet their own needs while reducing the impact of uncontrolled systems on the network.</p>

Table 11. Carnarvon trials covering basic control of DER energy storage and VPPs including primary inverter control for network support.

Experiment	Description	Key Findings	Comments and Observations
Battery Control (Trinkl 2020d)	This trial used direct control (via battery dispatch) to charge/discharge the DER battery. This enables a view of internal power flows within the DER and verifies that the Reposit system behaves as expected. (L, RR & A)	The trial showed that direct control behind the meter over DER batteries is possible and effective in changing the net power flows across properties' network connection points. The Reposit was successfully used as a node device to command the battery behind the meter to cease charging or discharging and charge or discharge at a stipulated rate and time within an acceptable margin of error. This battery control function can be used by Horizon Power to dispatch groups of batteries behind the meter with a variety of control strategies such as load shifting and peak shaving as well as increasing generation through discharging batteries on demand. DER systems with batteries can easily be registered and added to existing or new VPPs and switched between VPPs in the same way as DER systems with solar only. This is explored in the VPP Configuration and Control Experiments.	<p>The series of experiments demonstrated that Horizon Power is able to directly control a DER battery behind the meter and affect the net power flow of the property. The findings are limited due to small sample size and short time period. Each experiment was carried out on a single battery and the entire testing period was two days. Furthermore, the Reposit's existing battery dispatch function was used to control the battery, noting that this may not be the control mechanism that Horizon Power will use in the future.</p> <p>In each experiment the battery did not ramp at the rate that is stipulated for a solar generation; instead, it jumped from its current state (charging/discharging) to the commanded state within 10 seconds, 15 seconds or under 1 minute. The error in the charge/discharge rate was between 0.28% and 3.35%, within the 10% limit, in all cases, except for one instance where it was 13.33% due to a load coming online during this time. This indicates that the battery control functionality may be compromised by customers' behaviour who may concurrently change the load.</p> <p>The planned indirect battery control test (i.e. by requesting net curtailment) could not be carried out due to the DER already charging the battery using any excess solar. Price signals could not be used for battery control as the Reposit uses direct control to charge and discharge the battery.</p>

Experiment	Description	Key Findings	Comments and Observations
<p>VPP Configuration and Control (Trinkl 2020e)</p>	<p>The first part of this trial involved VPP and DER registration, assigning DER to new and existing VPPs and moving DER between VPPs. These actions were verified via examination of the VPP parameters. The second part involved curtailment of the VPP in net and gross modes for a VPP of many DER and a VPP of one, the SOLEX system in this case. (L, RR & A)</p>	<p>VPPs are an effective tool for utilities like Horizon Power to control aggregated customer DER, enabling the utility to gain access behind the meter to the customer DER and at the same time providing the customer added benefits such as battery optimisation with the Reposit. The mitigation strategies that can be implemented by using VPPs as a control system include reverse power flow, voltage rise and export limitation. The key findings regarding the VPP and DER registration were:</p> <ul style="list-style-type: none"> • Creation of new VPPs and DER in the Reposit fleet management portal is simple but not yet automated. • Control of DER mostly meets specifications in terms of response times, ramp rates and setpoint accuracy, with some minor excursions. • The Reposit system is capable of controlling both single and groups of smaller customer DERs, and larger commercial systems. • The Reposit system allows for the creation of multiple VPPs that can be used for different control strategies and applies the correct curtailment, through prioritisation, when one DER system is in multiple VPPs. Curtailments are all distributed equitably across the fleet of DER within a VPP. 	<p>Several of the experiments found that the VPPs are not staying within the 10% average of the setpoint. As has been suggested in the report, once this has been rectified by Reposit (who have been notified), further investigation and experimentation will be required.</p> <p>The unmanaged solar at some of the sites within the VPP prevented the setpoints from being achieved in several instances.</p> <p>There is some uncertainty in the results given that Horizon Power has no record of the actual individual system setpoints because they are internally generated by Reposit based on the VPP setpoint that Horizon Power sends.</p> <p>Furthermore, a number of data points could not be calculated due to specific conditions of the test and system, including potential response rates.</p> <p>For the subset of nodes that were tested, it was found that after the final control signal, when the experiments were finished, and the setpoint was moved high enough to not interfere with the generation, the ramp rate was very high, up to 88.78% nominal capacity per minute, far beyond the allowable limit of 16.66%, most likely due to the Reposit controllers using an exponential decay type approach to the setpoint.</p> <p>The results from the testing of the equitable distribution of active power curtailment across the fleet of DER within a VPP, indicated a variation in the final net export based on their nominal capacity, for example, 24.78% to 29.36%.</p>

Experiment	Description	Key Findings	Comments and Observations
<p>Feed in Management (Export Limit) (Trinkl 2020f)</p>	<p>This experiment aimed to evaluate if the Reposit system can be reliably used to ensure an export limit at a particular DER installation. Two DER systems, one with a zero export limit and one with a 1 kW export limit were investigated. (A)</p>	<p>The Reposit feed-in management function was successfully used to implement an export limit. The function provides the flexibility to remotely change the export limit if network conditions or customer arrangements change. Export limits other than 0kW are possible. WW and Reposit data (5 min averages, 8 weeks of data from two properties (14,787 readings) was used to investigate how often the export limit was exceeded and how far it was exceeded by. The export was kept below the set export limit 97.58% of the time, with a maximum deviation of 1.29kW.</p>	<p>The Reposit system provides HP with visibility and flexibility to change an export limit at a particular DER location. This may be desirable over hard-coding locally within the inverter, which cannot be as easily adjusted as network conditions and/or customer arrangements change. The ability to change export limits easily may also serve as a selling point for (unpopular) feed-in management measures, which could be reviewed and possibly adjusted on a regular basis.</p> <p>From a customer's perspective, the export limit is less restrictive if their solar PV system is combined with battery storage and/or net feed-in management (FiM) control, allowing for maximising the self-consumption of renewable energy.</p>
<p>Grid Credits (Trinkl 2020g)</p>	<p>This experiment was concerned with Grid Credits and whether the Reposit's Grid Credit system can be reliably used to reward the customer for ancillary services provided by their DER (such as a behind the meter activity of reducing load during the peak period by discharging a battery). (A)</p>	<p>The Reposit system was used to signal a customer's DER system to discharge their battery at 2kW for 30 minutes and to log and transfer the grid credit. Discharge using an in-advance scheduled request and an immediate request was evaluated at one customer system. Both requests activated discharge resulting in an average battery discharge power of 1.89kW and 0.95kWh energy transfer for the in-advance request, and 1.77kW and 0.88kWh for the immediate request. The average power and energy data recorded by the Reposit system was compared to average power and energy recorded by the WW for both tests showed that both systems yielded the same results in the in-advance request and a difference of 0.39% in the immediate request.</p>	<p>The experiments showed that there is a difference of 5 and 12% between specified power and exported power, with the exported power being lower than the specified power. The cause of this difference is unknown and can be determined by further focused tests in the future.</p> <p>Being able to signal the customers' batteries to discharge or charge at times that are most beneficial to HP is a desirable functionality. However, this functionality could be compromised by customers' behaviour, who may concurrently shift loads to counteract the requested battery discharge or charging action. The trial compared measurements by the Reposit system with the WW measurements. Both these measurement devices are unlikely to meet the metrological requirements of standard electrical metering apparatus (e.g. percentage error limits are defined for electricity meters of class 0.2, 0.5 and 1 as per AS62053.21:2018 and AS62053.22:2018). However, to be able to take advantage of and financially reward customers for desirable VPP functionalities non-standard measurement devices, such as the Reposit System, will need to become accepted by the industry.</p>

Experiment	Description	Key Findings	Comments and Observations
<p>DER Network Support (Trinkl 2020h)</p>	<p>The Volt-VAr response mode available in inverters of the new PV/battery systems in the Gibson St network was also investigated in a series of experiments carried out between June and August 2019. The reconfigured inverters used in these experiments make up 35% of the DER on the feeder. Six increasingly severe sets of volt response reference values and corresponding reactive power levels were applied (each set for a week) while collecting inverter real and reactive power data and voltage data, which was measured at the inverter and the net measurement point of the property.</p>	<p>The experiment results showed that the DER inverters responded as expected and absorbed reactive power according to the chosen settings, however, no significant change in network voltage due to the activation or varied configurations of Volt-VAr response mode within the inverters was observed. It was noted, though, that across the course of the experiments, as configurations resulting in higher and earlier reactive power absorption (i.e. reactive power absorption at lower voltages) were applied, the maximum real power export increased more than was expected due to seasonal variations. It seemed that the effect of the Volt-VAr response led to fewer PV inverters without Volt-VAr capability tripping off. These inverters (without Volt-VAr capability) stayed on and then pushed the voltage up to a voltage slightly lower than previous that made it unclear the Volt-VAr was having an effect when it in fact was.</p> <p>Following these experiments, the Gibson Street transformer tap was lowered by one tap position in late September 2019. While this action reduced the minimum voltage seen in the network, it also did not lead to the expected reduction of maximum voltages. This seems to also be related to the release of PV generation associated with inverters, which previously tripped off under high voltage conditions prior to the tap change.</p>	<p>Due to current PV penetration levels, PV system locations, the network configuration, and the mix of DERs with and without the power quality control functionality enabled in the network on which the experiment took place there is no clear evidence to state that Volt-VAr response modes will or will not mitigate voltage rise issues caused by DER. However, there are indications that with a sufficient proportion of Volt-VAr enabled systems on a network section Volt-VAr is effective at managing voltage rise. This implies further testing is required and has been planned for the next stage. The simulation studies provided in Chapter 4 also explore these effects further.</p> <p>This particular test series illustrates how challenging these trials on live grids are to extract definitive results in an uncontrolled environment to prove or disprove a hypothesis.</p> <p>Reactive power absorption utilising each PV inverters' available capacity can only compensate voltage rise caused by that inverter. This is self-evident considering the inverter rating and network impedance between the inverter and the upstream distribution transformer. The voltage rise caused by the real power export by the inverter would be commensurate with the voltage drop achievable via reactive power absorption in light of the network impedances presented in Deliverable 5 (Glenister et al. 2019) where X/R ratios are between 0.5 and 1. These ratios were calculated for the battery-PV trials systems outside the Gibson St LV network (Glenister et al. 2019). This suggests that a large percentage of systems need to participate in reactive absorption for it to be effective. A way to determine this fraction would be based on assuming systems without reactive power absorption capability are on the particular network alone. If these systems cause voltage rise problems, more systems with absorption capability are required. Thus, the systems with absorption capability are effectively invisible as far as voltage rise contribution is concerned.</p>

8 Tariffs and energy storage control

The project sought to explore the value proposition for customer connected batteries and how we could create a win-win outcome for both the customer and Horizon Power. We nominated the PV/Battery DER system of one trial participant (a primary producer business) to run an experiment to test the effectiveness of Time of Use (ToU) tariffs in managing a battery system connected behind the customer meter. The trial participant was aware that their Reposit box was optimising their battery function, but they were not asked to change their consumption behaviour in any way. The project team wanted to test the value of optimised battery operation for customers who are not in a position to significantly change their consumption behaviour.

8.1 Validated learnings

The charging and discharging of the battery system was automatically influenced by the application of a ToU tariff structure and by the Reposit product seeking to achieve an optimised outcome. The battery system was permitted to pre-charge from the network to avoid peak period tariffs for the customer.

The trial participant remained on their existing A2 tariff during the experiment; however, the Reposit box used to optimise the battery function was programmed with the new tariff. Had the participant actually opted to move to the ToU tariff employed, they would have experienced a better financial outcome with the Reposit box and DER, than they would have otherwise. Moving to the ToU tariff, in conjunction with a Reposit box and DER, lowered the customer's peak power and energy usage during network peak times.

The ToU tariff implemented for this experiment was the tariff that was available through Synergy (WA) at the time. This is shown in Table 12, below.

Table 12. Time of Use Tariff.

Banded/Time of Use Tariff		
Charges	Time	inc GST
Supply Charge		1.015496 \$/day
Off-peak (everyday)	9PM – 7AM	0.148405 \$/kWh
Shoulder (Weekdays)	7AM – 3PM	0.282139 \$/kWh
Peak (Weekdays only)	3PM – 9PM	0.538714 \$/kWh
Shoulder (Weekends)	7AM – 9PM	0.282139 \$/kWh
Feed in Tariff (HP -Carnarvon)		0.1056 \$/kWh

The DER system was installed on 24/01/2019 and was left running on a standard flat rate tariff until 14/06/2019. The above tariff was then implemented, and data gathered until 14/03/2020, giving 141 days of flat-rate data and 275 days of ToU data to compare with.

8.2 Change in DER behaviour

The implementation of the ToU tariff through a smart DER control device (Reposit Box) had a significant effect on the behaviour of the battery, and thus the power flows of the DER system and the customer's property.

Figure 31, below shows a typical day before the ToU tariff was implemented.



Figure 31. Typical day before ToU.

From Figure 31, it can be seen that this property has a high load during the day and evening and a relatively small solar system compared to the size of the load. This is leading to a situation where the battery was being underutilised and the customer was still drawing most of their power from the network during the afternoon peak period. Peak energy use is more costly for the customer and adds to the evening peak.



Figure 32. Typical day after ToU.

After the ToU tariff was implemented the smart DER control device (Reposit box) optimised the use of the battery to achieve the lowest possible cost of energy for the customer. As can be seen in Figure 32 above, the battery was partially pre-charged at a low rate throughout the night, during the off-peak tariff period. This then ensures that there are reserves of cheap energy for the customer to use during the shoulder and peak tariff periods during the day, thereby lowering the customer's electricity bills and benefiting Horizon Power by shifting their energy usage away from the peak.



Figure 33. Compensating for cloud cover.

Figure 33 above illustrates the advanced analytical abilities of the Reposit smart DER control device. During this period, the load was constant as the residents were away but had left a large cooling shed running for their fruit produce. Due to the very predictable load the Reposit box was able to not only pre-charge during the off peak period but also choose to draw some power from the grid during the shoulder period, as it had predicted that the fully pre-charged battery would not be enough to last through the entire peak period. Drawing some power from the shoulder is cheaper than drawing it later during the peak.

8.3 Utility benefit Time of Use tariff

The ToU tariff was found to have a significant positive impact, reducing both the maximum power draw and the total energy consumption of the customer from the network within the peak period. It was found that the ToU tariff in conjunction with a smart DER control device (Reposit Box) reduced the peak consumption kWh by 64% and the average max load power during the peak period by 67%. This reduction in peak consumption is without the customer being given a direct incentive or directive to change their behaviour. The change in network consumption during each period of the ToU tariff can be seen in Table 13, below.

Table 13. Consumption comparison.

Tariff Period	Consumption Flat Tariff (kWh)	Consumption Flat Tariff (%)	Consumption TOU (kWh)	Consumption TOU (%)	Change in Consumption (%)
Off Peak	1519	54	2200	78	43.36
Shoulder	637	23	391	14	-39.14
Peak	640	23	233	8	-63.99

The change in average peak network load during each period of the ToU tariff can be seen in Table 14 below.

Table 14. Average maximum load comparison.

Tariff Period	Average Max Load Flat Tariff (kW)	Average Max Load ToU (kW)	Change in Average Max Load (%)
Off Peak	2.121	2.178	2.66
Shoulder	2.157	1.788	-17.08
Peak	2.918	0.973	-66.64

Figure 34, below, shows a graphical summary of the consumption before and after the ToU was implemented.

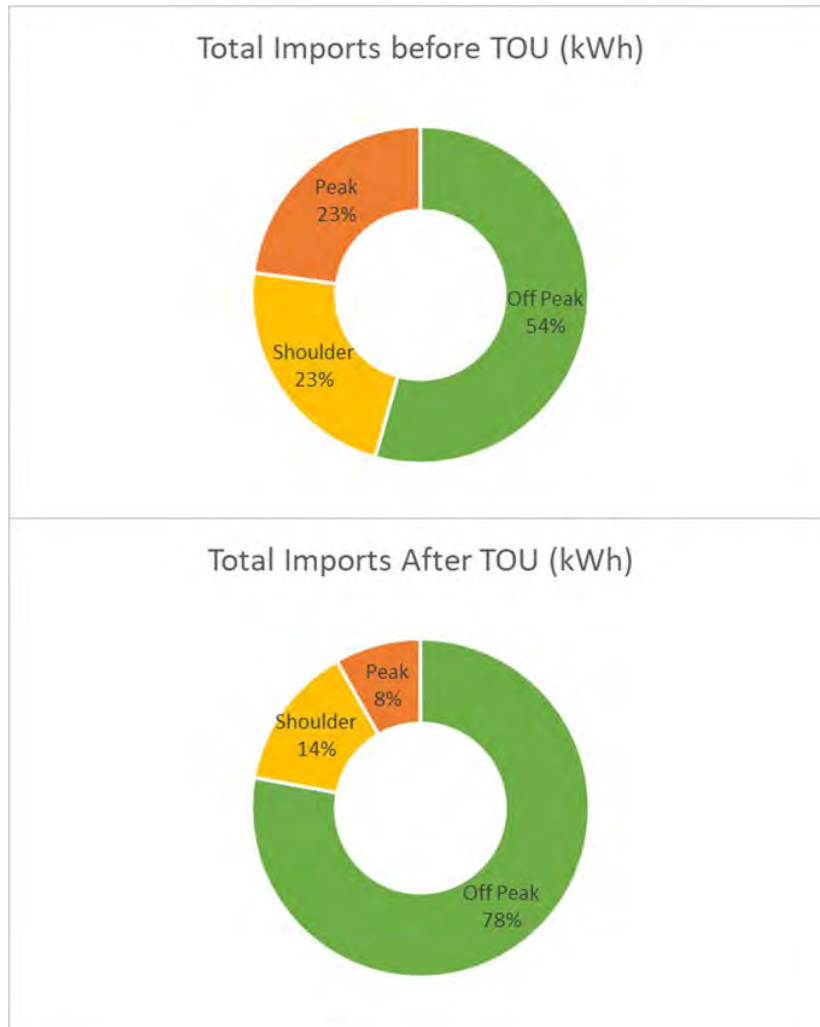


Figure 34. Graphical consumption comparison.

Figure 35, below, shows a graphical summary of the average maximum load before and after the ToU was implemented.

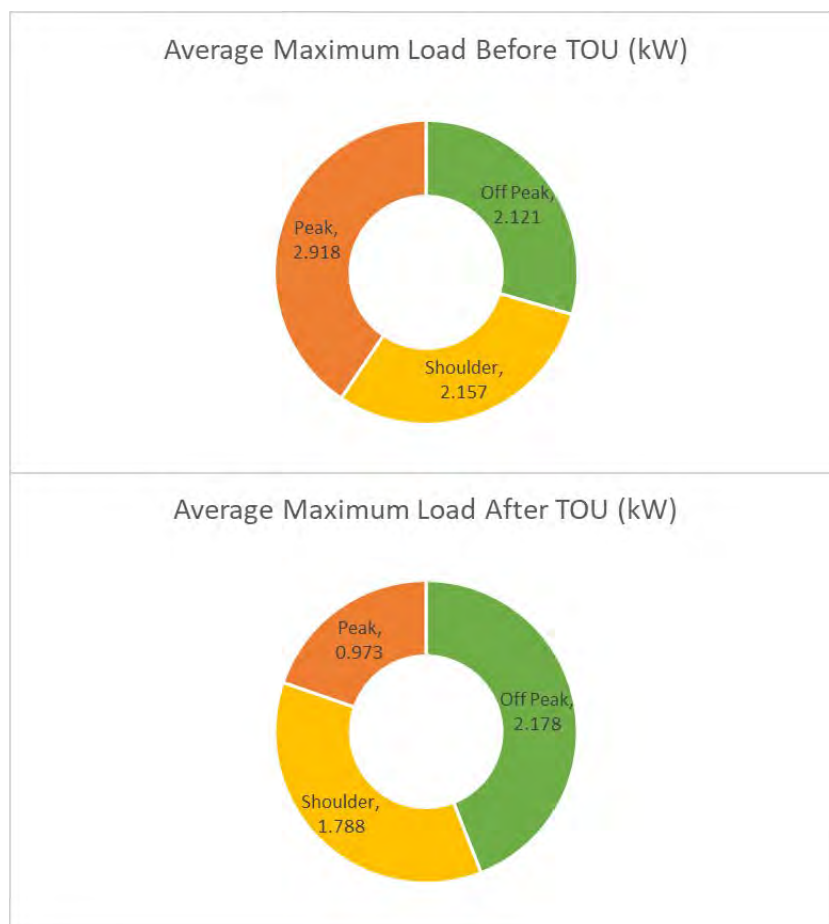


Figure 35. Graphical average maximum load comparison.

The reduction in peak load and consumption during the peak period is a tangible benefit to Horizon Power as the peak load in the evening is the driver behind network upgrades and augmentation. If the peaks can be smoothed out, infrastructure investments can be avoided.

8.4 Customer benefit Time of Use tariff

The implementation of the ToU tariff with a smart DER control device (Reposit Box) gave the customer a material financial benefit compared to both the ToU tariff without the smart DER control device and the flat rate tariff.

The ToU tariff with a smart DER control device, compared to the ToU tariff with DER but no smart control device, saved the customer \$836 per year or 36% of their annual electricity bill.

The full customer financial comparison can be seen in Table 15, below.

Table 15. Comparison of customer annual cost of energy.

Scenario	Annual Cost (\$)	Saving (\$)	Saving (%)
Flat Rate with DER	2402.94	0.00	0.00
ToU with DER	2302.04	100.90	4.20
ToU with DER and Smart Control	1465.80	836.24	36.33

Note: The annual figures were extrapolated from the 141 and 275 days of available data for the ToU with DER and ToU with DER and smart control device scenarios, respectively.

This additional benefit of \$836 or 36.33% per year, on top of the standard financial benefit that the solar and battery provide, would help to reduce the payback period of a battery for the customer.

8.5 Further experiments

The hypotheses around the ToU tariff have been validated for one property only. The next step would be to implement the same tariff structure and device on multiple properties to validate the hypotheses on a wider scale. An option would be to implement this structure on all (or as many as possible) of the DER systems on one transformer and observe the difference in power and energy flow at a transformer level.

It may be more cost-effective for Horizon Power to subsidise customer batteries to avoid network augmentation. This possibility requires further investigation.

It was not possible to implement MyPower⁷ in the current Reposit product. The dynamic nature of this tariff product offering renders it non-standard in the banded tariff space. This may be an issue for most smart devices and further investigation is required.

⁷ <https://www.horizonpower.com.au/mypower/>

9 Effects of cloud events on spinning reserve requirements

In order to manage increased PV penetration; the spinning reserve will need to be managed to accommodate changes in PV generation due to cloud shading of the distributed PV systems in Carnarvon. This section provides the relevant background on the generation and operating philosophy for the Mungullah Power Station and describes the existing spinning reserve strategy. PowerFactory simulation studies then investigate the impact of cloud events on the system performance to identify limiting factors on the design of an effective and reliable spinning reserve control strategy. Reactive power absorption, by DER inverters as part of the power quality functionality is also considered in these studies. A potential spinning reserve strategy using PV feed-in management and short-term solar forecasting is then presented, and a hypothetical cloud event and PV penetration scenario is used to explain the effectiveness of the strategy.

9.1 Existing spinning reserve strategy

The Mungullah power station (MPS) has a mix of gas and diesel-fired generating sets⁸. The gas generating sets are operated as a first priority whenever the gas generation capacity is greater than or equal to the load demand (Bruce 2012). The unit commitment philosophy at the MPS is to minimise the use of diesel as a fuel for electricity generation, hence the diesel generating sets have lower priority than the gas engine generators and are only started once all available gas engine generators are running.

The Carnarvon power system has a spinning reserve requirement of 100% of the prime operating capacity of the largest running machine (also known as N+1 Spinning Reserve), which is in line with the “Operating Philosophy for Mungullah Power Station” (Bruce 2012). Spinning reserve is implemented at MPS via set points to keep the difference between the load and running generation between 1.75 and 3.75MW. These setpoints maintain a minimum spinning reserve of 100% of the largest installed generator rating with a 250kW hysteresis. This hysteresis avoids machines turning on and off when the load crosses a machine on/off boundary.

Table 16. Spinning reserve “Load increasing” operation examples in Carnarvon (“X” indicates “running”).

Load (MW)	Gas Engines					Diesel Engines					SR (MW)
	G1	G3	G5	G10	G12	G2	G4	G9	G11	G13	
0 – 1.75	X	X									1.75 – 3.5
1.75 – 3.5	X	X	X								1.75 – 3.5
3.5 – 5.25	X	X	X	X							1.75 – 3.5
5.25 – 7	X	X	X	X	X						1.75 – 3.5
7 – 8.6	X	X	X	X	X	X					1.75 – 3.35
8.6 – 10.2	X	X	X	X	X	X	X				1.75 – 3.35
10.2 – 11.8	X	X	X	X	X	X	X	X			1.75 – 3.35
11.8 – 13.4	X	X	X	X	X	X	X	X	X		1.75 – 3.35
13.4 – 15	X	X	X	X	X	X	X	X	X	X	1.75 – 3.35

⁸ Five 1.75 MW gas fired generators and five 1.6 MW diesel fired generators

Table 16 and Table 17 show the spinning reserve implementation at MPS for increasing and decreasing load scenarios, respectively. The station automation system will schedule sufficient generators online to meet the current load and still have a reserve of 100% of the largest online generator to allow for (net) load changes before an extra generator is brought online. Each generator is assumed to reliably provide towards the required online capacity up to its rated output, taking high-temperature de-rating into account.

Table 17. Spinning reserve “load decreasing” operation examples in Carnarvon (“X” indicates “running”).

Load (MW)	Gas Engines					Diesel Engines					SR (MW)
	G1	G3	G5	G10	G12	G2	G4	G9	G11	G13	
0 – 1.5	X	X									2 – 3.5
1.5 – 3.25	X	X	X								2 – 3.75
3.25 – 5	X	X	X	X							2 – 3.75
5 – 6.6	X	X	X	X	X						2.15 – 3.75
6.6 – 8.2	X	X	X	X	X	X					2.15 – 3.75
8.2 – 9.8	X	X	X	X	X	X	X				2.15 – 3.75
9.8 – 11.4	X	X	X	X	X	X	X	X			2.15 – 3.75
11.4 – 13	X	X	X	X	X	X	X	X	X		2.15 – 3.75
13 – 15	X	X	X	X	X	X	X	X	X	X	1.75– 3.75

9.2 Impact of cloud events on the system performance

The impact of cloud shading induced power changes on MPS in the short term is modelled in PowerFactory using load ramping events in balanced RMS simulations. These simulations assume insufficient time for control actions and simulate the power station response to cloud induced power ramps on the net load seen at MPS. Reactive power absorption by DER inverters, as part of the power quality functionality, is also modelled from a system perspective. The estimated amount of reactive power absorption is based on the simulated PV capacity.

The PowerFactory model “Carnarvon Generation Model – Nov 2017” was used to perform these simulations with the one-line diagram showing the MPS in Figure 60 (in the Appendix). This model was provided to the authors at Murdoch University by Horizon Power. The simulations performed are listed in Table 18 with the criteria used to assess the simulation outcomes listed in Table 19, where these criteria have been derived from the generation philosophy and MPS operating philosophy (Kerrigan 2012, Bruce 2012).

Table 18. RMS PowerFactory simulations performed.

	PowerFactory simulation
1.	Carnarvon (CRN) power system with 3MW of PV.
2.	CRN power system with 6MW of PV. No changes to power station operation.
3.	CRN power system with 11.4MW of PV capacity. Maximum PV scenario described in (Glenister et al. 2020).
4.	Ramping of load on single gas and diesel generators to ascertain the ramp-rate capability of each type of generation.
5.	Investigation into minimum loading of MPS.

Table 19. Criteria used to assess PowerFactory RMS simulations.

Phenomenon of interest	Limits
Frequency	±1Hz (Normal operating range) ±2Hz (Abnormal <2Hz PELS ⁹ , >2Hz UFLS ¹⁰)
Load Following	±1Hz (Normal operating range) ±2Hz (Abnormal <2Hz PELS, >2Hz UFLS)
Power Reserve	1.75 – 3.75MW (Frequency regulation)
Reactive Power	1704 kVAr (0.6 x 2840 kVA)
Minimum Loading	30% – 50% of machine rating

9.2.1 Background and simulation descriptions

Data (SCADA and WW) made available as part of the Carnarvon DER trials project was for the period 2017 – 2020. On 1st July 2019, 10MW of PV hosting capacity was made available for new distributed PV systems to be installed across all Horizon Power’s networks. Within six months of this date, the amount of installed PV capacity in Carnarvon went from about 1MW to 3.1MW. This required a re-evaluation of the situation with respect to the PowerFactory simulations. The assumptions made in the simulations are based on an analysis of data from 2017 to 2018 when the PV capacity was 1MW (Glenister et al. 2019b, Glenister et al. 2020). The estimates of the size of cloud shading induced power changes from this analysis are shown in Table 20. From these values, the largest change in PV generation that is likely is 40% of the installed PV capacity for 300-second power ramps and 25% of installed PV capacity for 60-second power ramps. These factors correspond to PV generation decreasing, which is seen as more critical than PV generation increasing.

Table 20. Derived factors from previous work on this project (S. Glenister et al. 2019b) used to scale power ramps for PowerFactory RMS simulations.

Parameter	Value	Comment (Analysed WW data 2017 – 2018 interval)
WW systems as a percentage of all PV systems in CRN based on the change in PV generation.	52%	Based on a comparison of changes in PV generation from WW data and net load changes in SCADA data.
A measure of WW PV systems capacity	584.8kW	This is based on the sum of the peak outputs of each WW based system. Measured peaks are not time coincident.
Maximum WW PV generation increase	215kW	From SCADA 406kW change. 300 seconds time interval.
Maximum WW PV generation decrease	202kW	From SCADA 400kW change. 300 seconds time interval.
Maximum 60s WW PV generation increase	148kW	60s time interval.
Maximum 60s WW PV generation decrease	130kW	60s time interval.

⁹ Pre-emptive Load Shedding

¹⁰ Under Frequency Load Shedding

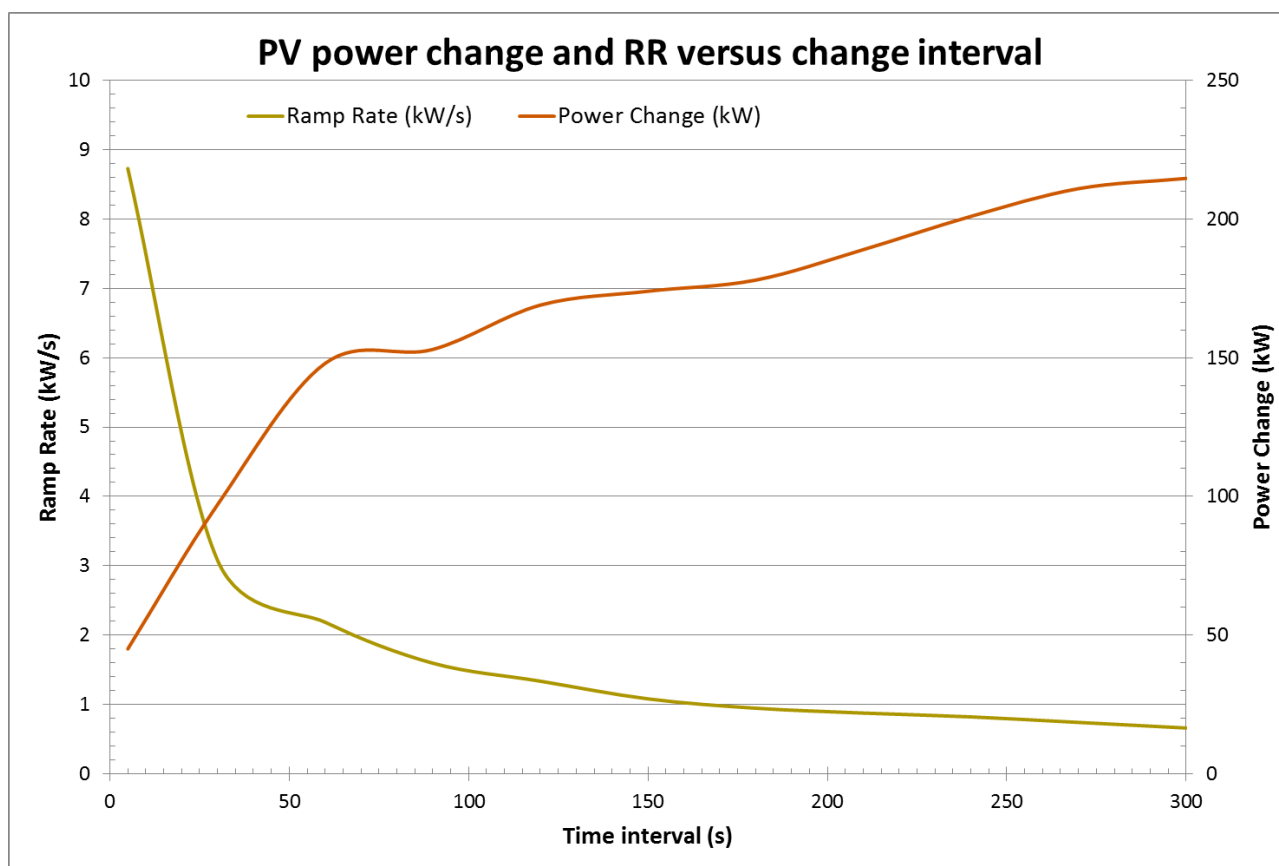


Figure 36. PV power change and Ramp-Rate (RR) versus time duration of the change in PV power generation (Glenister et al. 2019b).

Ramp-rates for changes in PV generation are considerably lower than power ramps seen due to large load changes and mass inverter trip events. Large changes in PV generation occur over larger time intervals on the order of 300 seconds. Ramp-rates for PV changes start to approach values commensurate with inverter trip and large load change events for small changes in PV generation. In Figure 36, depicting the ramp-rates and PV magnitude change versus time interval, it is evident that the ramp-rate increases rapidly for short duration events with a corresponding decrease in PV power change. This graph was derived from the analysis performed in previous work as part of this project (Glenister et al. 2019b).

Despite this data covering only one year, there are other studies indicating similar types of phenomena in terms of larger changes in PV generation occurring over longer time intervals (Sayeef 2012). With these temporal phenomena, highlighted by Figure 36, factored into the simulations, the power change events for 300 seconds and 60 seconds were used as templates for the simulations. The ramp-rates corresponding to these power change intervals are 0.66kW/s and 2.2kW/s, respectively, and are significantly below 9.7kW/s, which corresponds to 1.75MW (gas engine capacity) over 180 seconds (gas generator start time). One issue with these measured ramp-rates is that in order to estimate them for a higher installed PV capacity, they will increase in proportion to any increase in capacity. For example, if the capacity of the WW equipped PV systems were to double, then these ramp-rates can be expected to double. Inverter trip induced power ramp-rates as high as 42kW/s have been observed in one case but are typically around 15kW/s (Glenister et al. 2019b, Sayeef 2012).

To estimate the contribution to reactive power in the system, inverters are assumed to absorb reactive power as the voltage increases as a consequence of the Volt-VAr power quality mode. Since the voltages in Carnarvon are often around 250 V, this implies that inverters will be absorbing reactive power even at low

PV penetration levels on LV networks. Only post-2015 inverters are Volt-VAr equipped, corresponding to 67% of the installed inverter capacity in April 2020. At higher penetrations and over time, as old systems fail or get replaced, this proportion will increase. For example, with 6MW of PV capacity (one of the simulated scenarios), the proportion of Volt-VAr inverters is assumed to be 83%. To include the effect of Volt-VAr as seen at MPS, aggregate assumptions were made, and these are listed in Table 21.

Table 21. Reactive power estimation factors used for the PowerFactory simulations.

Reactive power absorption occurs when there is PV generation.
The amount of absorption is proportional to the PV capacity.
All inverters configured with maximum reactive absorption of 60% of inverter capacity.
70% of the maximum possible reactive power absorption is seen at the HV bus bar in Iles Rd.

9.2.2 Simulation results

Initially, the simulations were establishing a benchmark for how the generators perform, in particular with respect to frequency under load ramping. Load power ramping was chosen as a way to determine the performance under cloud shading conditions, since the effect on the net load seen at the power station due to the cloud shading of PV manifests itself in terms of power ramps over 60 to 300 seconds for the most significant power level changes. Shorter time frames have smaller and less noticeable net power changes at the power station.

Figure 38 shows the performance of the gas engine generators to load ramps with ramp-rates between 12 and 50kW/s. These ramp-rates are well in excess of what cloud shading would cause on the net load at the system level. The power ramps applied in these simulations can be seen in Figure 61 in Appendix 3. The fourth ramp, in Figure 38, had a similar value to the third ramp, but the reduction in frequency was significantly smaller. This occurred because three generators were applied to the latter case, reducing the ramping rate seen by each generator. This shows that the effects of power ramps are reduced with more generation online. Additionally, the largest frequency decline did not cause the frequency to drop to 49Hz; the threshold frequency below which Pre-emptive Load Shedding (PELS) is triggered (Bruce 2012). Figure 63 shows the response of the diesel generators to the same ramp-rate load increases that were used for the gas generators (shown in Figure 62). The gas generator response was more sluggish (higher damping factor) when contrasted with the diesel response, although the diesel generators' frequency excursion for the same ramp-rate was larger but still short of dropping to 49Hz. Diesel generators will never be online by themselves at MPS.

In this model and shown in the one-line diagram (Figure 60 in Appendix 2), MGP 11kV B-BOARD refers to the 11kV switchboard B, where 5 of the generators' outputs are combined; MGP 22kV B refers to the 22kV bus bar between the output of the tap changing 25MVA transformer and the 22kV express feeder B, both at MPS; and CRN 22kV B2 refers to a section of the Iles Rd 22kV bus bar. The express feeders, connecting MPS and the CRN 22kV switch board are 5.5km in length. Also, in the model for the case of the minimum load scenario the total load seen by the power station was $3.63 + j1.1439$ MVA and for the maximum load scenario it was $12.1 + j3.81$ MVA (the j terms represent the reactive power positive for absorbing). Table 22 shows the initial loads for the various simulations and the change in power, reactive power and the final load. For the simulation results the real and reactive power values are somewhat different from the load values shown in Table 22 due to network losses and reactive power generation by the network. The express feeders A and B in particular supply about 0.7MVA of reactive power. Each HV feeder had particular load values, which are shown in Table 26 in Appendix 2, with power factors varying between 0.9 to close to 1. The overall power factor was 0.95; thereby, the reactive power absorption from MPS was not excessive and well within the generator 0.8 lagging capability. The voltage changes seen in the simulations were small to insignificant, see Figure 66.

Figure 37 shows the voltage at the MGP 11kV Board B, MGP 22kV B bus bar and the CRN 22kV B2 bus bar. These results are from three simulations that assumed 11.4MW, 6MW and 3MW of installed PV capacity. Net load increases of 3.4MW, 2.4MW and 1.2MW, respectively, were simulated for these cases. Associated with the load increase were PV generation and reactive power absorption decreases, causing the voltage changes shown in Figure 37. These load changes can be seen in Figure 64 in Appendix 3.

Table 22. Scenarios for various PV penetrations and cloud induced power changes based on experience from WW data.

PowerFactory MPS Model					
	P + jQ (MVA) (Initial Load)	PV (MW)	ΔPV generation (MW)	Volt-Var induced ΔQ	Final P + jQ (MVA)
Minimum Load Scenario	3.63 + j1.1439	3	1.2	0.45	4.83 + j0.69
	3.63 + j1.6202	6	2.4	1.05	6.03 + j0.57
	3.63 + j4.7	11.4	4.7	2.25	8.33 + j2.45
Max Load	12.1 + j3.81	11.4	4.7	2	7.4 + j5.81

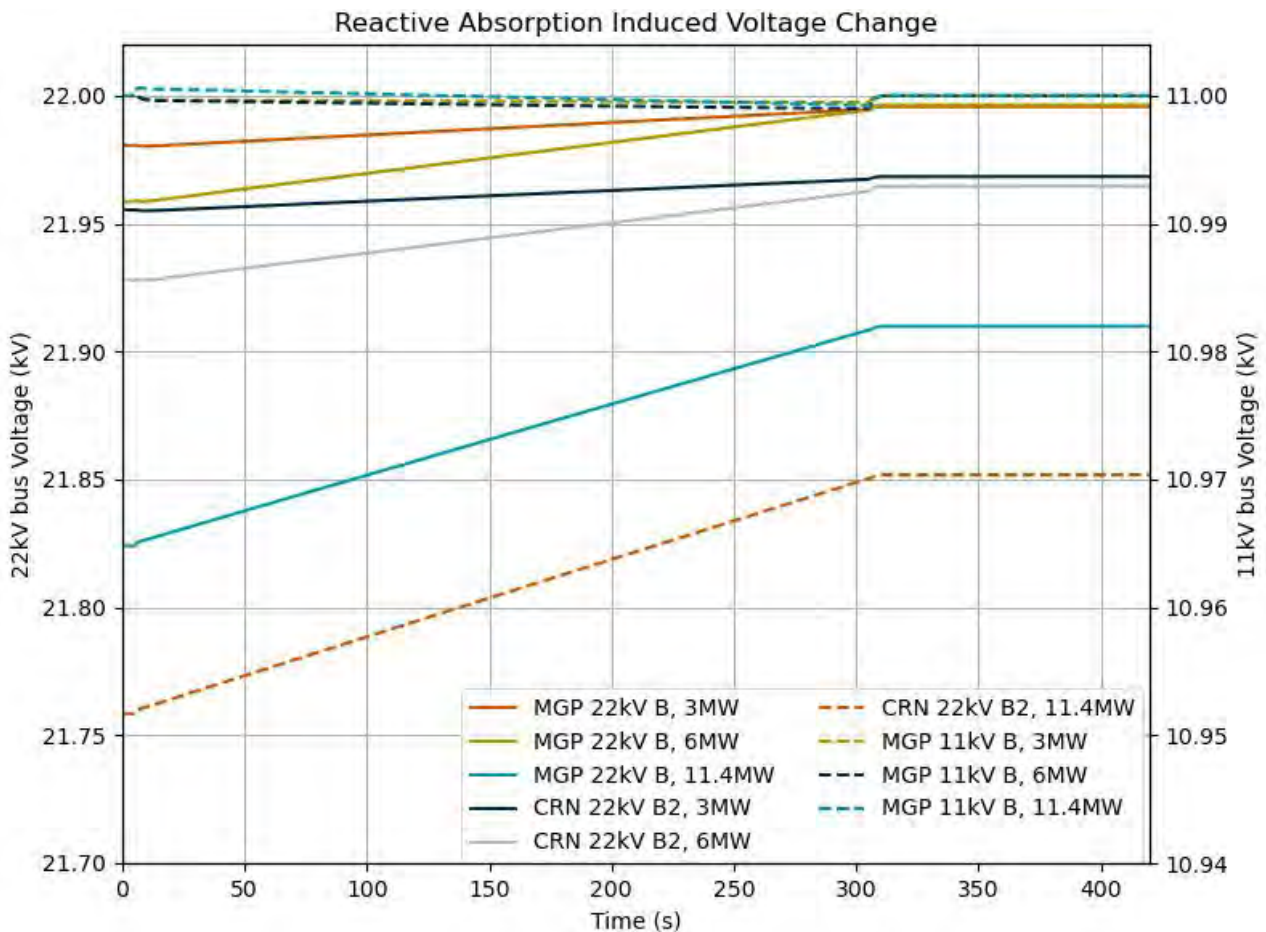


Figure 37. Voltage at the MGP 22kV B bus bar, CRN B2 bus bar and MGP 11kV Board B. Load increase due to a 3.4MW, 2.4MW and 1.2MW decrease in PV output power over 300 seconds corresponding to 11.4MW, 6MW and 3MW of installed PV capacity, load initially minimum. Reactive power absorption by the network decreased due to inverter Volt-Var systems backing off, causing the voltage to rise.

The net increase for the 11.4MW case was limited to 3.4MW so as to not over load the generators keeping the total load to 7MW (4x 1.75MW, see Figure 64). However, the reactive power decrease was the full 2.25MVAR. The reasoning behind this was to see the effect on the system voltages without the frequency and voltage collapsing.

The voltage changes seen in Figure 37 are 90V, 37V and 15V increases for the three cases on the 22kV bus bars. Also, the average voltage difference between the MGP 22kV B and CRN 22kV B2 bus bars is 60.0V, 31.4V and 26.5V for the 11.4MW, 6MW and 3MW cases, respectively (see Figure 60). However, the total difference between the nominal voltage and voltage at CRN 22kV B2 during maximum absorption of 4.7MVAR was 240V, about 1% of nominal voltage. The voltage changes seen on the 11kV bus at MGP 11kV B-BOARD (see one-line diagram in Figure 60) were around 1V. Figure 66 in Appendix 3 shows the voltage on MGP 11kV B-BOARD during these power ramps in Figure 64. There appeared to be adequate reactive power provision even at very high PV penetration levels with large reactive absorption. These voltage differences were on the order of 0.1 – 0.3% of the nominal voltage. This suggests reactive power provision is unlikely to be an issue from a voltage management perspective.

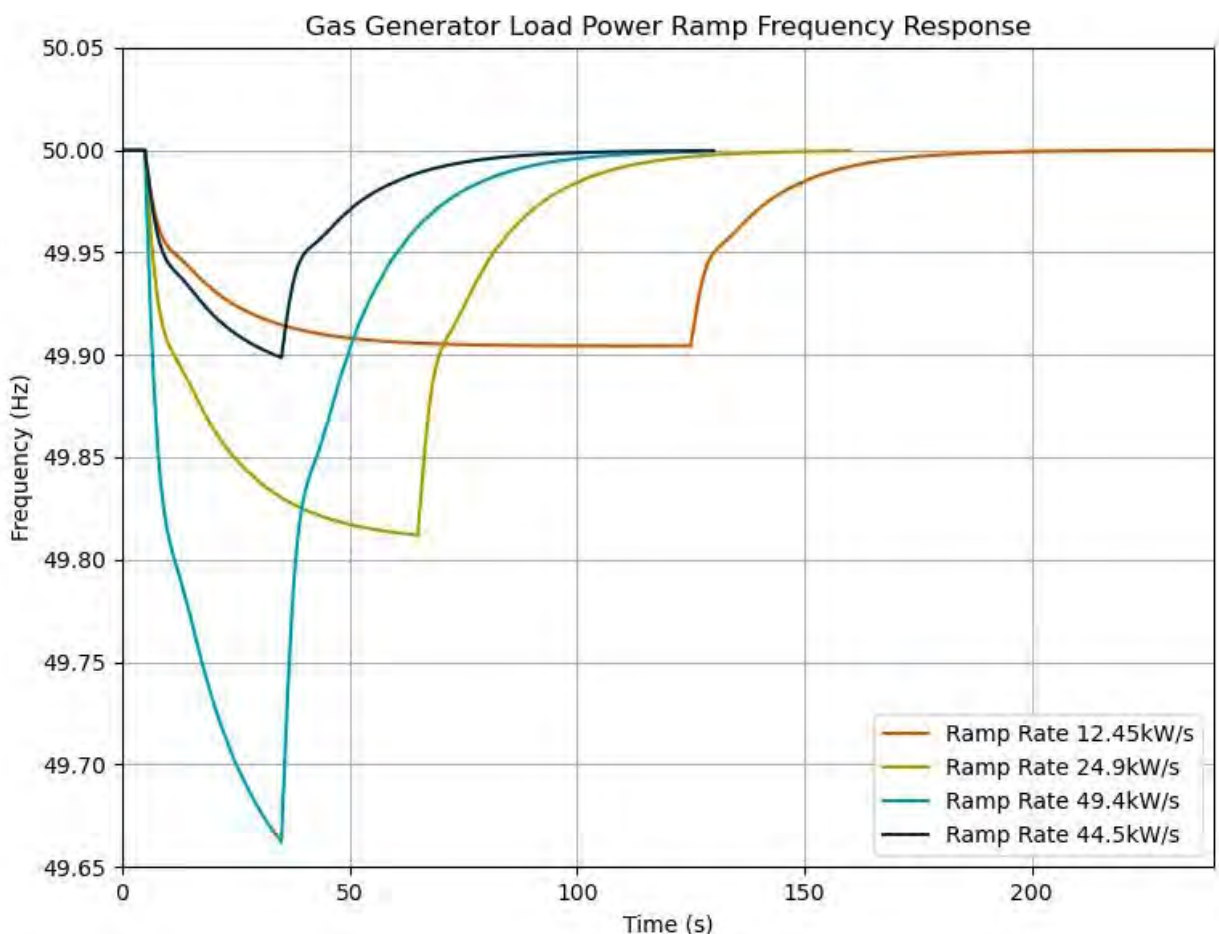


Figure 38. Frequency response of gas engine generators to the load ramps. Load ramps are shown in Figure 60 (Appendix).

Applying the reactive power factors from Table 21 to estimate the proportion of reactive power seen in the power ramping simulations for the 3MW of PV capacity case, results in:

$$3 \times 0.4 \times 0.75 \times 2/3 \times 0.7 = 0.42\text{MVAR absorbing.}$$

Where,

- 3 is the installed PV capacity (3MW)
- 0.4 is the fraction of capacity that the PV power changes by (1.2MW / 3MW)
- 0.75 is the ratio of reactive power to real power, corresponding to 60% reactive power of inverter capacity (factor used in inverter power quality modes)
- 2/3 is the assumed fraction of the inverter population in Carnarvon that has power quality mode functionality (Volt-VAr)
- 0.7 is the assumed aggregated fraction of Volt-VAr capacity of Volt-VAr capable inverters.

This corresponds to a power factor for the change in power (1.2MW) and change in reactive power (0.42MVAR) of 0.944. Previous simulation work associated with the Volt-VAr power quality mode on PV inverters gave rise to power factors of between 0.94 to 0.97, depending, among various factors, on the number of participating inverters (Calais et al. 2020).

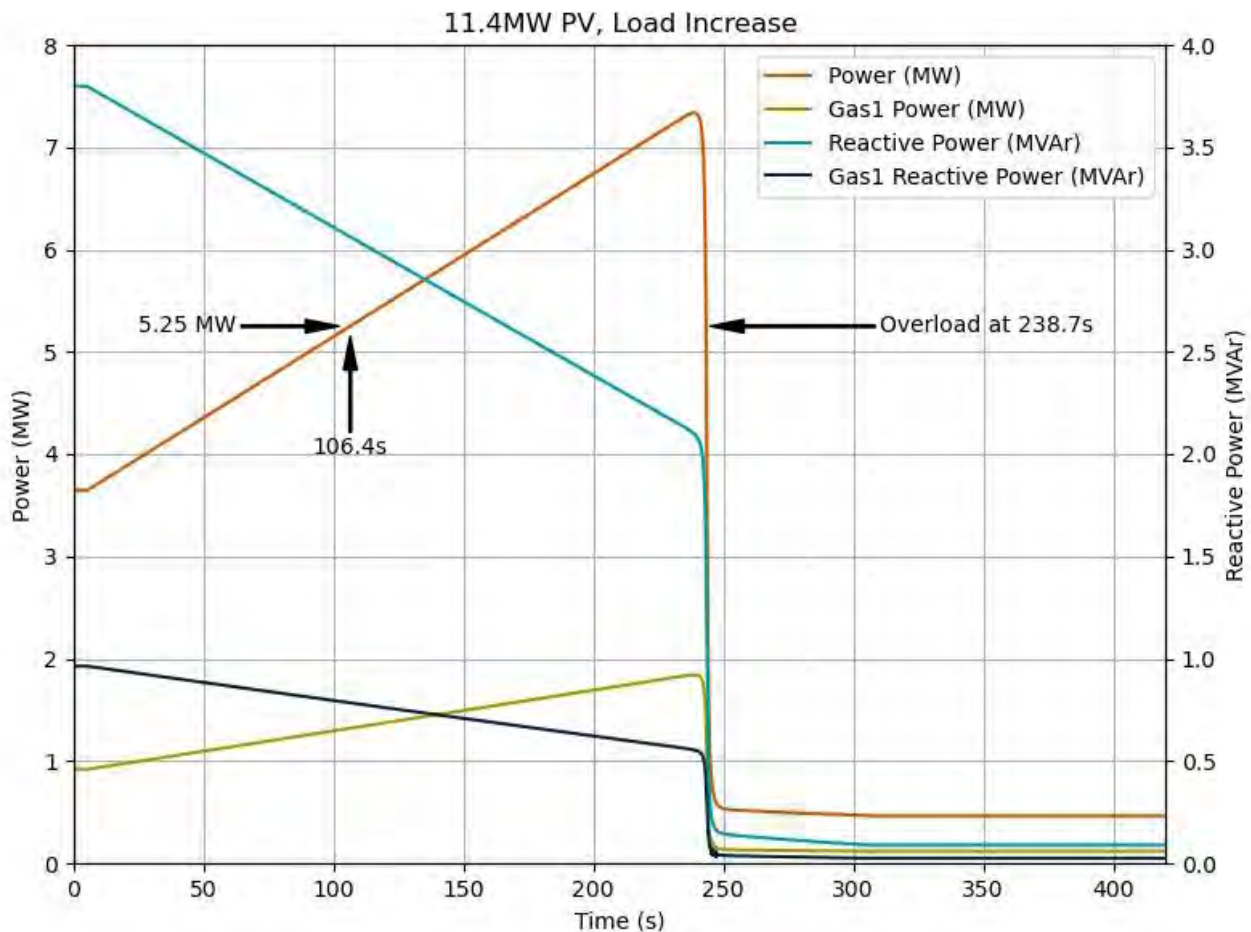


Figure 39. Load increase due to a 4.7MW decrease in PV output power over 300 seconds, assuming 11.4MW of installed PV capacity, load initially minimum. The total load and one gas generator load are shown. Reactive power decreased and spinning reserve dropped from 1.75MW to 0 in 132 seconds.

For the 6MW and 11.4MW cases, more of the inverters in Carnarvon were assumed to have power quality modes giving rise to power factors around 0.91, slightly increasing the reactive power consumption relative to the previous work (Calais et al. 2020).

It is expected that as penetrations increase and the prevalence of overvoltage increases, Volt-VAR systems will be pushed harder. The Horizon Power standard for inverter interconnection has 240V to 265V as the absorption range. However, the new Australian standard AS/NZS 4777.2:2020 (Standards Australia 2020), brings Volt-VAR on at a voltage of 240V to 255V for the Australian region C, which corresponds to isolated or remote power systems (Regions A and B are for interconnected applications).

Large load ramping caused by cloud shading at various installed PV capacities were simulated, and the results are shown in Figure 40. The net load power ramps are shown in Figure 67, Figure 68 and Figure 39. These ramps show the total and per generator power and reactive power changes seen at MPS. The initial load corresponds to the minimum load in the “Carnarvon Generation Model – Nov 2017” for the 3MW scenario. For the 6MW and 11.4MW scenarios reactive power was increased, resulting in $3.63 + j1.6202$ MVA and $3.63 + j4.7$ MVA for the initial loads, respectively. Four gas engine generators were online for this simulation, corresponding to a minimum spinning reserve of 1.75MW and an online capacity of 7MW.

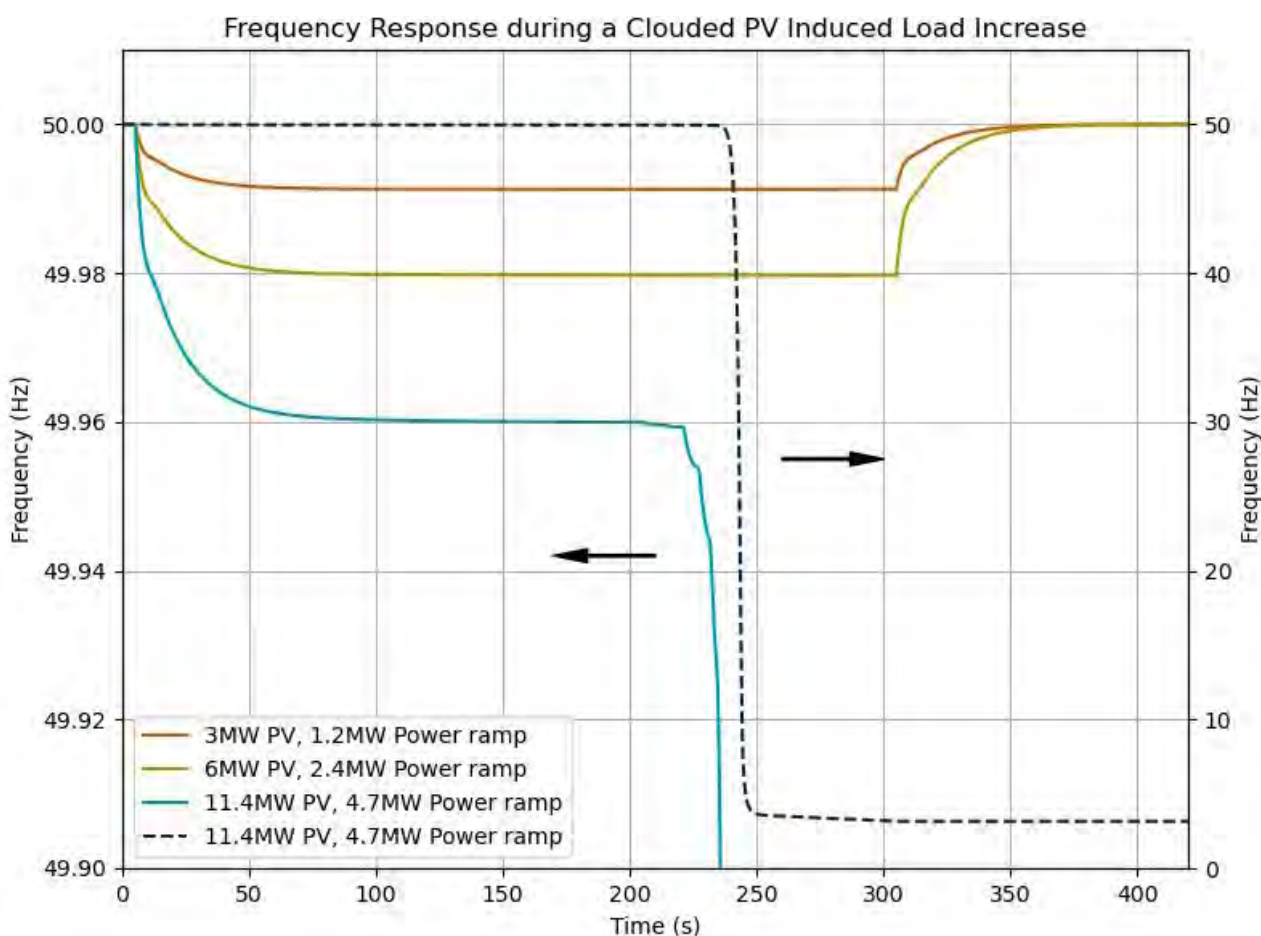


Figure 40. Frequency response to load increases due to cloud shading of PV for 3, 6 and 11.4MW of PV capacity.

From Figure 40 it is clear that for a 300-second power ramp, the frequency regulation at MPS was more than adequate provided there is no overloading of generation. However, the simulations assumed that no control intervention occurs because the time frame (5 minutes) is within the update cycle of the supervisory

control systems (i.e. DERMS) and there is no PV forecasting. For the 4.7MW load increase, the generation became overloaded, as is apparent in Figure 39 and Figure 40. A forecasting system will alleviate this by allowing a supervisory control system time to pro-actively curtail the PV in a timely fashion to enable the spinning reserve to be appropriately adjusted.

If the power station automatic control (which is not modelled in the RMS simulations) is considered, there still appears to be a shortfall in time for the 11.4MW PV scenario (4.7MW load increase) simulation. As can be seen in Figure 39, the load increases past 5.25MW at 106 seconds. From this point until generation overload (duration of 132 seconds), the spinning reserve is below 1.75MW. When the spinning reserve reaches 1.75MW as net load increases, the power station control initiates the start process for the next generator, which in this case is a gas engine generator with a minimum start time of 180 seconds. Additionally, with a PV curtailment system operating based on the DERMS system and assuming an update period of 5 minutes, there is the possibility of a shortfall in generation at high penetration levels of PV since this shortfall can occur within the DERMS update period.

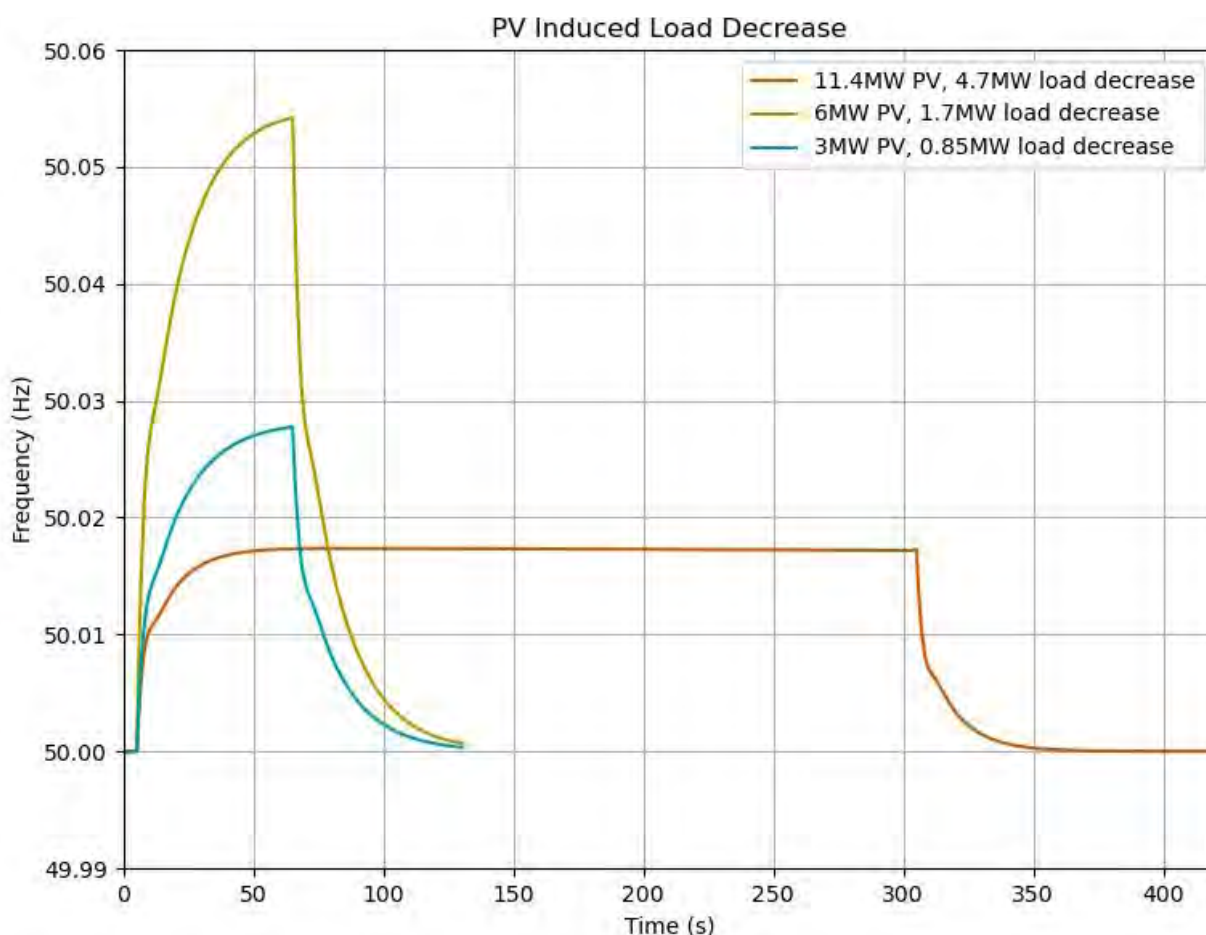


Figure 41. Frequency response to load decreases due to cloud unshading of PV for 3, 6 and 11.4MW of PV capacity.

Figure 41 shows the frequency response of the generation for the minimum load scenarios for 3MW and 6MW of PV capacity for load decreasing and PV output increasing. In the case of 11.4MW of PV capacity, the maximum load scenario was used, since the minimum load scenario would result in reverse power flow for decreasing load. Also, the 11.4MW case was over 300 seconds, whereas the 3MW and 6MW cases were for 60-second ramps. Figure 69, Figure 70 and Figure 71 in Appendix 2 show the power and reactive power ramps for these cases.

For the 60-second cases, the PV increase was 28% of the installed capacity instead of 25% for PV decrease, as was reflected in the measured cases from previous work (Glenister et al. 2019b). From Figure 41, it is apparent that the PV induced load reduction does not impact the frequency regulation. In all three cases, the load dropped such that the spinning reserve rose above 3.75MW; consequently, a generator would turn off and in the 11.4MW of PV case, three diesel generators turn off.

These simulations demonstrated that the MPS frequency regulation system can easily manage any cloud shading induced power ramping, provided there is sufficient load to prevent reverse power or sufficient reserve to avoid starting a generator. Although diesel generators can start quickly enough, for 6MW of PV, an estimated maximum 60 second PV shading induced net load increase would cause a 1.5MW load increase in 60 seconds and this is very close to the minimum spinning reserve margin. Moreover, Table 23 provides problematic PV capacities beyond which it is increasingly likely a generation shortfall will occur if no measures are taken, such as solar forecasting, to pro-actively manage the installed PV capacity. In particular the issues highlighted are relevant for a forecasting system where pre-emption of spinning reserve is the only mechanism used to manage the cloud induced load ramping (i.e. enough generation must be on-line at all times). The forecasting system allows for the adjustment of the spinning reserve in anticipation of a short fall and, equally, to reduce spinning reserve for efficiency when appropriate. Secondly, a feed-in-management system will only alleviate problems caused by high PV penetrations if it is able to curtail before the commencement of a PV cloud shading induced large net load ramp.

Table 23. Problematic installed PV capacities for starting gas engine generators.

Power ramp duration	Factor relative to installed PV capacity	Problematic ramp-rate based on 180s generation start time	Problematic installed PV capacity
300s	40%	9.72kW/s	7.29MW
60s	25%	29.2kW/s	7MW

The “Factor relative to installed PV capacity” entries in Table 23 are the percentage of PV capacity determined from earlier work (Glenister et al. 2019b, Glenister et al. 2020). Analyses performed in this work estimated the maximum PV ramp-rate for a given installed PV capacity. “Problematic ramp-rate based on 180s generation start time” assumes a spinning reserve of 1.75MW and 180 seconds to start the next generator. These factors all lead to the “Problematic installed capacity” values, where beyond this capacity, PV shading induced power ramps will exceed the minimum spinning reserve within the assumed next (gas) generator start time in the absence of pro-active PV management systems.

9.3 A Short-term Solar Forecasting and Feed-in Management based spinning reserve strategy

Previous work by Horizon Power in collaboration with IBM investigated the value of forecasting in the management of distributed energy resources. This investigation based on predictive weather models, AMI, SCADA and GIS data was aimed at reliable prediction of PV generation and energy demand at the power station (for 15 min intervals) 24 hours in advance and at a confidence of 95%. The work is described in more detail in Appendix 3 and identified a number of challenges, specifically related to the prediction of PV generation. Key findings from the work point towards the need for disaggregation between demand and generation in the data to accurately correlate the effects of external factors on generation and demand, and for replacing the Deep Thunder weather model irradiance forecasts with sky camera-based irradiance forecasts to improve solar PV forecasts specifically on cloudy days. These findings shaped the scope of the Carnarvon DER Trials and the work presented in this report, including an investigation into an example application of sky camera-based forecasts and DER feed-in management for power system control in Carnarvon, which is presented below.

9.3.1 Sky camera-based forecast system integration into power station control systems

The example skycamera based forecast system integration into the power station control system discussed here is centred around a control signal, which indicates a significant drop (in PV power) in the next x minutes (control signal value = 0) or no significant drop in the next x minutes (control signal value = 1) (Dickeson 2020). A *significant drop* is defined by a certain amount (drop threshold) by which the PV power is predicted to drop. The minimum prediction lead time x is related to the maximum time required for the control system changes to take effect, i.e. the starting time for a generator or the latency in the control of a PV system or a group of PV systems for example through a Virtual Power Plant (VPP).

There are several options to use the described control signal for power station control:

1. Adjustment of the spinning reserve under clear weather conditions: A correct prediction of clear weather (control signal value = 1) allows for operation with decreased spinning reserves. Given a suitable system load, this may result in a significant reduction of fossil fuel generation and/or the runtime of more expensive thermal generators (Power and Water Corporation 2019).
2. Ramp rate control during cloud events using PV curtailment: A correct prediction of a cloud event (control signal value = 0) can be used for ramp rate control of PV by pro-actively ramping down or curtailing PV output.
3. Ramp rate control during cloud events using PV curtailment and battery storage: A correct prediction of a cloud event (control signal value = 0) can be used for ramp rate control of a combined PV/battery system, by pro-actively ramping down the combined output of the PV/battery system.
4. Adjustment of the spinning reserve under cloudy conditions: A correct prediction of cloud cover that causes significant PV power drops allows for the increase of spinning reserve by selecting to start/increase spinning reserve. This option (as opposed to options 2 and 3) could result in foregoing PV curtailment but may lead to generators operating at suboptimal loading.

9.3.2 Potential benefits of a spinning reserve strategy using short-term solar forecasting with feed-in management

A hypothetical cloud event was used in this section to demonstrate the potential benefits of a spinning reserve control strategy using a short-term solar forecasting system in combination with PV feed-in management and generation control. The scenario was chosen to align with Carnarvon conditions with more than 5MW of installed PV capacity. The underlying assumptions are listed in Table 24.

Table 24. Scenario assumptions.

Scenario duration	1 hour
Simulation time step	1 minute
Load (not masked by PV)	7.7MW (assumed constant for the scenario duration)
PV fluctuation	2.4MW (decrease) over 5 minutes, 2.88MW (increase) over 6 minutes
Available PV power	1.9-4.78MW during the scenario
Net load seen by the power station	2.9-5.9MW
Generator start time	3 minutes
Generator stop time	1 minute
Forecast system	The forecast system can reliably predict available PV power 10 min ahead (forecast uncertainties are not considered). A forecast signal = 1 indicates available PV output under clear sky conditions, a forecast signal = 0 indicates a significant drop and a variable available PV output.
Feed-in management response time	< 5 minutes (begin of ramping after a set point was sent)
Feed-in management ramp rate limit	10% of nominal managed PV capacity (assumed to be 5MW) per minute
Battery energy storage	Not considered

Figure 42 presents the existing spinning reserve strategy’s operation for Carnarvon for the scenario. When applying the set points of the existing spinning reserve strategy (see Table 16 and Table 17), the scenario’s conditions initially led to the operation of three gas engines with an average of 65% loading. As soon as the cloud event led to the decrease in available PV power (instant “1” indicated in Figure 42), the spinning reserve dropped. Once the spinning reserve was below 1.75MW, the fourth gas engine start was initiated. Before the fourth gas engine became available, the decrease in available PV power further reduced the spinning reserve to a minimum of 0.41MW. Once the fourth gas engine started, the sustained drop in PV power again caused the spinning reserve to drop below 1.75MW (instant “2” in Figure 42), which initiated the start of the fifth gas engine. As the clouds disappeared and the available PV power increased, the spinning reserve exceeded 3.75MW (instant “3” in Figure 42), and one of the five gas engines switched off and disconnected over a one minute period. A few minutes later, due to the sustained increase in PV power, the spinning reserve exceeded 3.75MW again, and another gas engine switched off. During this period of high spinning reserve, the average generator loading reached values below 50% (down to 42%). Once the period of stable available PV power of 4.78MW was reached, the system operated again with three gas engines, with an average generator loading of 56%.

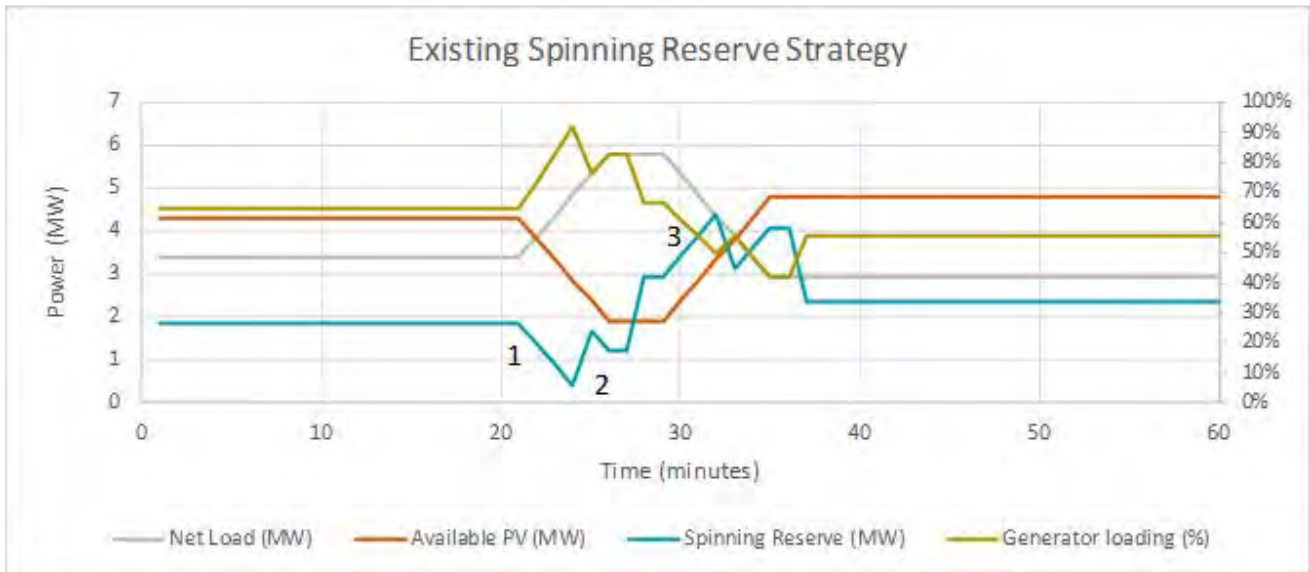


Figure 42. A hypothetical cloud event scenario and the existing spinning reserve strategy operation.

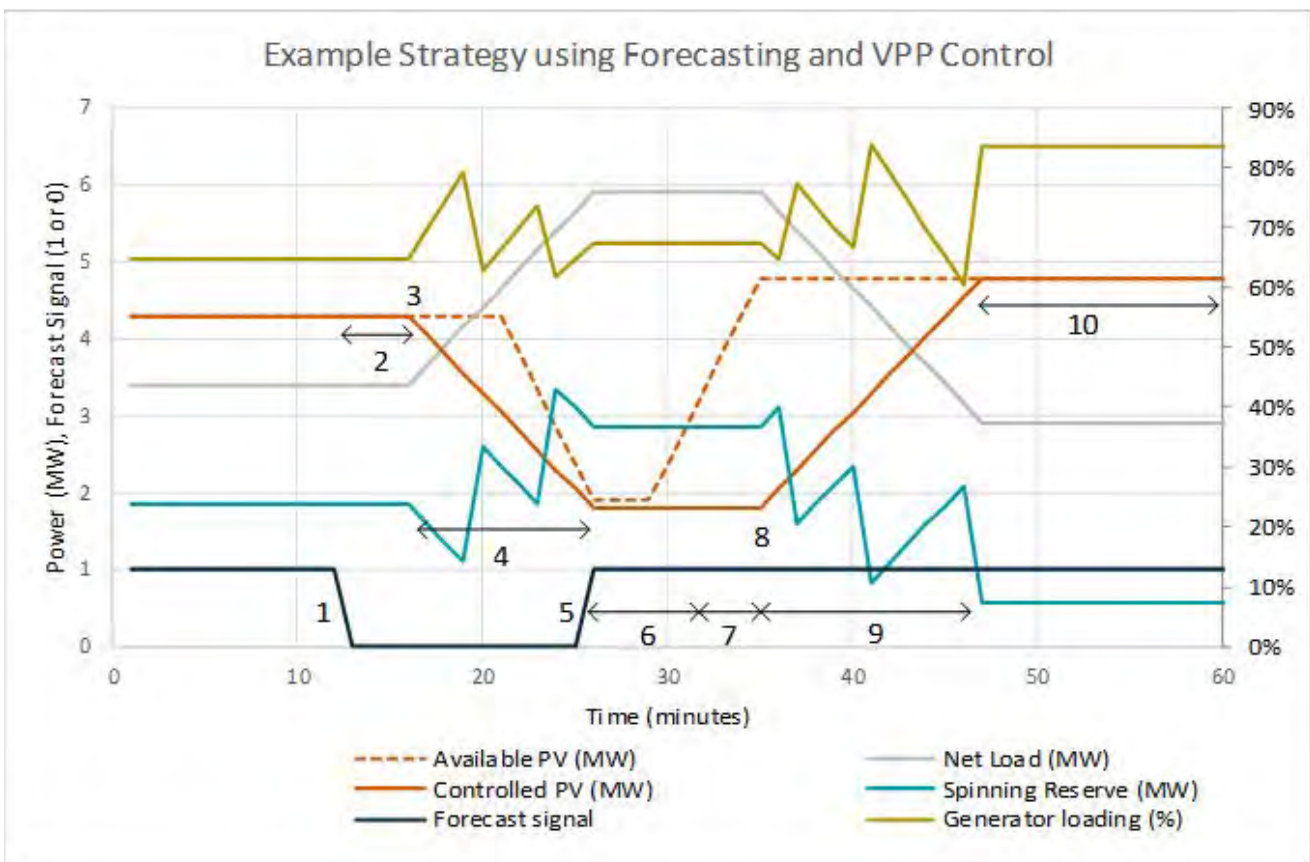


Figure 43. The hypothetical cloud event scenario and the application of an example spinning reserve strategy using a short-term solar forecasting system in combination with PV feed-in management and generation control.

Figure 43 presents the same cloud event but applied a spinning reserve strategy using a short-term solar forecasting system in combination with PV feed-in management and generation control. The strategy applied the forecast information to enable:

1. Pro-active ramping of managed PV and concurrent adjustment of spinning reserve during the cloud event while ensuring that average generator loading remains above or equal to 60%.
2. Operation at the reduced spinning reserve when extended clear sky conditions are detected.

At the beginning of the scenario, the initial operation of three gas engines with an average 65% loading was the same as before. At instant “1” in Figure 43, the forecasting system predicted a significant drop in 10 minutes. The system control consequently sent a VPP set point to pro-actively ramp down the amount of managed PV in the network. The prediction window of 10 minutes of the forecasting system was linked to the latency of the control system with respect to the ramping of these managed PV systems (period “2” in Figure 43). The Carnarvon DER Trials determined the latency of VPP control using Horizon Power’s Distributed Energy Resource Management System (DERMS) in combination with the Reposit system and found the response time of this control system (to begin ramping after a set point is sent) to be within five minutes (Trinkl 2020e). A latency of fewer than five minutes was assumed in this scenario. The setpoint value will depend on the amounts of managed and unmanaged PV on the network and the predicted drop. The ramping of managed PV commenced at instant “3” in Figure 43, and a ramp limit of 10%/min of nominal managed PV capacity (5MW) was observed during the ramp down. Based on the forecast and the implemented curtailment, generator starts were initiated so that that spinning reserve levels and average generator loadings ranged between 1.1-3.4MW and 62-79%, respectively (period “4” in Figure 43). At instant “5” in Figure 43, the forecast system predicted that stable PV generation would be available in 10 minutes. Nevertheless, the managed PV remained curtailed (period “6” in Figure 43), as the system observed a minimum time where changes to the selection of generation units remain in place (e.g. a minimum run time) while monitoring the solar forecasting information. Once the period of intermittent irradiance has passed, the managed PV can be released. Again, period “7” relates to the response time of the VPP control, followed by the start of the ramp-up at instant “8” in Figure 43. During the ramp-up (period “9” in Figure 43), generator stops were initiated based on the forecast and chosen ramp-rate. During the ramp-up, spinning reserve and generator loading ranged between 0.84-3.1MW and 65-84%, respectively. As the forecast system confirmed stable, clear sky conditions, the spinning reserve could be adjusted to allow for a more economical operation of fossil generation (period “10” in Figure 43). By running two gas engines only, the spinning reserve dropped to 0.58MW, resulting in 83% average generator loading (if three gas engines were operated instead, the spinning reserve would be at 2.3MW and average generator loading at 56%) during this final period of the scenario.

The application of the example strategy described above underlines the following benefits of a solar forecasting system in combination with PV feed-in management:

- Prior to cloud events, pro-active ramping of managed PV and knowledge of future available PV output, with a lead time that is greater than the start time of generators, allows for adjustment of the spinning reserve during cloud events while ensuring that generator loading remains at desirable levels.
- An accurate prediction of a sustained clear weather period allows for the operation of the power station with decreased spinning reserve. Given a suitable system load, this may result in significant fuel savings and operational benefits (reduced runtime of expensive generators).

The example strategy and its application to the hypothetical scenario are simplified and limited. Key aspects that are not considered are load changes and load forecast uncertainties. Horizon Power's previous work with IBM explored demand predictions in Carnarvon with 15-minute resolution. Demand forecasting models such as the one described in Appendix 3 will need to be improved and combined with short-term solar forecasting to enable the implementation of the example strategy.

The above example also does not consider the impact of batteries (power station integrated centralised batteries and/or distributed batteries, which can be unmanaged or managed by a supervisory system controller) and solar forecast uncertainties. Knowledge of the forecast uncertainty will improve the system control robustness and allow for adjustment of control decisions, if necessary. The next section provides insights into forecast uncertainties of an example skycamera based forecasting system, the WobaS system.

10 All-sky imager based nowcasting system WobaS

10.1 Introduction to the WobaS system

Solar irradiance can be highly variable over space and time, even for small time intervals, e.g. 15 minutes and within the area of a small town. To improve grid operation, irradiance maps and forecasts of such maps for approximately the next 20 minutes can be used. Forecasts with a forecast horizon of up to 6 hours or less are also called nowcasts. All-sky imagers (ASI) nowcasting systems can determine current and future irradiance maps, which can improve the operation of electricity grids with a high solar PV penetration. The basic principle of such nowcasting systems (Quesada. Ruiz et al., 2014, Kazantzidis et al., 2017, Blanc et al., 2017) is to take photos of the entire sky where clouds are detected. The cloud height can be detected by stereo photography, using two or more cameras, or similar approaches (e.g. Kassianov et al., 2005). This height information enables the computation of the 3D coordinates of the clouds and corresponding shadow maps, which can be transferred to irradiance maps with local irradiance measurements or clear sky models. The cloud movement vectors are derived from a series of images and are used to predict future cloud positions and irradiance maps. A variety of different methods to create these maps is available from the literature. The WobaS¹¹ nowcasting system uses one or more all-sky imagers to create global horizontal, global tilted and direct normal irradiance maps. A single-camera system can only provide accurate point forecasts for the location of the camera, beyond this area it requires another source of cloud height measurement, for example, a ceilometer at a nearby airport. Typical WobaS nowcasting systems use two ASIs, mounted at a distance of between 500 m and 2 km from each other. Mobotix Q24, Q25 or Q26 surveillance cameras with fisheye lenses are used (Figure 44, left). Every 30 seconds, new sky images with a 3 MP or 6 MP resolution are taken. An example all-sky image is shown in Figure 44 (right).

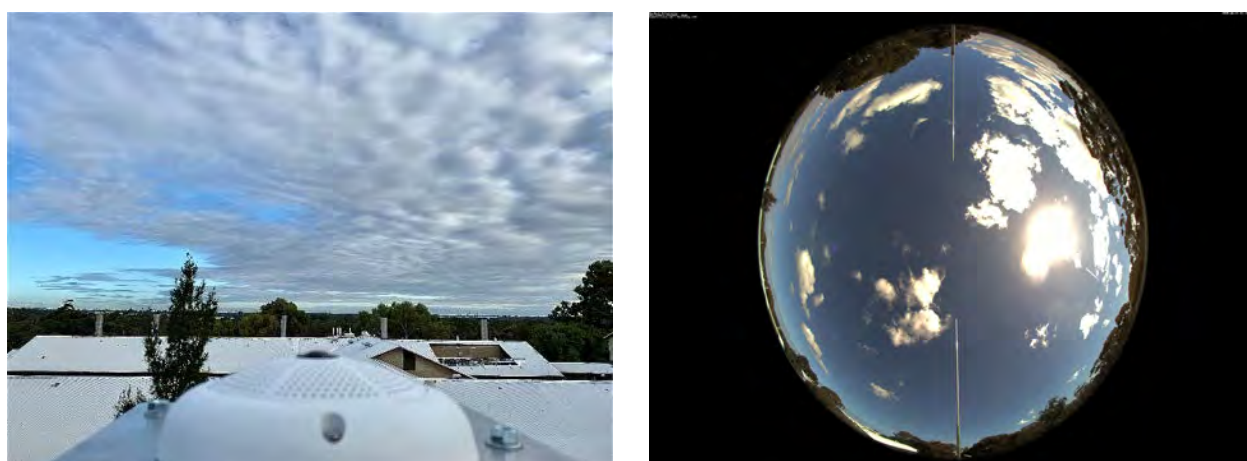


Figure 44. (Left) Mobotix all-sky imager at Murdoch University; (Right) all-sky image at Murdoch University.

The nowcasting software also needs access to irradiance data at the location of the camera. Direct normal irradiance (DNI), GHI and the diffuse horizontal irradiance (DHI) are used in the software with GHI and DNI either being measured or obtained from a model for the area where the camera is positioned. DHI can be estimated directly from photos. New nowcast results are created with each image series.

¹¹ WobaS stands for “Wolkenkamera basiertes Nowcasting System” (cloud camera based nowcasting system)

The nowcast results consist of irradiance maps with a spatial resolution down to 5 m for an area of up to 64 km² per ASI pair and lead times up to 20 minutes ahead. 21 maps are created for each evaluated image series with lead times from 0 to 20 minutes ahead in one-minute intervals. Figure 45 illustrates a DNI map with the corresponding clouds and the positions of the ASIs. Each detected cloud is treated as an individual object with distinct attributes such as geolocation, motion vector and transmittance. This enables nowcasts during complex and frequent multi-layer conditions. The processing chain of the nowcasting system can be described by eight distinct steps:

1. Clouds are segmented using a 4-D clear sky library (CSL) or a convolutional neural network (CNN), accounting for different atmospheric conditions see (Wilbert et al., 2016; Hasenbalg et al., 2020; Kuhn et al., 2017).
2. 3D cloud coordinates, including cloud height, are determined by a stereo photography block correlation approach with difference images (Nouri et al., 2019b).
3. Cloud motion vectors are derived from three sequential image series by a block correlation approach with different images from a single ASI (Nouri et al., 2019b).
4. Future cloud positions are predicted using the cloud motion vectors (Nouri et al., 2018).
5. Cloud transmittance properties are measured for a few clouds that shade the ASI (and the ground-based irradiance measurement station if available). For the remaining cloud objects, transmittance estimations according to their height are used. The estimations are based on a probability analysis of historical cloud height and transmittance measurements, and on recent transmittance measurements and their corresponding cloud height (Nouri et al., 2019c).
6. Cloud shadows are obtained through a projection of cloud objects on a topographical map with ray tracing (Nouri et al., 2018).
7. Shadow projections are combined with the clear sky irradiance and the cloud transmittance properties to spatial DNI maps (Nouri et al., 2018). GHI maps are derived using the DHI measurement, and a transposition model is used to derive the global tilted irradiance in the planes of interest.
8. Real-time uncertainties of the nowcasting system are determined (Nouri et al., 2019d).

The nowcasts are provided as data files and graphs about 12 seconds after the image acquisition for a common desktop PC (8x3.6GHz Intel Core i9-9900K, 2x16GB DDR4-2666 and PNY Quadro RTX 4000 8GB GDDR6).

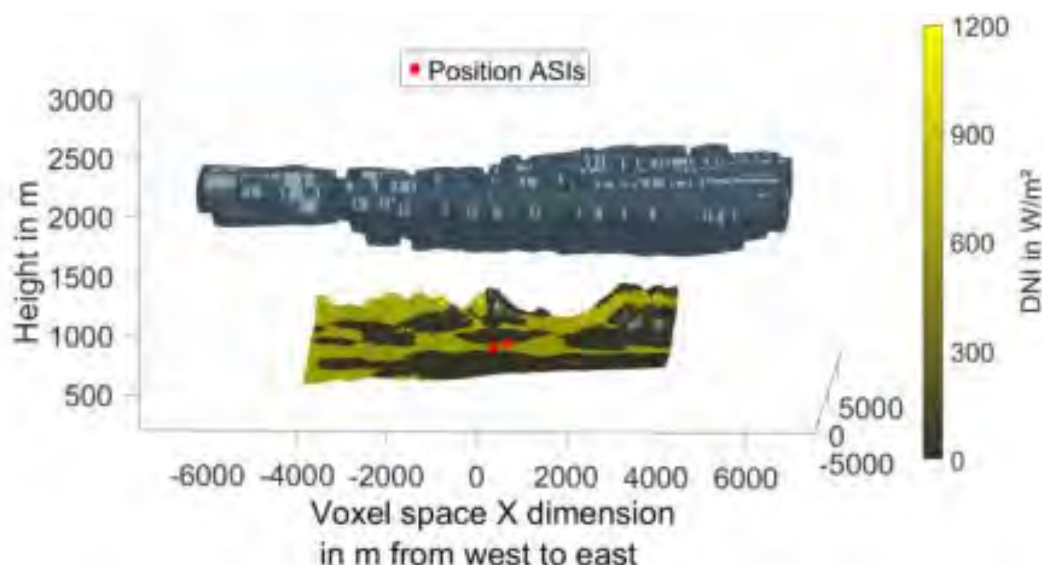


Figure 45. Cloud models and topographical map around CIEMAT's PSA with spatial DNI information.

10.2 General accuracy information for the WobaS System

For the application of ASI nowcasting, it is important to know its performance under all relevant atmospheric conditions at the site of interest. The WobaS system was tested at five different sites in Germany (Solar Tower Jülich and Oldenburg), Portugal (University of Evora) and Spain (CIEMAT’s Plataforma Solar de Almeria (PSA), La Africana 50MW solar power plant). In total, more than 4.5 years of data was analysed (Nouri et al., 2020). Currently, further systems are also being tested at Murdoch University in Australia and another site in the Arabian Peninsula. The system performance has been analysed for different atmospheric conditions. The performance of the system for Carnarvon was estimated based on the experience with these existing systems, as so far, no WobaS system has been installed in Carnarvon for a more direct performance assessment. After a short summary of the evaluations at the five sites, the findings and recommendations for Carnarvon will be presented.

The evaluation of the five sites used a set of ground-based DNI measurements at 1 min resolution as a reference. The average deviation between the reference irradiance and the nowcast for the corresponding pixel in each of the maps was calculated for every 1min interval. Mean absolute deviations (MAD), and root mean square deviations (RMSD) discretised over the DNI variability classes were then derived. The evaluation was done by separating the data in different temporal DNI variability classes from Schroedter-Homscheidt et al. (2018) Nouri et al. (2019d). The variability classes describe conditions ranging from the clear sky (class 1) to completely overcast (class 8) (Table 25). Figure 46 shows the results for different variability classes, and Figure 47 shows the overall results, considering the data of all classes.

Table 25. Description of DNI variability classes.

Class	General description of temporal DNI variability
1	Almost clear sky conditions with low temporal DNI variability and very high clear sky index
2	Almost clear sky with low temporal DNI variability and high clear sky index
3	Almost clear sky with intermediate temporal DNI variability and high/intermediate clear sky index
4	Partly cloudy with high temporal DNI variability and intermediate clear sky index
5	Partly cloudy with intermediate temporal DNI variability and intermediate clear sky index
6	Partly cloudy with high temporal DNI variability and intermediate/low clear sky index
7	Almost overcast with intermediate temporal DNI variability and low clear sky index
8	Overcast with low temporal DNI variability and very low clear sky index

The system was found to perform best for classes 1-3. Around 70% of the PSA data belong to such conditions. Deviations for more complex and variable (especially multilayer) conditions were higher, as it is more challenging to detect and model the clouds. However, overall, the ASI system outperformed a smart persistence nowcast that assumed that the Linke turbidity does not change during the next 20 min. The study showed that the nowcast errors within the same variability class and elevation angle interval were similar, independent of the evaluated site. This means that the expected average nowcast accuracy at a new site can be derived based on the measured performance at the five test sites. The deviations decrease as the solar elevation angle increases, as clouds close to the centre of the image can be analysed better. The remaining deviations within the different classes and elevation intervals can be explained by the effects of cloud height, cloud type, cloud speed, the image resolution, aerosol optical depth and the distance between the cameras. We expect that the conditions at the PSA are among the most challenging. PSA is about 30 km away from the Mediterranean Sea and surrounded by four mountain ranges, which leads to fast-changing complex conditions consisting of multiple layers of scattered cloud cover.

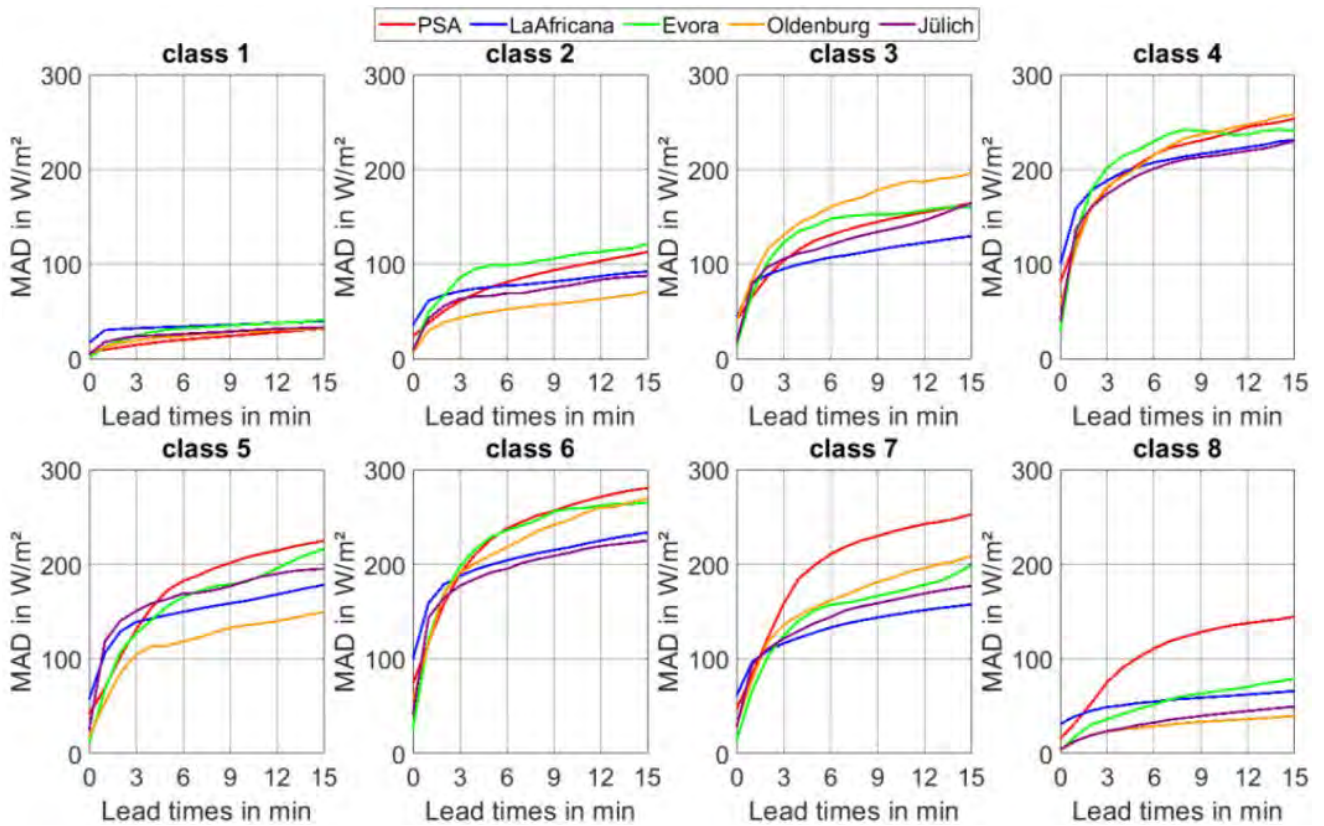


Figure 46. MAD for DNI at the 5 sites for different DNI variability classes (from Nouri et al., 2020).

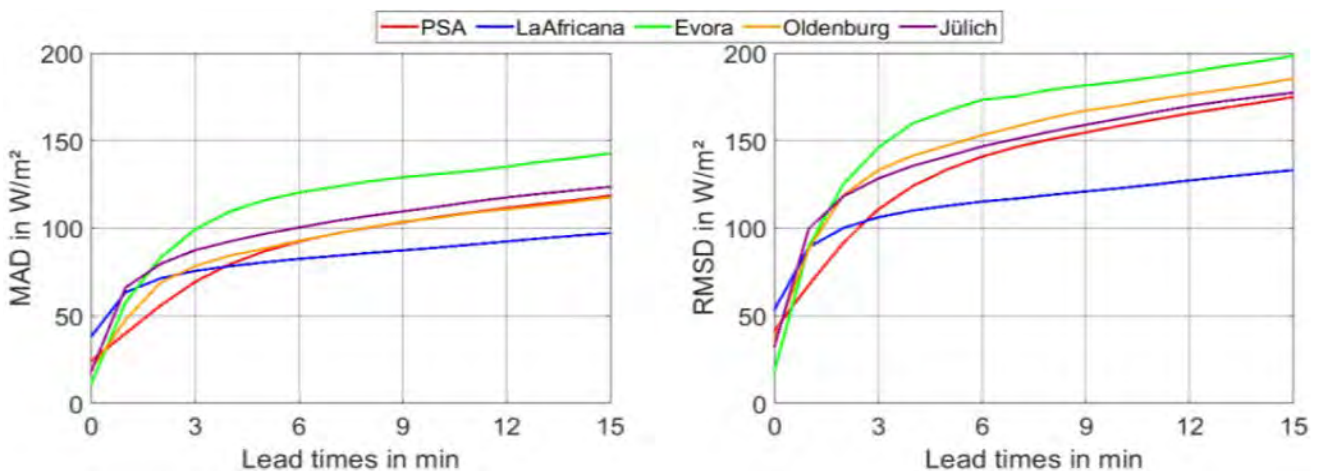


Figure 47. Overall MAD and RMSD for DNI at the 5 sites (from Nouri et al., 2020).

At PSA and Oldenburg, evaluations in terms of GHI are also available. The uncertainty for GHI is lower than that for DNI (Figure 48), as the GHI is influenced less by clouds than the DNI. For the plane of array irradiance, the uncertainty is between the DNI and GHI uncertainty and closer to the GHI uncertainty.

10.3 Accuracy estimation for Carnarvon

In order to convert these accuracy estimates to the case of Carnarvon, the latitude, typical cloud conditions and types and overall cloudiness at Carnarvon were considered in comparison to the already investigated sites. Carnarvon is much closer to the equator than the five sites (24.9°S vs. 37.1°N at PSA, the site among the five that is closest to the equator). This leads to much higher average solar elevation angles at Carnarvon and thereby a higher nowcasting accuracy. For the cloud types, a series of all-sky images obtained with a different camera system from Carnarvon were compared to WobaS images from the other sites. No specific cloud or aerosol conditions were found in these sky images, which were not already observed at the other sites.

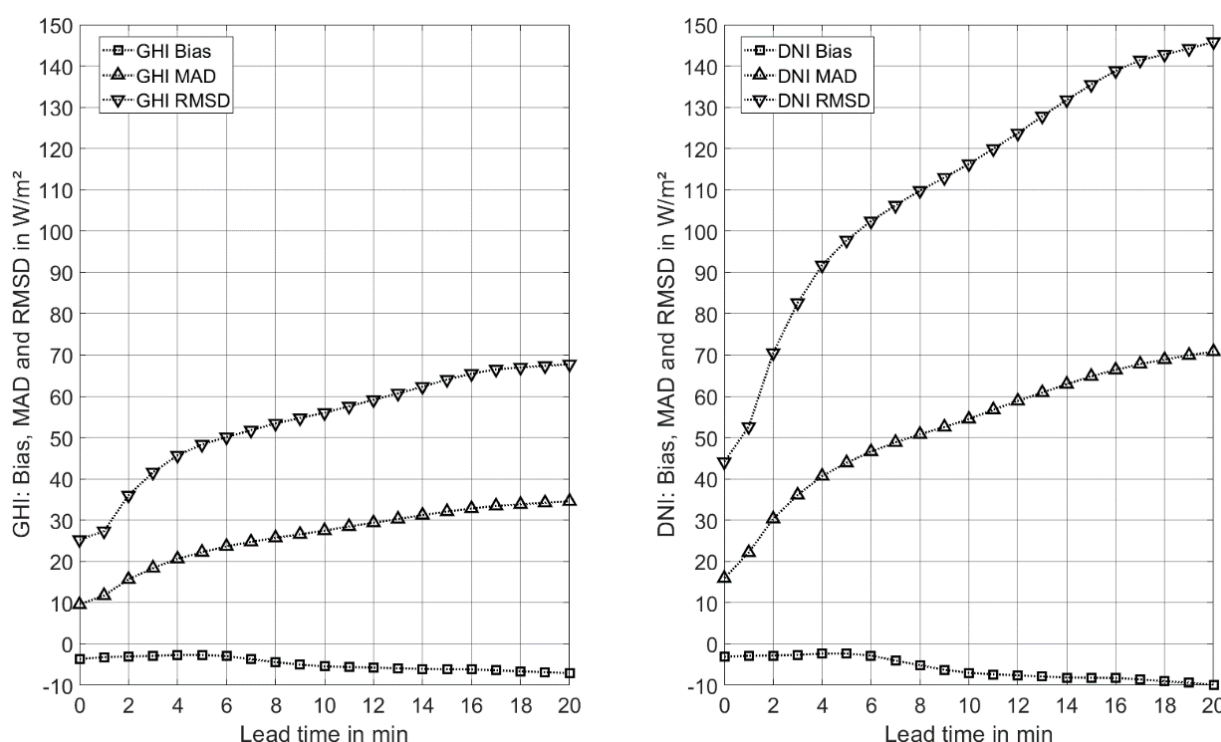


Figure 48. GHI and DNI error metrics for the ASI system at PSA (24.09.2019 to 28.11.2019). The error metrics are derived from a spatially averaged irradiance nowcast over an area of 1 km² and the averaged signal from 8 reference stations distributed within this area. Bias refers to the average deviation.

Additionally, a one-year long GHI time series from Carnarvon was evaluated and compared to the other sites. The GHI data revealed that Carnarvon is much less cloudy than the WobaS test sites. This is visualised in Figure 49, which shows the 1-minute GHI data as the colour plotted for the day of the year on the x-axis and the hour of the day on the y-axis. Missing data is shown in white. For PSA, cloudy periods in spring, autumn and winter are clearly visible with low GHI throughout great parts of those days and high GHI variation. The lower cloudiness in Carnarvon compared to the already investigated sites can also be seen in climate data. For example, (Meteoblue, 2020) states 14 to 24 sunny days per month for Carnarvon, but only 10 to 18 sunny days for PSA.

Therefore, we expect that the uncertainties will be lower overall for the WobaS system in Carnarvon than at the previously investigated sites. For a lead time of ten minutes, a temporal average of 1 min and without spatial averaging, we expect MAD well below 100 W/m² for DNI and below 60 W/m² for GHI.

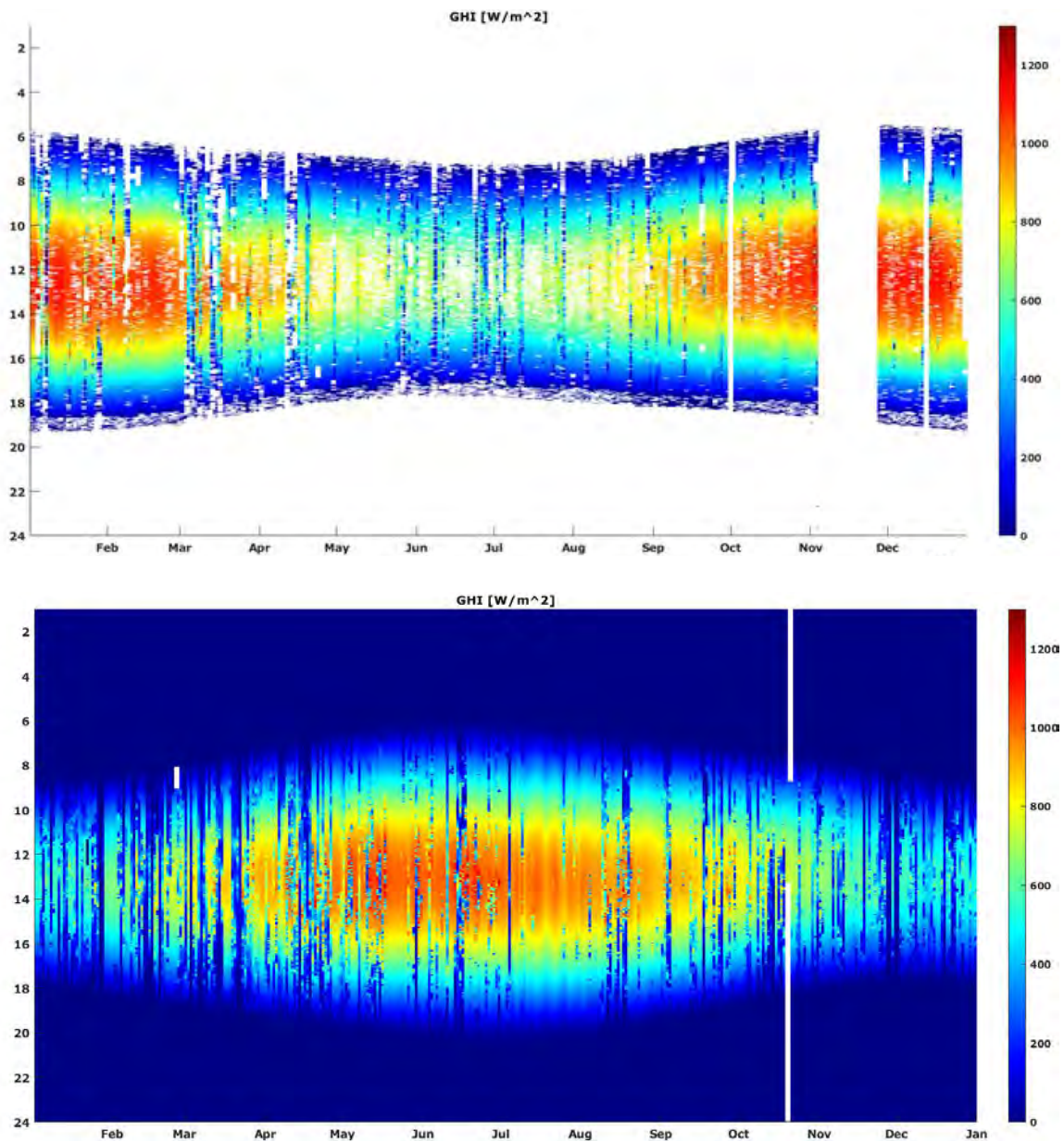


Figure 49. Colour-coded GHI plot with hour of the day on the y-axis and time within the year on x-axis for Carnarvon (upper plot, 2019) and PSA (lower plot, 2010).

10.4 Modelling aggregated PV generation from all-sky-imager based irradiance forecasts

WobaS provides the option to predict the plane of array (POA) irradiance for each PV installation, or each zone of a PV installation, separately. For this prediction, a CSV-table is passed to WobaS, which defines the properties of each PV installation by the geographic coordinates of its corner points, tilt angle, azimuth angle and the albedo of the surrounding near field. Based on a digital elevation model, WobaS then predicts mean POA irradiance and mean DNI for each of the defined areas, and for each forecasted time stamp. To also take into account the shading effect of nearby buildings, trees, etc., a higher resolution digital surface model can be considered (Tereci et al., 2009). These data sets are collected to create solar cadastres, and several companies offer the creation of this type of data.

With irradiance data specific to the orientation of the PV system, the resulting PV power can be modelled. For example, the pvlib toolbox (Holmgren et al., 2018) can be utilised to convert the irradiance data into the power output of each PV installation. If available, additional meteorological data and specific information on the PV system (especially specifications of modules and inverters) can be included. Otherwise, default values are applied. The cell temperature and temperature-dependent efficiency can be estimated based on ambient temperature, wind speed and the effective irradiance on the cell. Incidence angle effects and spectral losses can also be considered. Additionally, a soiling factor can be applied to account for optical losses due to dust or pollen on the modules. AC power output from the grid-connected inverter can then be modelled, considering the inverter’s present efficiency and clipping if the inverter is at its maximum rated power. Finally, for each timestamp, the AC power of all grid-connected PV installations in an area of interest can be added together to obtain the aggregated PV generation within that area.

10.5 System configuration for Carnarvon

The majority of Carnarvon’s PV systems are distributed within the area that can be covered by a WobaS system with one ASI pair located at East Carnarvon and Morgantown, for example as shown in Figure 50 (the location of the ASI indicated by the red crosses). The ASIs are about 1km apart from each other. The WobaS system covers about 8x8km² per camera pair. As some of the larger PV installations are located in the North and South Plantations, another ASI pair could be added (depicted as black crosses in Figure 50). The WobaS system is modular and can be enhanced by an arbitrary number of cameras to create a network (Blum et al., 2019). The cameras could be positioned on rooftops and powered either by small PV and battery systems or a 230V connection. The images of all cameras could be transferred to the evaluation computer via a 4G modem in the camera cabinet or via a LAN internet connection, if available.

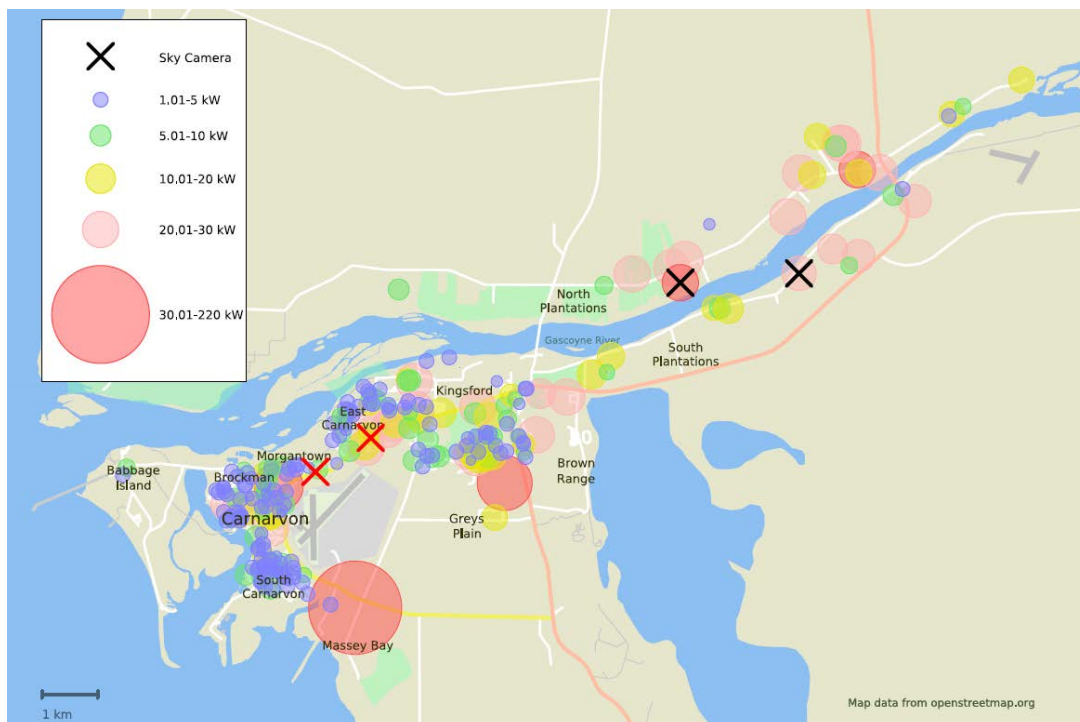


Figure 50. Example positions of two ASIs to cover Carnarvon’s PV systems.

11 Hosting capacity calculation approaches

11.1 Horizon Power's existing approaches to calculating hosting capacity

11.1.1 Calculation of power system hosting capacity

Horizon Power uses and assesses a range of deterministic criteria to calculate the overall total hosting capacity for its power system, including the:

- Operational reserve and step load criteria
- Maximum loading criteria
- Minimum loading criteria

The operational reserve and step load criteria seek to ensure that the real power fluctuations of renewable energy installations on Horizon Power's systems do not exceed the operating reserve and step load capability available on those systems. These criteria include a renewable energy fluctuation factor, which is a measure of the amount of fluctuation, associated with renewable energy systems, seen at the power station when considering issues such as PV system diversity, the effect of cloud events and maximum renewable installation output ranges.

The operational reserve and step load criteria also consider the effect of both unmanaged DER and managed DER. Unmanaged DER has no associated remote control or communication. Managed DER includes various forms of generation control, such as Feed-in Management (FiM) or renewable energy smoothing, which reduce the variability and improve the controllability of those installations. Typically, managed installations have a reduced impact on the power system and allow for an increased level of hosting capacity. The technical requirements for managed and unmanaged DER installations are covered in Horizon Power's DER Technical requirements, available at www.horizonpower.com.au.

The maximum loading criteria seek to ensure that the maximum capacity of installed generators on Horizon Power's systems are not exceeded when dispersed renewable energy installations are operating at minimum output.

The minimum loading criteria seek to ensure that the minimum loading capability of installed generators on Horizon Power's systems are not exceeded at times of minimum day time load and high renewable installation output.

Consideration of the most limiting criteria gives rise to the total hosting capacity limit. The total hosting capacity provides a clear indication of the maximum amount of renewable energy that can be connected to each electrical system.

In addition to the deterministic criteria identified, power system network and dynamic stability studies are undertaken to identify hosting capacity limits. These power system studies may identify additional constraints or additional available hosting capacity.

11.1.2 Calculation of local network hosting capacity

The hosting capacity at any point on the network is determined by the most limiting of the following criteria:

- Voltage regulation
- Thermal ratings
- Fault levels
- Power quality
- Voltage stability
- Voltage flicker

Appropriate simulation tools and models are required to calculate hosting capacity for all relevant nodes. The highest DER capacity that meets all of the applicable criteria is the hosting capacity of the network. Within the simulation model, steady-state load flow studies are conducted for a suitable range of credible operational scenarios, including minimum, maximum and typical load and generation patterns on the network. Voltage and network loading violations are assessed, taking note of the maximum capacity that does not violate network limitations at any point of the network. Typical equipment under consideration include transformer, cables and overhead lines. As part of the network studies, analysis is undertaken to ensure maximum network fault levels do not exceed plant ratings and the minimum network fault levels do not compromise the minimum required fault levels to enable adequate operation of protection systems. Power quality checks are also completed, including an assessment of harmonic content limitations, and voltage flicker limitations, noting the maximum capacity that does not violate network limitations at any point of the network.

11.2 Suggested hosting capacity calculation approach

Horizon Power's existing methodologies to calculate renewable energy hosting capacity, as described in the previous sub-sections and in (Edwards and Tayati 2013), have primarily focused on system-level impacts, i.e. impacts related to spinning reserve and generator loading capability, generator start times and generator step load capabilities. In order to achieve very high levels of distributed renewable energy generation in remote networks, local issues and adverse effects at distribution network levels become increasingly important to address. The voltage studies performed as part of the Carnarvon DER Trials have confirmed that voltage rise issues exist in some LV networks and will increase as PV penetration rises. Hence, to determine hosting capacity in remote networks, an approach is required which includes the LV distribution network perspective and considers adverse impacts at a local level as well as at the system level.

There are different approaches to calculate the hosting capacity in LV networks as described in the literature (e.g., deterministic, stochastic, time-series based). Each method has its own advantages and disadvantages. The method shown in Figure 51, adopted from Navarro-Espinosa et al. (2016), is suggested here to calculate the hosting capacity for a Carnarvon LV network. Random load profiles can be generated for the customers based on historical load profiles (using AMI data). Similarly, PV profiles can be generated using data from the irradiance sensor. The Monte Carlo method can be used to generate the random profiles of the load and PV. The PV systems and capacity can be randomly assigned to the customers according to the considered PV penetration level. Any platform (e.g., MATLAB, Python, DPL) can be used to create the load and PV profiles, which are then applied to the network for a load flow analysis to calculate the impact metrics. For each PV penetration level, the load flow analysis is performed for a number of scenarios from the randomly created load and PV profiles. CDFs are calculated at each penetration level to determine the probability of violation of a metric's limit.

The process is repeated for increasing PV penetration levels and, finally, the CDFs are investigated to identify the probability of violating the limits of the impact metrics for each PV penetration and to select the level as the hosting capacity, which has acceptable probability of violating the limits of the impact metrics.

It is important to identify the impact metrics and their limits. In the literature, voltage violations and asset overloading are primarily considered among the parameters limiting the hosting capacity. In addition, protection, power quality and power losses are also considered. However, the impact metric for a parameter can be defined in several ways, based on the utility's technical requirements. For example, in Navarro-Espinosa et al. (2016), the impact metrics to consider the voltage violation is calculated as the number of non-compliant nodes (based on the technical requirement of the network operator).

The approach described above determines the hosting capacity for one LV network. The process needs to be repeated for other LV networks. Once all of the LV network hosting capacities are determined, the impact of these hosting capacities needs to be studied at the HV feeder level and system level to determine the remote system's hosting capacity.

This approach also allows for the examination of methods to increase PV hosting capacity and DER integration, which can be implemented as part of the studies performed at LV network, HV feeder and system levels. Cost optimisation simulation tools, models and processes can be used in conjunction with these studies to assess the cost-benefit of methods to increase PV hosting capacity and DER integration.

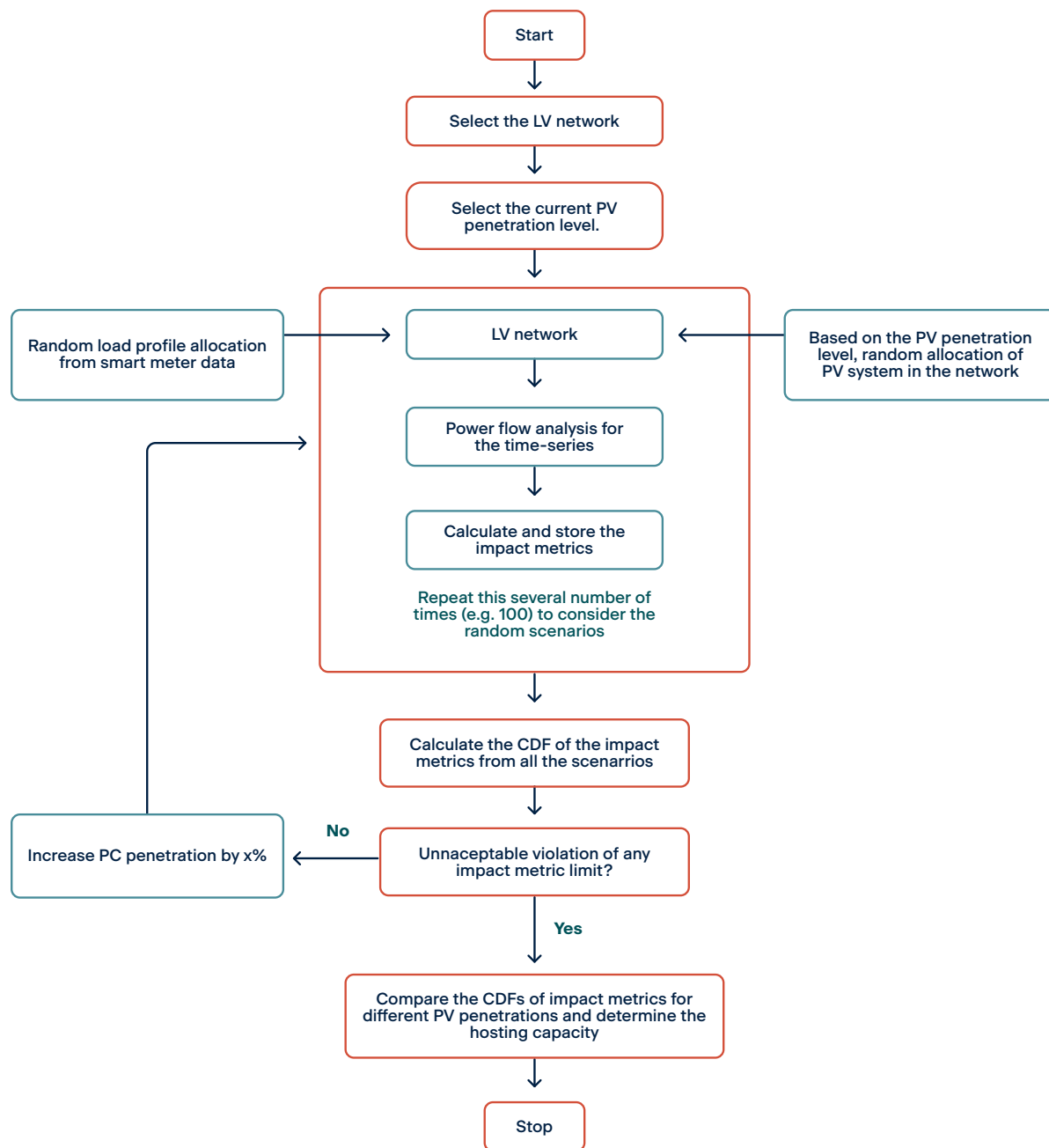


Figure 51. Flowchart of a stochastic approach to determine the PV hosting capacity of an LV network.

The approach presented in Figure 51 will provide the probable maximum PV capacity an LV network can host. However, further studies may be required to assess the impact of a PV connection to a specific node in a network. The *IEEE Guide for Conducting Distribution Impact Studies for Distributed Resource Interconnection* (IEEE 2014) provides a comprehensive resource for such studies. The document provides detailed guidance on review criteria, when certain impact studies are appropriate, the data requirements for the impact studies, how they should be performed and how the results should be evaluated. The types of studies covered range from preliminary review and conventional studies to special system impact studies.

The German standard VDE-AR-N 4105:2018-11 “Generators connected to the low-voltage distribution network – Technical requirements for the connection to and parallel operation with low-voltage distribution networks” (Verband Deutscher Elektrotechniker 2018), outlines the process followed to perform a network connection evaluation of a power generation system performed by network operators in Germany. Annex D of the standard provides an example for a 20kW PV system connection evaluation, which considers the impedance of the network at the Point of Common Coupling (PCC), the maximum apparent connection power and the type and operating mode of the power generation system or storage unit. The evaluation verifies the permissible slow voltage change of 3% (as defined in the standard) and establishes if the rating of electrical equipment with respect to constant current and short-circuit currents is suitable. The evaluation also verifies other aspects of system interaction, for example, rapid voltage change (by considering maximum switching current factors), flicker and harmonics.

An alternative approach to calculating the hosting capacity is provided by a tool in DigSILENT PowerFactory (available since the 2019 version). A measure of the network hosting capacity is calculated by applying DER to one node at a time and increasing the PV generation injected at the node until a metric is violated (DigSILENT 2019). This tool represents an upper limit of the amount of PV capacity that can be connected to distribution feeders without violating system constraints and without any network expansion. Therefore, given a performance or system robustness index, the tool can automatically identify the hosting capacity limit of the feeder and report the limiting factors of the hosting capacity for each node. In terms of the system constraints, this tool can consider voltage limits, overloading and power quality.

12 Recommendations

This section provides recommendations for managing different aspects of DER based on the work done within the project and relevant literature and practices.

Several recommendations resulting from the voltage studies and associated project work are provided below:

- Recommendations to overcome voltage issues need to be network segment specific and based on individual LV network behaviour. Distribution transformer tap setting changes are suggested for networks where there are clear trends, i.e. occurrence of high voltage events only or occurrence of low voltage events only. On networks with both high and low voltage events, network-specific studies into voltage rise mitigation measures are recommended. In such cases, effective use of voltage response mode capabilities of inverters becomes increasingly important. Further solutions could include the use of distribution transformers with online tap changing and line drop compensation capabilities or network reinforcements, specifically for networks where infrastructure replacements are scheduled.
- To maximise the benefits of the voltage response modes (i.e. Volt-Watt and Volt-VAr) of inverters which meet AS/NZS4777.2:2015, measures need to be in place to ensure that DER inverter settings are set appropriately. These include:
 - Maintaining a detailed DER registry: A database containing the DER documentation (including connection phase information) should be established and maintained for each LV network.
 - Ensuring that appropriate DER inverter settings are implemented: Utilities should put all efforts on ensuring that appropriate inverter settings are implemented, that efficient DER data collection and data storage processes are in place and that compliance with standards is monitored.
- Load and PV generation phase balancing should be explored as a measure to reduce voltage issues and voltage imbalance on LV networks. For three phase inverters or single-phase inverters used in a three-phase combination the voltage balance mode is recommended to be enabled.

Horizon Power must broaden its communications to include DER system retailers, suppliers and installers, especially those resident and operating in the Southwest Interconnected System (SWIS) serviced by Western Power and Synergy, where different inverter settings are required.

In addition, Horizon Power must seek to:

- Close the loop with regards to the installer applications to ensure application requirements are implemented
 - Installers could be required to provide evidence upon installation that the systems have been installed correctly. This could include photos of the installation as well as the settings.
- Developing processes to ensure that PV-inverter systems which are replaced due to age related failure or product defect comply with the Horizon Power technical requirements and AS 4777 standard in force at the time of replacement, and that Horizon Power's records are updated accordingly.
- Developing customer contact and follow up processes to ensure any non-compliant systems identified in future audits are rectified.
- Implementing PV inverter system audits and follow up processes into Horizon Power's Business as Usual (BaU) practices.
- Work with industry and relevant organisations to raise awareness through improved engagement and professional development programs.

- Work with relevant industry working groups and OEMs to develop the ability for the utility to remotely read/set inverter settings, not only the inverter manufacturer. Advocate to include this as part of AS4777.
- Investigate the privacy implications of capturing customer's inverter passwords and create a process for doing so.
- The hypotheses around the ToU tariff have been validated for one system on one property only. The next step would be to implement the same tariff structure and system on multiple properties to ensure the same outcome. An option would be to implement this structure on all (or as many as possible) of the DER systems on one transformer and observe the difference in power and energy flow at a transformer level.
- It may be more cost-effective for Horizon Power to subsidise customer batteries to avoid network augmentation. This possibility requires further investigation.
- It was not possible to implement MyPower¹² in the current Reposit product. The dynamic nature of this tariff product offering renders it non-standard in the banded tariff space, this may be an issue for most smart devices. Further investigation is required.
- In networks where voltage rise issues and phase imbalance are limiting hosting capacity, solutions could include the use of in front of the meter grid-scale batteries (e.g. community batteries), which can provide voltage regulation and load balancing services (Wang et al. 2019). Given the demonstrated consumer and private investor preferences through the uptake of DER on the Carnarvon network, in-front of the meter batteries can enable more customers to continue to connect DER. Furthermore, these batteries could be sized to maintain continuity of supply in islanded microgrid mode during system faults/supply interruptions. Implementation of in-front of the meter batteries is in line with suggested actions of the recently released WA Climate Policy (Government of Western Australia 2020), which lists deployment of utility batteries in regional communities to enable more households and businesses to install solar PV systems as part of the Energy Transformation Strategy.

General recommendations arising from the Carnarvon DER Trials include:

- Inverter tests performed as part of the Carnarvon DER Trials led to several recommendations towards the development of the AS/NZS4777.2 in a variety of areas. Given the potential impact on system stability in microgrids during widespread inverter tripping events (which were observed during the Carnarvon DER Trials), it is essential to ensure that inverters can ride through rapid frequency changes and large load switching induced phase shifting of the network voltage without disconnection from the network.
- It is recommended that utilities engage in activities that investigate and demonstrate the technical capabilities of VPP's. Specifically, research into the integration of VPP control into power system management and control in combination with load and renewable energy resource forecasting and centrally controlled battery systems for operational reserve management is recommended.
- As distributed renewable energy penetration and the uptake of DER increases, visibility, control and situational awareness of DER on the distribution network will become more and more important for maintaining a reliable electricity supply. For example, studies performed during the Carnarvon DER Trial project highlighted:
 - Visibility of localised voltage issues is necessary for implementing effective voltage rise mitigation approaches.

¹² <https://www.horizonpower.com.au/mypower/>

- Situational awareness of DER is necessary for estimating system wide power fluctuations caused by DER.
- Operational reserve regimes incorporating short term solar forecasting in combination with PV feed-in management can provide benefits such as reduced fuel consumption and increased hosting capacity.
- Utilities should invest in developing tools for visualising and controlling LV network flows with controllable DER.
- To achieve very high levels of distributed renewable energy generation in remote networks, local issues and adverse effects at distribution network levels become increasingly important to address. The voltage studies performed as part of the Carnarvon DER Trials have confirmed that voltage rise issues exist in some LV networks and will increase as PV penetration rises. Hence, to determine hosting capacity in remote networks, new approaches are required, which include the LV distribution network perspective and consider adverse impacts at a local level, as well as at the system level.

13 Summary

This Technical Report # 2 covers further work on the Carnarvon DER trials in a range of areas and key findings are summarised below.

Unmasking of load for a subset of the Carnarvon load demonstrated that fluctuations seen in the net load are largely due to cloud shading induced PV generation fluctuations. Also, the largest unmasked load for this load subset occurred mainly in the summer months and around the middle of the day. This may reflect that these particular consumers are proactively using PV generated power when it is available.

Minimum load in Carnarvon occurred on 8th June 2019 at 14:09. This appeared to be not significantly impacted by PV generation due to the PV capacity being only 1MW in association with the misalignment in time between minimum load and maximum irradiance. The next two lowest load minimums had very similar characteristics, and load levels with one of these in August 2019, at a time by which more PV hosting capacity had been released.

A closer investigation into voltage variations at specific sites on two LV networks has been performed for sample cloudy and clear days. The voltage varied with the PV output power following the cloud events. However, the extent of the variation may depend on the simultaneous load variation, network topology, lead-in cable and distance from the transformer. Some sites are more prone to reaching higher voltages often compared to others. Inverter trips were observed during periods of higher voltages. The adopted measures to mitigate voltage issues need to be selective and based on individual LV network behaviour. Horizon Power is already analysing the application of power quality response modes and phase balancing to mitigate voltage rise issues. An inverter settings audit on the respective network is also in place.

In response to the inverter trips that were observed during periods of high voltage in the LV network, the Horizon Power project team started to explore the potential of applying advanced analytics to customer meter data in order to identify single phase solar PV systems that would benefit from being re-allocated to other network phases that are less congested and with fewer high voltage excursions. Synchronised 1-minute interval data was collected and then analysed using constrained k-means clustering to develop a process to identify single-phase PV systems on the network and their impact on system voltage at times of peak solar insolation. The constrained k-means algorithm was found to complete the phase identification with a high accuracy. Overall, the results from this study have shown that phase identification enables the balancing of DER in the network, improving the outlook for hosting capacity by reducing the peak voltage events that can cause inverter trips.

An audit of approximately 135 inverters from residential and commercial PV systems in Carnarvon was carried out by the Horizon Power project team to check for compliance with Horizon Power's technical requirements. The inverter audit was prompted by the unexpected behaviour of legacy PV systems in the town, which was observed during the LV network voltage study, i.e. inverters tripping multiple times a day. Results from the inverter audit to date indicate there is a problem with the installation of inverters in Horizon Power's system, particularly with inverter settings and FiM compliance. Out of the 135 inverters that were audited, only 2 could be confirmed as compliant. A combination of installers being unaware of Horizon Power's technical requirements and a lack of accountability for non-compliant installations are identified as potential causes to the low rate of compliance. Visibility and control of Solar PV was explored through a series of extensive experiments carried out by Horizon Power on the battery/PV systems with Reposit boxes used for the Carnarvon Trials 1 and 2. Table 10 and Table 11 provide summaries, key findings and observations on these experiments, which were completed during the trials and covered pre-requisite functions, basic control of an individual node and basic control and administration of VPPs. The basic functionality of the Reposit system was tested in terms of the acquisition of data, data quality, loss of communications and its effect on VPP operation and prosumer internet service data volumes (Table 10).

Tests covering basic control of DER energy storage and VPPs examined direct battery control via battery dispatch, VPP configuration and control testing for correct VPP operation and feed in management (for export limit). A further experiment investigated the Reposit's grid credit system and finally, a series of experiments around power quality response mode functionalities (DER network support) and specifically the Volt-VAR response mode to mitigate voltage rise was also performed (Table 11). Time to respond, ramp rates and how accurately does the system achieve the desired setting or setpoint are recurring themes in a number of the experiments involving VPPs and are important considerations from a system control point of view. Of importance was that VPPs behave in the desired manner, which is the net export power adjusts to a Reposit node setpoint within 5 minutes. Experiments on VPP configuration and control and the export limit feed in management demonstrated the Reposit product as an attractive solution to DER from the prosumer and network operator perspective.

Time of Use tariffs can be an effective means of managing a battery system connected behind the customer meter for customers who are not in a position to significantly change their consumption behaviour. The experiment that was carried out to test the effectiveness of the ToU tariff structure found that the behaviour of the DER system was influenced by the application of the ToU tariff. An optimised outcome that benefited the customer and Horizon Power could be achieved through the application of the tariff structure. The customer benefited from a lower electricity bill (assuming they were actually on the nominated ToU tariff), whilst Horizon Power benefited from reduced power and energy consumption during the afternoon/evening peak.

Spinning reserve control strategies can be used to manage increased PV penetration in Carnarvon and accommodate for changes in PV generation due to cloud shading of distributed PV. The relevant background on the generation and operating philosophy for the Mungullah Power Station and a description of the existing spinning reserve strategy has been provided. PowerFactory simulation studies investigated the impact of cloud events on the system performance to identify limiting factors on the design of an effective and reliable spinning reserve control strategy. The simulations demonstrated that the frequency regulation capability of the Mungullah Power Station is not affected by PV cloud shading induced power ramping as long as reserve capacity is available, and reverse power flow is avoided. However, with the 3-minute start time of the gas generators, under very high penetration scenarios, the power ramp-rate will be problematic, causing a shortfall in available time to start the next gas engine generator. The estimated installed PV capacity thresholds where this will occur have been provided.

A potential spinning reserve strategy using PV feed-in management and short-term solar forecasting has been presented and has been contrasted in its operation against the existing spinning reserve strategy by using a hypothetical cloud event scenario. The application of the strategy under this scenario highlights the following benefits of using a solar forecasting system in combination with PV feed-in management:

- Proactive ramping of managed PV and knowledge of future available PV output prior to cloud events with a lead time that is greater than the start time of generators, allowing for adjustment of the spinning reserve during cloud events while ensuring that generator loading remains at desirable levels.
- Accurate prediction of a sustained clear weather period, allowing for the operation of a power station with decreased spinning reserve, which can result in significant fuel savings and operational benefits.

The potential strategy is simplified and limited in that it does not consider the impact of batteries, load changes and load forecast uncertainties as well as solar forecast uncertainties. Knowledge of the forecast uncertainty will improve the system control robustness and allow for adjustment of control decisions, if necessary.

An example skycamera based forecasting system, the WobaS system has been presented to provide insights into forecast uncertainties. WobaS provides the option to predict the plane of the array irradiance for each PV installation, or each zone of a PV installation, separately. With irradiance data specific to the

orientation of the PV system, the resulting PV power can be modelled. The performance of the system for Carnarvon was estimated based on the experience with five existing WobaS systems in Germany, Portugal and Spain. Carnarvon is much closer to the equator than the five sites, leading to much higher average solar elevation angles at Carnarvon and thereby a higher nowcasting accuracy. Furthermore, GHI data reveals that Carnarvon is much less cloudy than the WobaS test sites. Therefore, the uncertainties are expected to be lower overall for the WobaS system in Carnarvon than at the previously investigated sites. Specific recommendations for the placement of skycameras in Carnarvon for the inclusion of a WobaS system into power system control have been provided.

Horizon Power's existing methodologies to calculate renewable energy hosting capacity have primarily focused on system-level impacts, i.e. impacts related to spinning reserve and generator loading capability, generator start times and generator step load capabilities. To achieve very high levels of distributed renewable energy generation in remote networks, local issues and adverse effects at distribution network levels become increasingly important to address. The voltage studies performed as part of the Carnarvon DER Trials have confirmed that voltage rise issues exist in some LV networks and will increase as PV penetration rises. Therefore, to determine hosting capacity in remote networks, an approach is required which includes the LV distribution network perspective and considers adverse impacts at a local level as well as at the system level. A stochastic approach to determine the PV hosting capacity of an LV network as presented in this report is suggested. The process would need to be repeated for other LV networks. Once all LV networks' hosting capacities are determined, the impact of these hosting capacities need to be studied at the HV feeder level and system level to determine the whole remote system's hosting capacity. This approach also allows for the examination of methods to increase PV hosting capacity and DER integration.

14 References

- Blanc, P., Massip, P., Kazantzidis, A., Tzoumanikas, P., Kuhn, P., Wilbert, S., Schüler, D. and Prah, C. (2017). ShortTerm Forecasting of High Resolution Local DNI Maps with Multiple Fish-Eye Cameras in Stereoscopic Mode AIP conference Proceedings 1850. doi: 10.1063/1.4984512
- Blum, Niklas, Thomas Schmidt, Bijan Nouri, Stefan Wilbert, Esther Peerlings, Detlev Heinemann, Thomas Schmidt, et al. (2019). "Nowcasting of Irradiance Using a Network of All-Sky-Imagers." Paper presented at the EU PVSEC 2019 Proceedings, Marseille.
- Bruce, M. (2012). Operating Philosophy for Mungullah Power Station DM# 3534657, Horizon Power.
- Dickeson, G. (2020). "Final evaluation report for SETuP Skycamera Trial". Power and Water Corporation Solar Energy Transformation Project. Ekistica.
- Calais, M., et al. (2020). Development, testing, implementation and analysis of PV generation and feed-in management control methodologies in Carnarvon. Deliverable 10. Distributed Energy Resources (DER) Trials in Carnarvon.
- Glenister, S., et al. (2019a). Development of spinning reserve control strategies during cloud events, using PV generation management, PV feed in management and short term solar forecasting tools. Deliverable 4. Distributed Energy Resources (DER) Trials in Carnarvon.
- Glenister, S., et al. (2019b). Statistical assessment of the impacts of time of day and seasonal weather variation on PV generation at different levels of penetration in Carnarvon. Deliverable 2. Distributed Energy Resources (DER) Trials in Carnarvon.
- Glenister, S., et al. (2020). Statistical assessment of the impacts of time of day and seasonal weather variation on PV generation at different levels of penetration in Carnarvon. Deliverable 7. Distributed Energy Resources (DER) Trials in Carnarvon.
- Hasenbalg, M., P. Kuhn, S. Wilbert, B. Nouri, and A. Kazantzidis. (2020). "Benchmarking of Six Cloud Segmentation Algorithms for Ground-Based All-Sky Imagers." *Solar Energy* 201 (2020/05/01/ 2020): 596–614. <https://doi.org/https://doi.org/10.1016/j.solener.2020.02.042>
- Holmgren, W., C. Hansen and M. Mikofski (2018). "pvlib Python: A python package for modelling solar energy systems." *Journal of Open Source Software* 3(29): 884.
- Kassianov, E., Long, C.N. and Christy, J. (2005). Cloud-base-height estimation from paired ground-based hemispherical observations. *J. Appl. Meteorol.*, 44 (8), 1221–1233. doi: 10.1175/JAM22771.
- Kazantzidis, A., Tzoumanikas, P., Blanc, P., Massip, P., Wilbert, S., Ramirez-Santigosa, L. (2017). Short-term forecasting based on all-sky cameras. In *Renewable Energy Forecasting*; Kariniotakis, G., Ed.; Elsevier Science., 153–178.
- Kerrigan, R. (2012). Generation Philosophy for Horizon Power's Systems 3436691 Bentley, Horizon Power.
- Kuhn, P., Nouri, B., Wilbert, S., Prah, C., Kozonek, N., Schmidt, T., Yasser, Z., Ramirez, L., Zarzalejo, L., Meyer, A., Vuilleumier, L., Heinemann, D., Blanc, P. and Pitz-Paal, R. (2017). Validation of an all-sky imager based nowcasting system for industrial PV plants, *Prog Photovolt Res Appl.*, 1-14 (2017). doi: 10.1002/pip.2968
- Meteoblue. (2020). https://www.meteoblue.com/de/wetter/historyclimate/climatemodelliert/tabernas_spanien_2510746 and https://www.meteoblue.com/en/weather/historyclimate/climatemodelliert/carnarvon_australia_2074865, last accessed 20.10.2020.
- Moghbel, M., et al. (2019). Technical Report #1. Carnarvon Distributed Energy Resources (DER) Trials. Horizon Power.

- Nouri, B., Wilbert, S., Blum, N., Kuhn, P., Schmidt, T., Yasser, Z., et al. (2020). "Evaluation of an All Sky Imager Based Nowcasting System for Distinct Conditions and Five Sites." In solarPaces 2019 conference proceedings published in AIP conference proceedings 2020.
- Nouri, B., Wilbert, S., Kuhn, P., Hanrieder, N., Schroedter-Homscheidt, M., Kazantzidis, A., Zarzalejo, L., Blanc, P., Kumar, S., Goswami, N. and Shankar, R. (2019a). "Real-time uncertainty specification of all sky imager derived irradiance nowcasts." *Remote Sensing*, 11(9): 1059.
- Nouri, B., Kuhn, P., Wilbert, S., Hanrieder, N., Prah C., Zarzalejo, L., Kazantzidis, A., Blanc, P. and Pitz-Paal, R. (2019b). Cloud height and tracking accuracy of three all sky imager systems for individual clouds. *Sol. Energy* 177, 213–228. doi: 10.1016/j.solener.2018.10.079
- Nouri, B., Wilbert, S., Segura, L., Kuhn, P., Hanrieder, N., Kazantzidis, A., Schmidt, T., Zarzalejo, L., Blanc, P. and Pitz-Paal, R. (2019c). Determination of cloud transmittance for all sky imager based solar nowcasting. *Sol. Energy* 181, 251–263. doi: 10.1016/j.solener.2019.02.004
- Nouri, B., Wilbert, S., Kuhn, P., Hanrieder, N., Schroedter-Homscheidt, M., Kazantzidis, A., Zarzalejo, L., Blanc, P., Kumar, S., Goswami, N., Shankar, R., Affolter, R. and Pitz-Paal, R. (2019d). Real-Time Uncertainty Specification of all Sky Imager Derived Irradiance Nowcasts. *Remote Sens.* 11(9), 1059. doi: 10.3390/rs11091059
- Nouri et al., 2018. Nouri, B., Kuhn, P., Wilbert, S., Prah C., Pitz-Paal, R., Blanc, P., Schmidt, T., Yasser, Z., Ramirez Santigosa, L. and Heineman, D. (2018). Nowcasting of DNI Maps for the Solar Field Based on Voxel Carving and Individual 3D Cloud Objects from All Sky Images, AIP Conference Proceedings. Vol. 2033. doi:10.1063/1.5067196
- Power and Water Corporation (2019). *Solar/Diesel Mini-Grid Handbook*. 2nd Edition. Daly River Solar Research Project. Power and Water Corporation. Darwin, Australia.
- Quesada-Ruiz et al., 2014 Quesada-Ruiz, S., Chu, Y., Tovar-Pescador, J., Pedro, H., Coimbra, C. Cloud tracking methodology for intrahour DNI forecasting. *Sol. Energy* 102, 267–275 (2014).
- Sayeef, S., et al. (2012). CSIRO Solar intermittency: Australia's clean energy challenge. Characterising the effect of high penetration solar intermittency on Australian electricity networks.
- Schroedter-Homscheidt, M., Kosmale, M., Jung, S. and Kleissl, J. (2018). Classifying ground-measured 1 minute temporal variability within hourly intervals for direct normal irradiances, *Meteorol. Z.* doi: 10.1127/metz/2018/0875
- Standards Australia (2015). Grid connection of energy systems via inverters Part 2: Inverter requirements. Sydney, SAI Global Ltd. AS/NZS 4777.2.2015.
- Standards Australia (2020). Draft Grid connection of energy systems via inverters, Part 2: Inverter requirements. Sydney, SAI Global Ltd. DR AS/NZS 4777.2.2020.
- Tereci, A., Schneider, D., Kesten, D., Strzalka, A., Eicker, U. (2009). Energy saving potential and economical analysis of solar systems in the urban quarter Scharnhäuser Park. *Proceedings of ISES Solar Congress*, pp. 1814–1822
- Trinkl, P. (2020a). Experiment Plan and Report: Data Visibility, Version 2. Carnarvon Distributed Energy Resources (DER) Trials. Bentley, Horizon Power.
- Trinkl, P. (2020b). Experiment Plan and Report: Loss of Communications, Version 2. Carnarvon Distributed Energy Resources (DER) Trials. Bentley, Horizon Power.
- Trinkl, P. (2020c). Experiment Plan and Report: Customer Internet Connection, Version 2. Carnarvon Distributed Energy Resources (DER) Trials Bentley. Horizon Power.

Trinkl, P. (2020d). Experiment Plan and Report: Battery Control, Version 2. Carnarvon Distributed Energy Resources (DER) Trials Bentley. Horizon Power.

Trinkl, P. (2020e). Experiment Plan and Report: VPP Configuration and Control, Version 2. Carnarvon Distributed Energy Resources (DER) Trials Bentley. Horizon Power.

Trinkl, P. (2020f). Experiment Plan and Report: Feed in Management (Export Limit), Version 2. Carnarvon Distributed Energy Resources (DER) Trials Bentley. Horizon Power.

Trinkl, P. (2020g). Experiment Plan and Report: Grid Credits, Version 2. Carnarvon Distributed Energy Resources (DER) Trials Bentley. Horizon Power.

Trinkl, P. (2020h). Experiment Plan and Report: DER Network Support, Version 2. Carnarvon Distributed Energy Resources (DER) Trials Bentley. Horizon Power.

Wilbert et al., 2016. Wilbert, S., Nouri, B., Prah, C., Garcia, G., Ramirez, L., Zarzalejo, L., Valenzuela, L., Ferrera, F., Kozonek, N. and Liria, J. (2016). Application of Whole Sky Imagers for Data Selection for Radiometer Calibration. In: EU PVSEC 2016 Proceedings, 1493–1498, doi: 10.4229/EUPVSEC20162016-5AO.8.6

15 Appendices

15.1 Appendix 1

15.1.1 Calculations for the unmasked load of a customer and the aggregated unmasked load for customers with WWs

The unmasked load for a customer is calculated by

$$P_i^{\text{UML}}(t) = \sum_{j=1}^{k(i)} P_{i,j}^{\text{GEN}}(t) + \sum_{j=1}^{l(i)} P_{i,j}^{\text{NETT}}(t) - \sum_{j=1}^{m(i)} P_{i,j}^{\text{BAT}}(t) \quad (1)$$

where $P_i^{\text{UML}}(t)$ is the UNMASKED LOAD of customer i at time t . $P_{i,j}^{\text{GEN}}$, $P_{i,j}^{\text{NETT}}$ and $P_{i,j}^{\text{BAT}}$ represent the reading of the GEN, NETT and BAT WWs, respectively, while $k(i)$, $l(i)$, and $m(i)$ are the total number of GEN, NETT and BAT WWs for customer i . $P_{i,j}^{\text{NETT}}$ is positive when the customer imports power from the grid and negative otherwise. $P_{i,j}^{\text{BAT}}$ is positive when the battery is charging and negative when it is discharging.

The aggregated UML of the customers with WWs is calculated as

$$P_{\text{Agg}}^{\text{UML}}(t) = \sum_{i=1}^{N(t)} P_i^{\text{UML}}(t) \quad (2)$$

where $N(t)$ is the number of customers with available WW readings at time t . It is to be noted that the unmasked load of a customer can only be calculated when the readings from all the WWs of that customer are available (i.e. no missing data at that timestamp). Therefore, normalisation is required to observe the unmasked load fluctuations over time. The normalised aggregated unmasked load is calculated as

$$P_{\text{Agg_Nor}}^{\text{UML}}(t) = \frac{P_{\text{Agg}}^{\text{UML}}(t)}{\sum_{i=1}^{N(t)} \text{Max}(P_i^{\text{UML}})} \quad (3)$$

where $\text{Max}(P_i^{\text{UML}})$ denotes the maximum unmasked load of customer i over the analysis period.

Now the unmasked load fluctuation can be calculated as

$$UMLF_{\Delta t}(t) = P_{\text{Agg_Nor}}^{\text{UML}}(t) - P_{\text{Agg_Nor}}^{\text{UML}}(t - \Delta t) \quad (4)$$

Where Δt is the time interval (e.g., 30s, 60s, ..., 5 min) to calculate the fluctuation.

The unmasked load fluctuation factor is the maximum fluctuation over the analysis period, as defined in (5).

$$UMLFF = \text{Max}(UMLF_{\Delta t}(t)) \quad (5)$$

15.1.2 Aggregated unmasked load, normalised aggregated PV and the aggregated net load plots

Figure 46 and Figure 47 show the normalised aggregated unmasked load, the normalised aggregated PV and the aggregated net load on 22nd August 2019. From Figure 46, it is seen that the aggregated unmasked load is relatively constant with the net load exhibiting an inverted solar profile. During the day the net load is negative due to PV export. Also apparent in Figure 46, and implied by Figure 3 from (Glenister et al. 2020) and Figure 2, is that the fluctuation of the net load is dominated by the fluctuation of the PV generation for this subset of the Carnarvon network. Figure 47 is an instance of this for the largest PV change on 22nd August 2019. In this case the net load is a reflection of the PV change.

The loads for the same time and duration on the same day (22nd August 2019) as Figure 47 for the express feeders A and B are shown in Figure 48. Although the express feeder load increases, the increase is slower and about twice the size at 500kW (see Figure 48b) compared with an aggregated net WW load change of 250kW. This is likely due to the other unmonitored PV systems on the Carnarvon network contributing to the fluctuations.

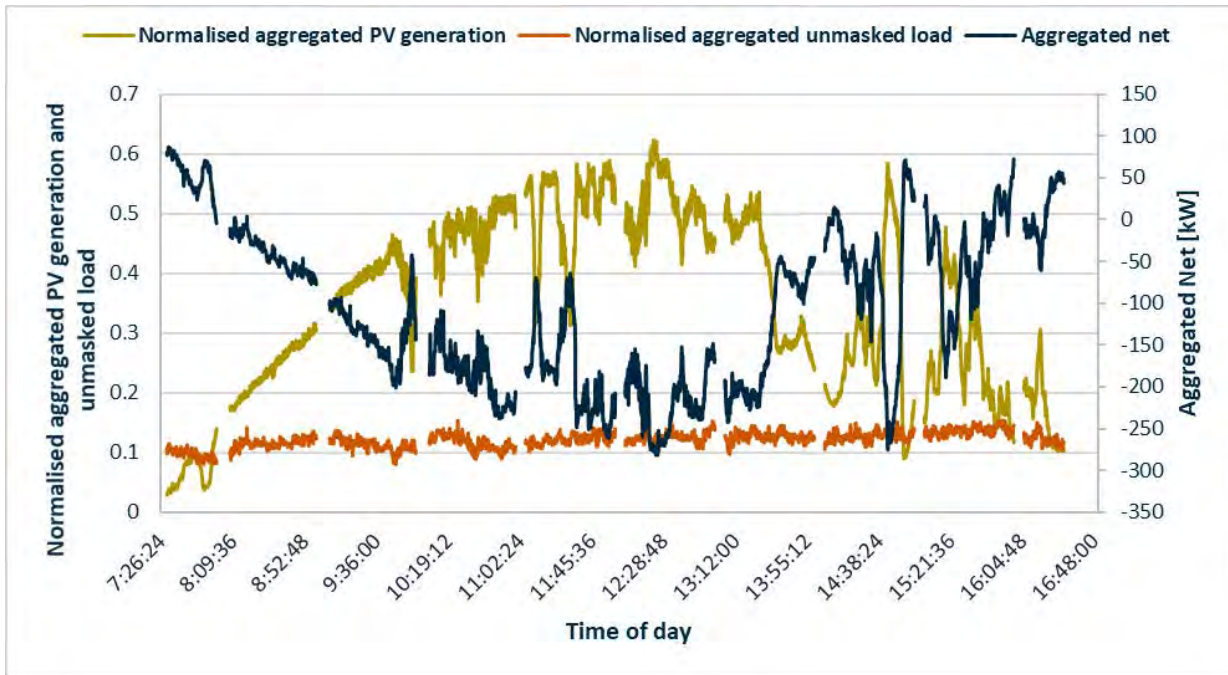


Figure 52. PV generation, net load and unmasked load for all WW systems on 22/08/2019.

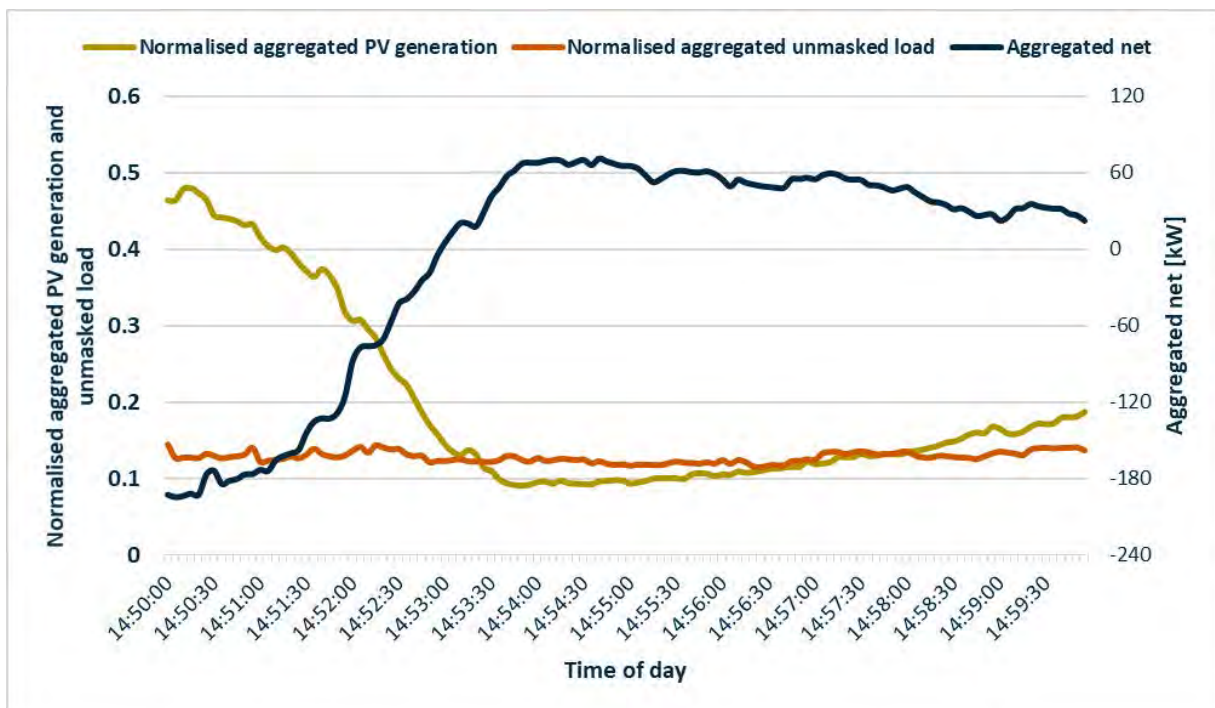
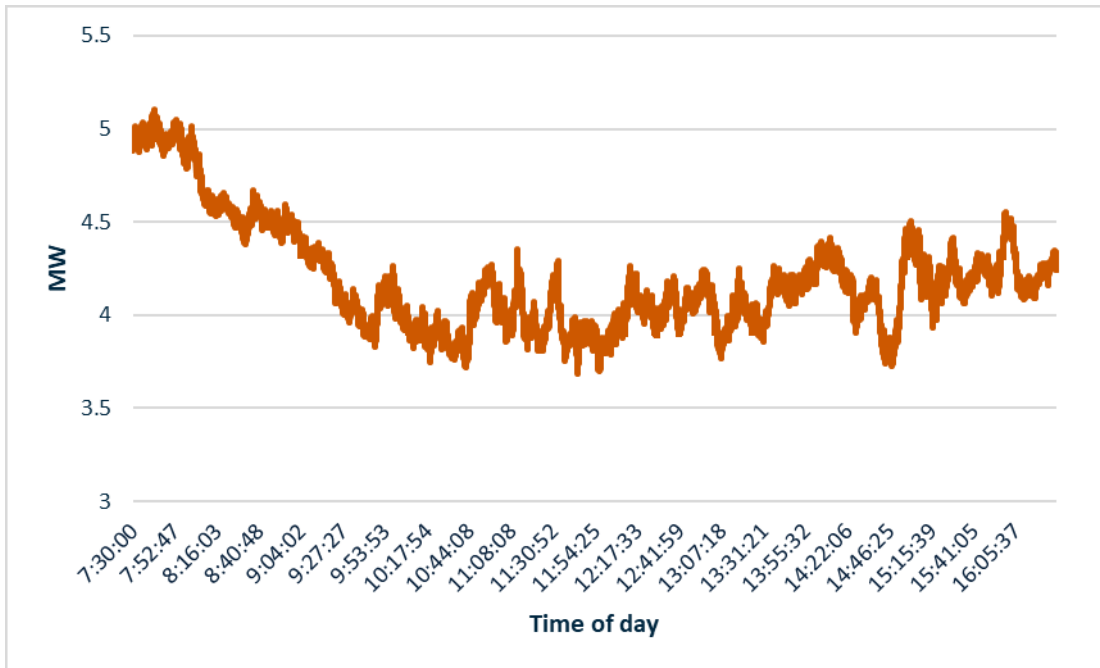
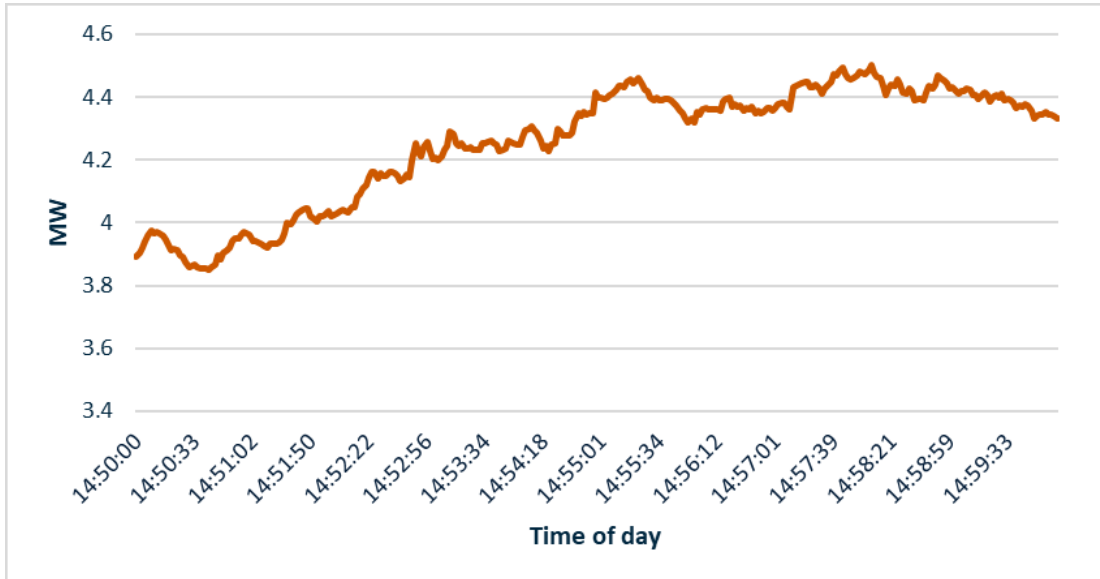


Figure 53. An expanded view of Figure 52 around the time of the largest change in PV generation on 22/08/2019.



(a)



(b)

Figure 54. a) Express feeders A and B net load for Carnarvon on 22nd August 2019 over the same time period as in Figure 3 of Glenister et al. (2020). (b) An expanded view, showing the power changes between 14:50 and 14:59.

15.2 Appendix 2

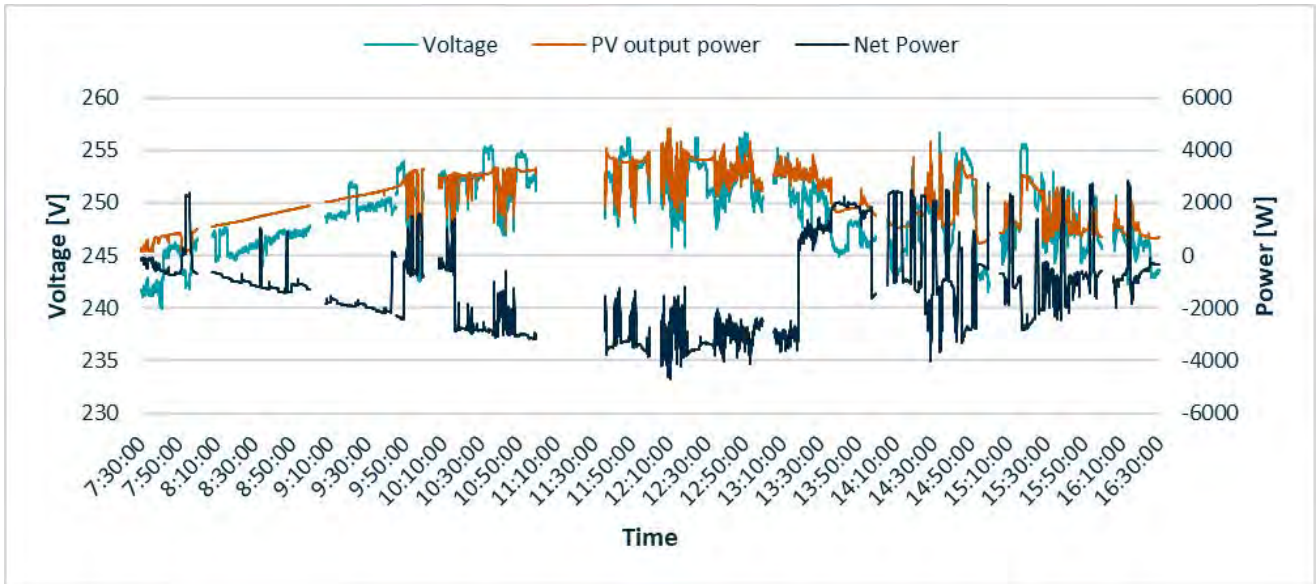


Figure 55. Voltage, PV output and net power for Site A2 on 22nd August 2019.

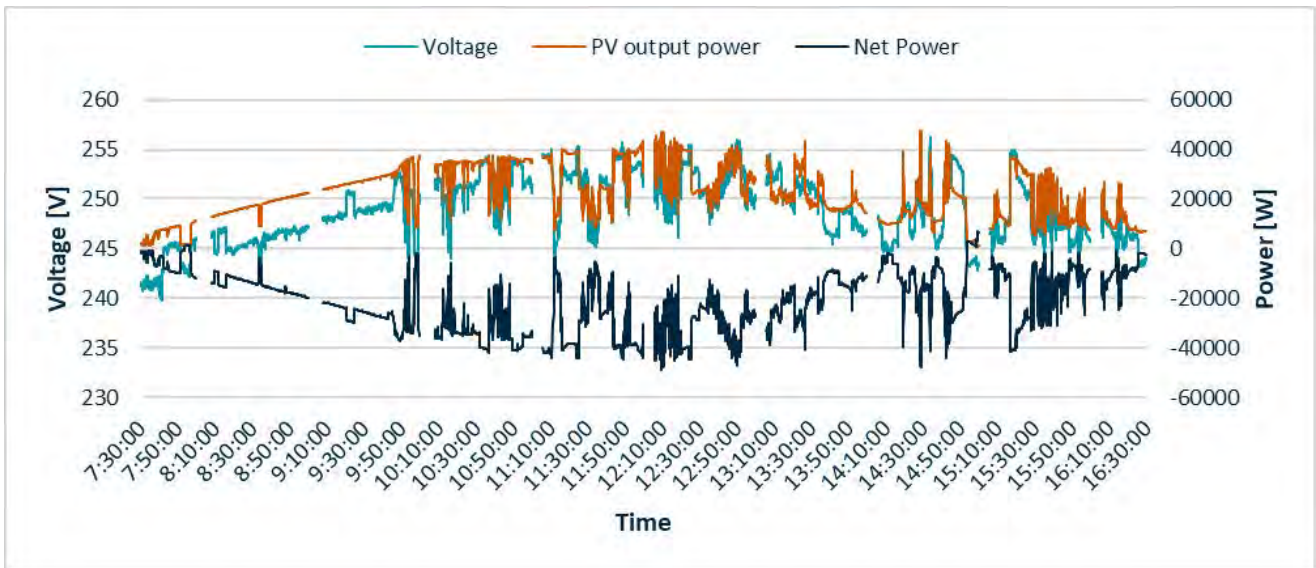


Figure 56. Voltage, PV output and net power for Site A8 on 22nd August 2019.

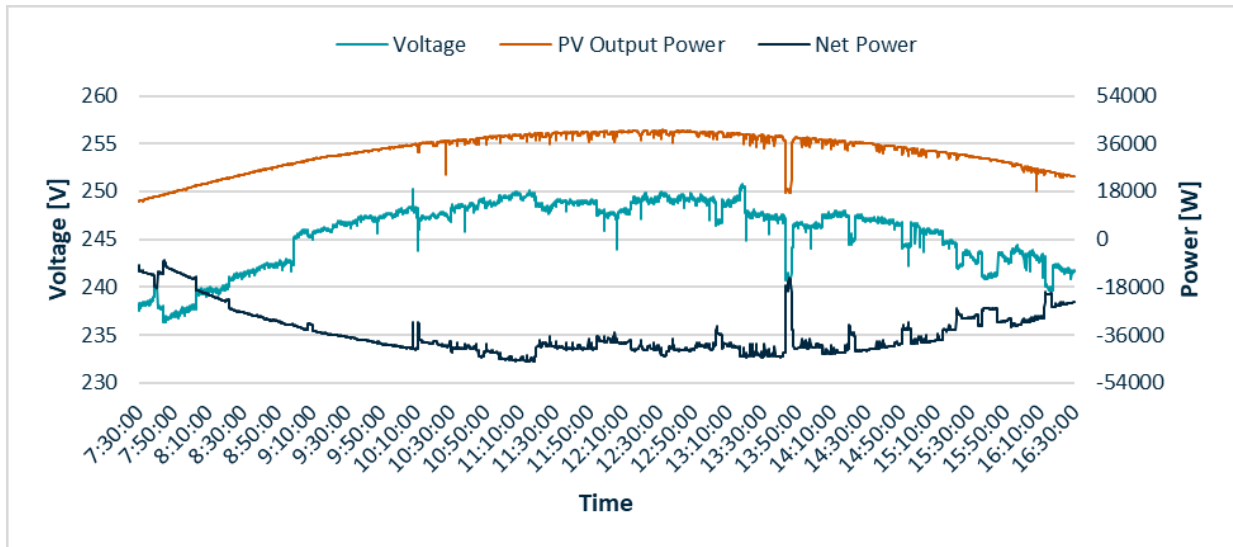


Figure 57. Voltage, PV output and net power for Site A8 on 31st January 2020.

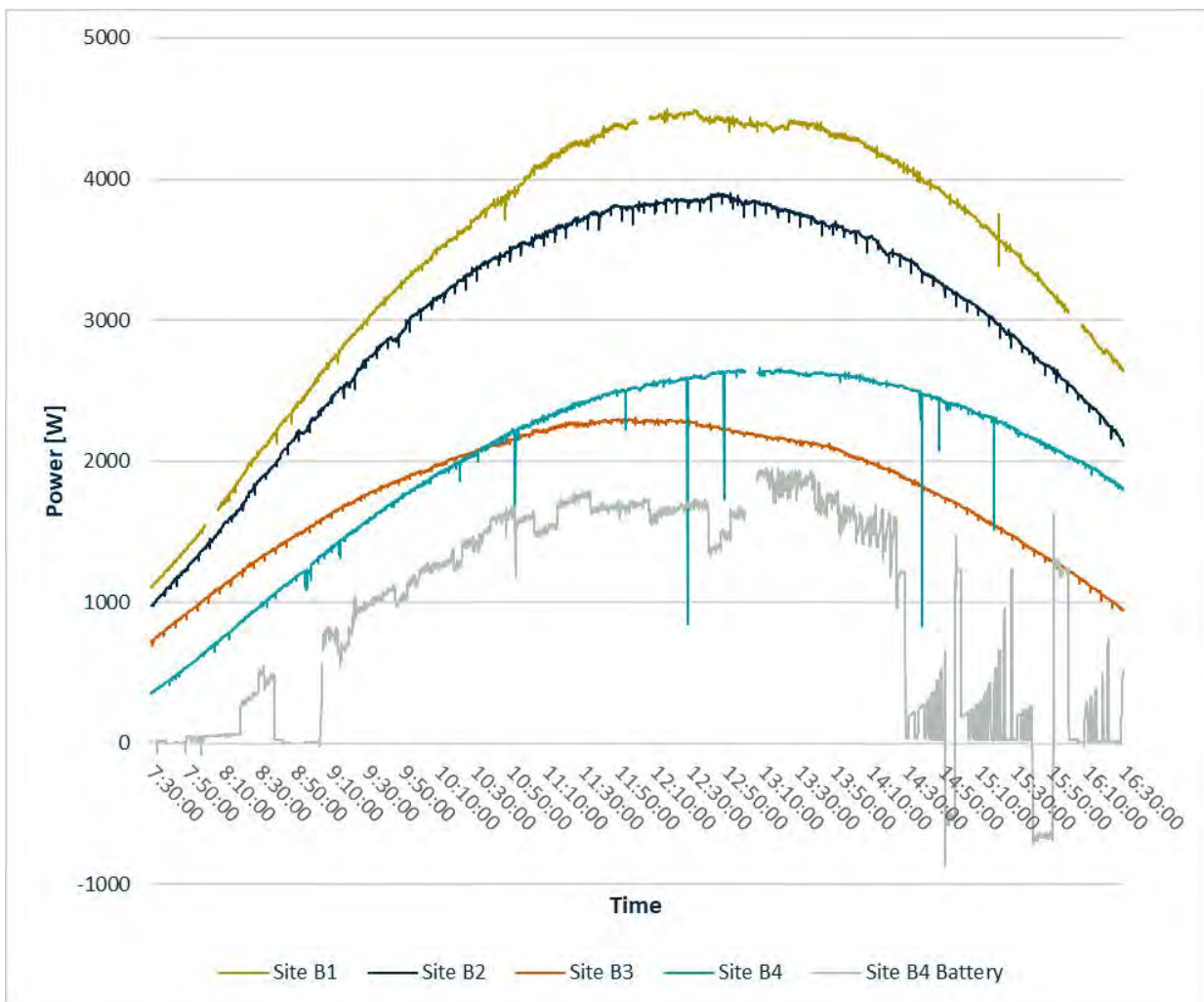


Figure 58. PV output and battery power for Network-B sites on 31st January 2020.

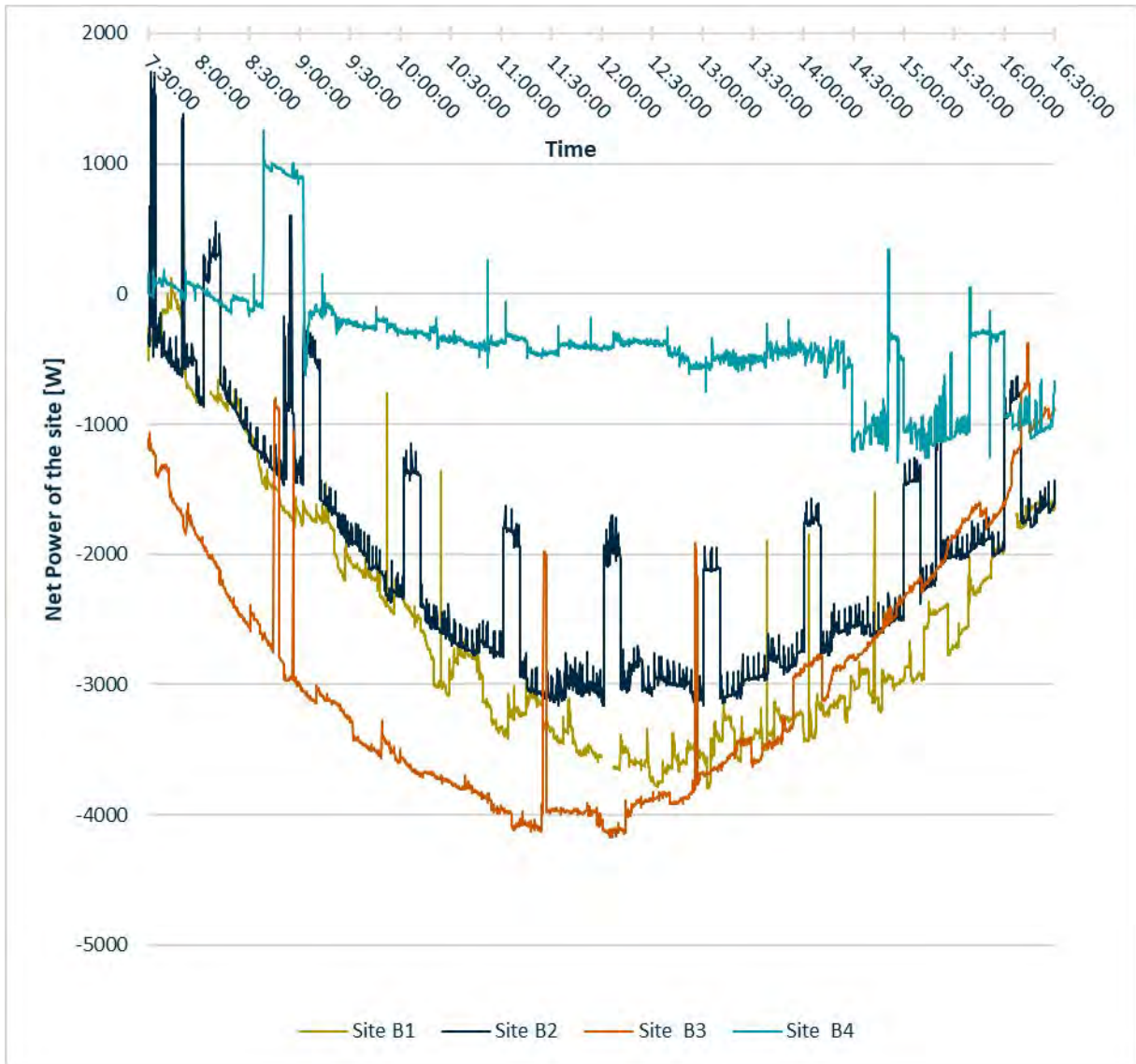


Figure 59. Net power for Network-B sites on 31st January 2020.

15.3 Appendix 3

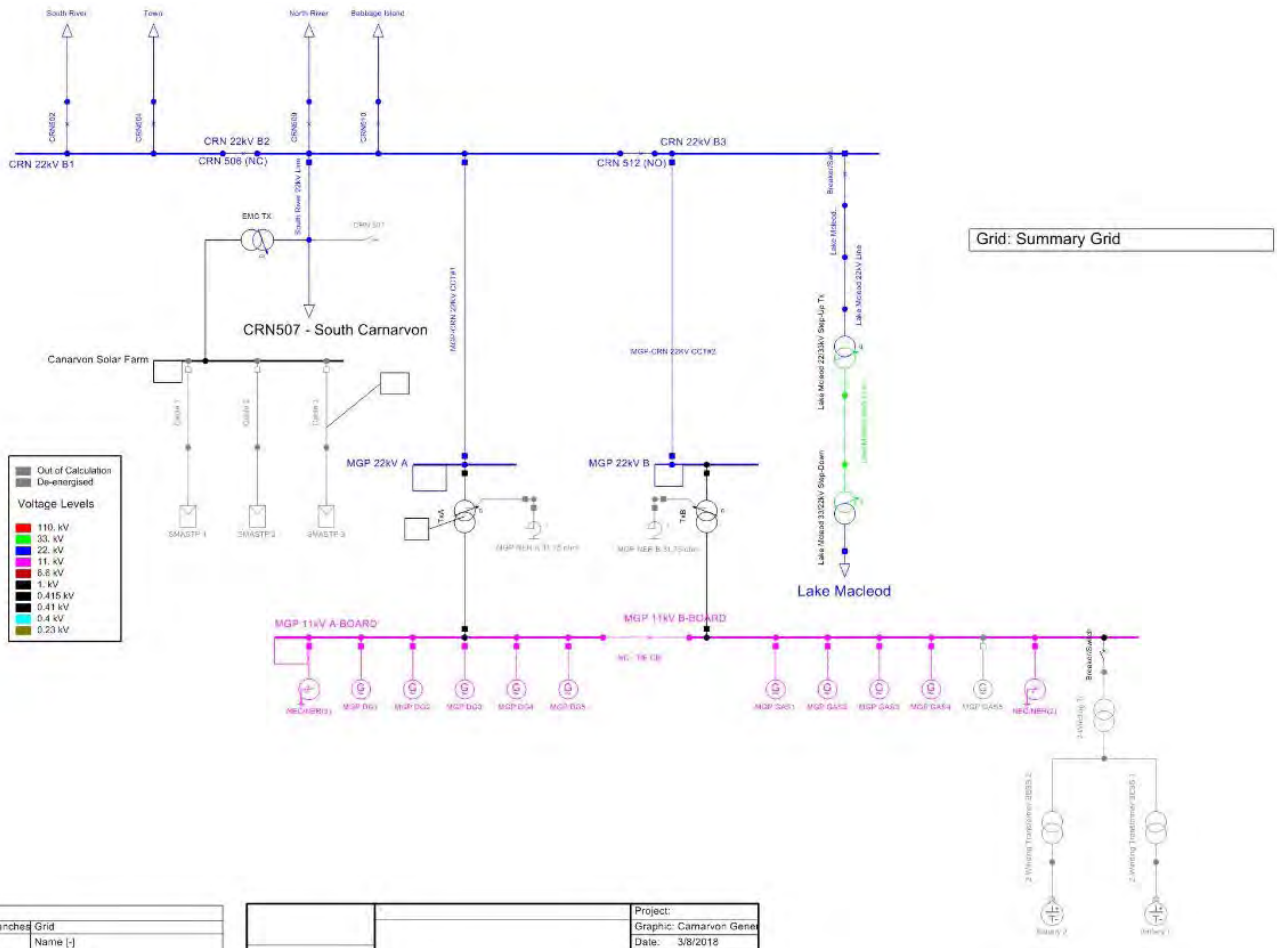


Figure 60. "Canarvon Generation Model – Nov 2017" PowerFactory model online diagram.

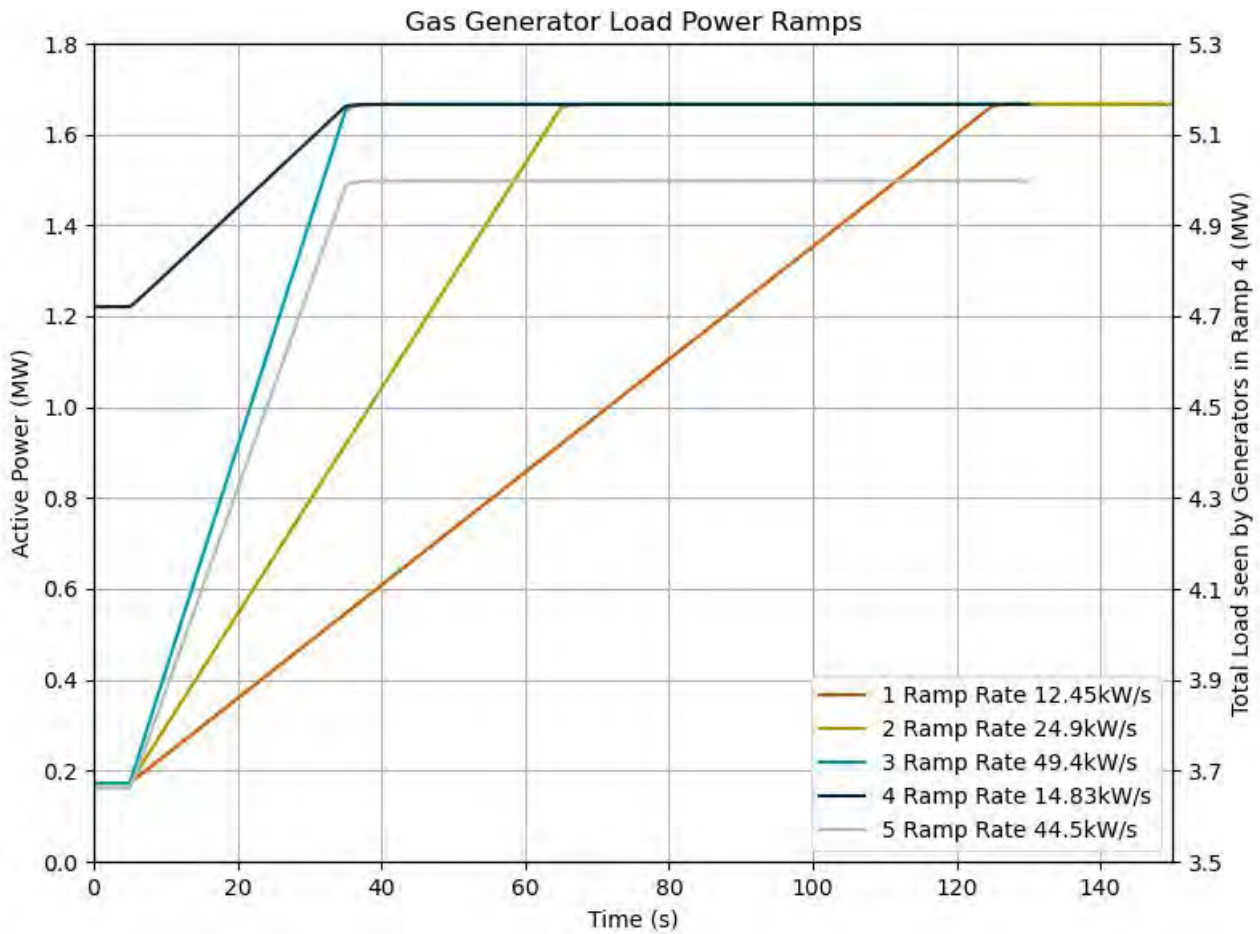


Figure 61. Gas engine generator load ramps used to test performance of the gas engine generators. The right y axis is 3.5 – 5.3MW for the 5th curve only and easy comparison between the 3rd and 5th power ramps. The 4th curve shows the per generator ramp corresponding to the total power ramp in the 5th ramp.

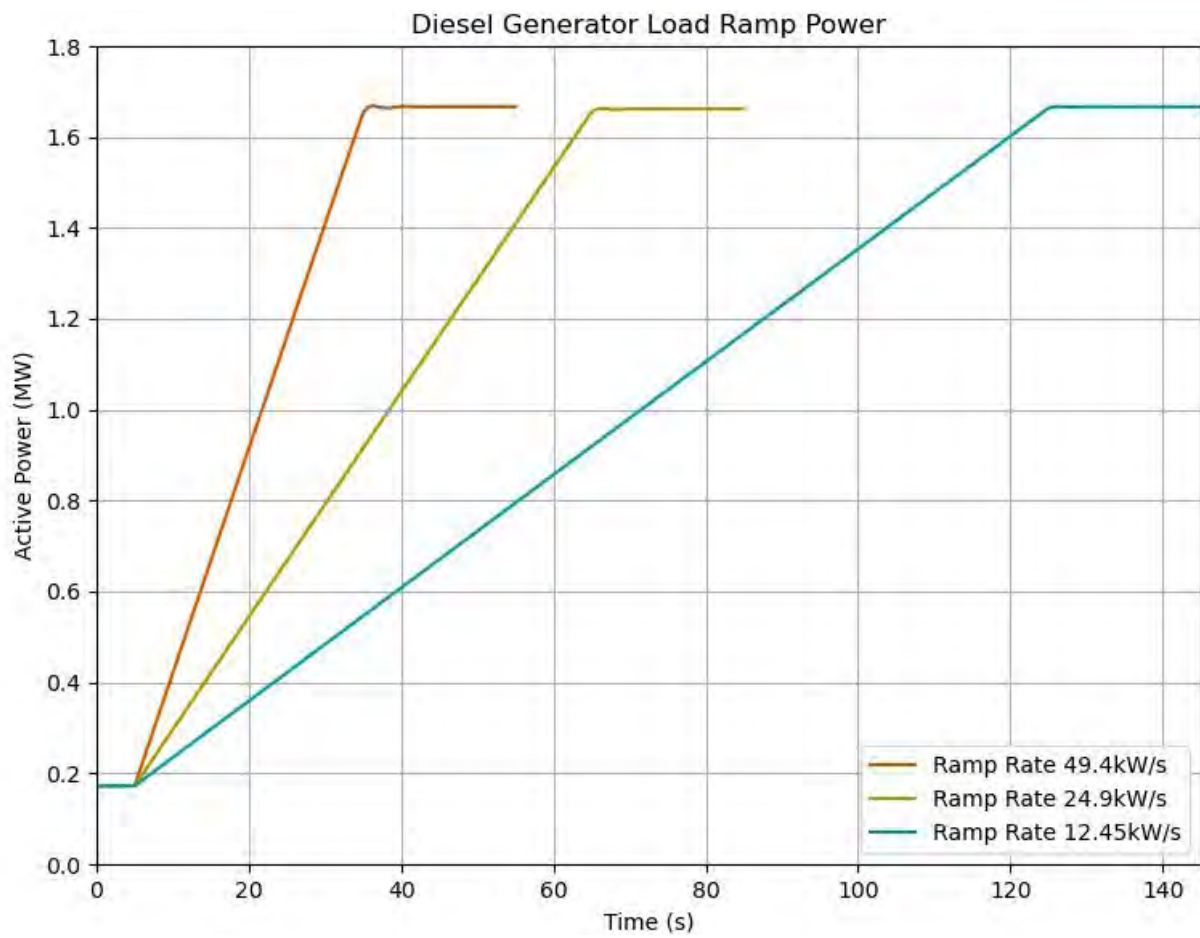


Figure 62. Diesel engine generator load ramps used to test performance of the diesel engine generators.

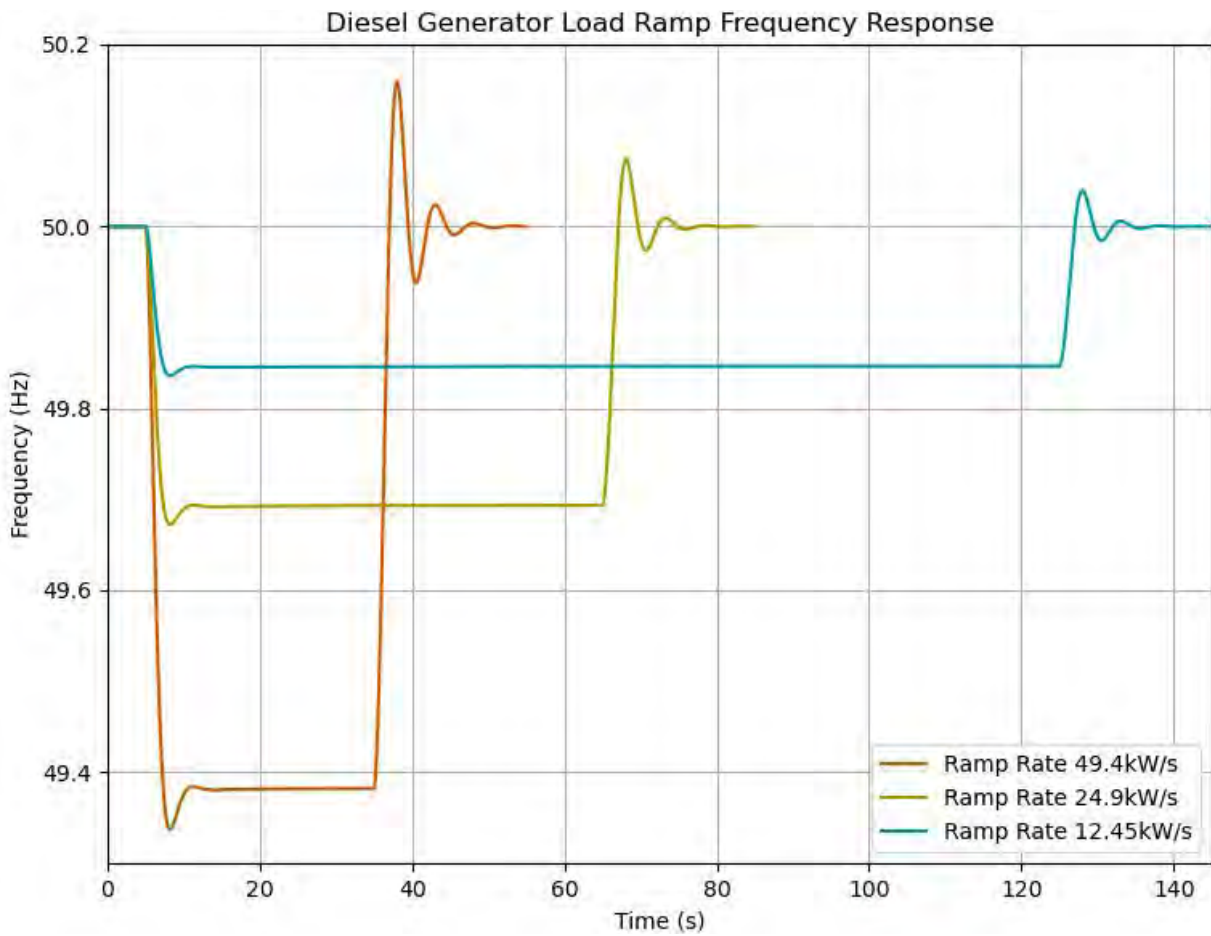


Figure 63. Diesel engine generators frequency response to load ramping. The load ramps are shown in Figure 62.

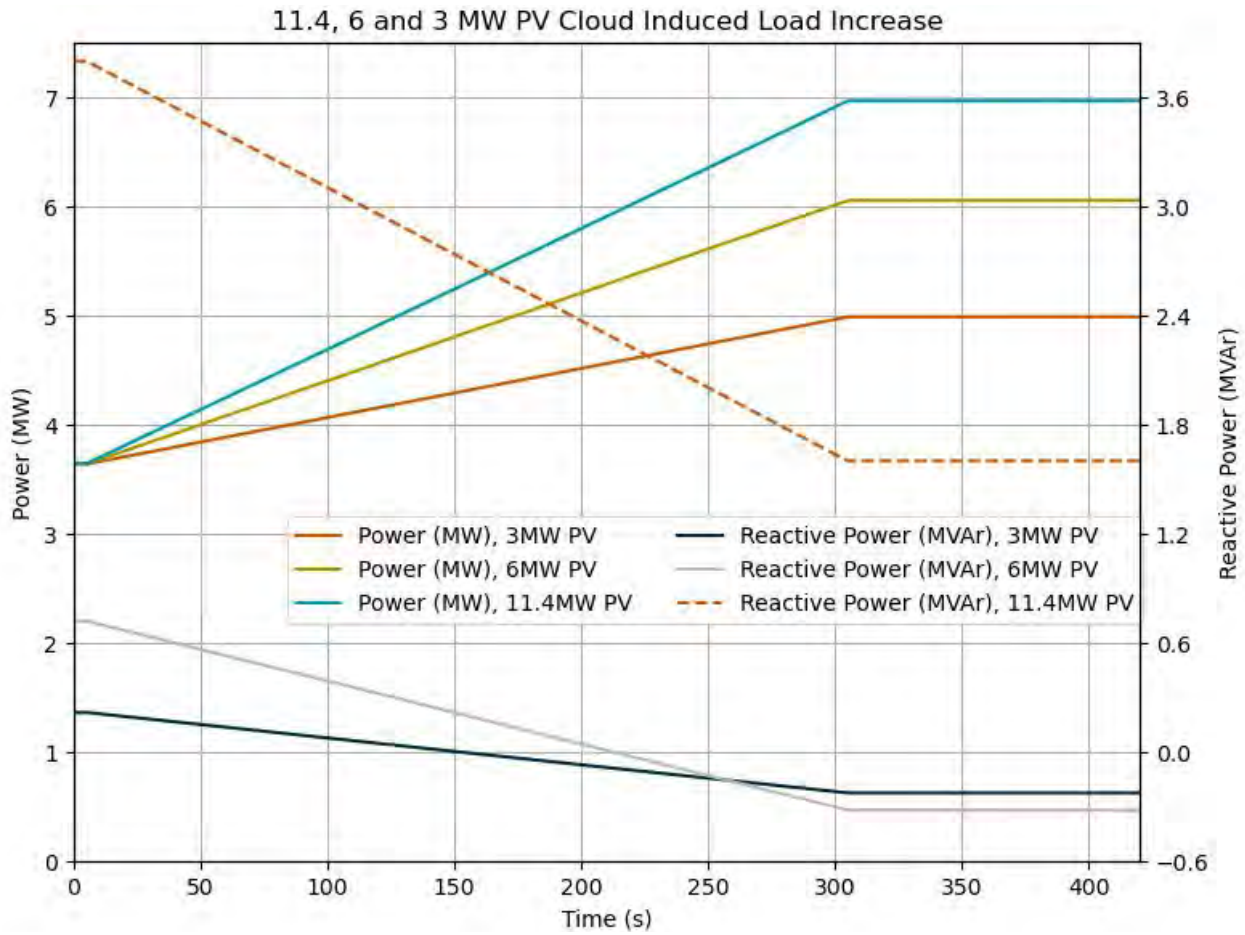


Figure 64. Real power and reactive power changes corresponding to the voltage changes shown in Figure 37. The 11.4MW PV scenario net load power increase stops at 7MW to prevent overloading of the generators.

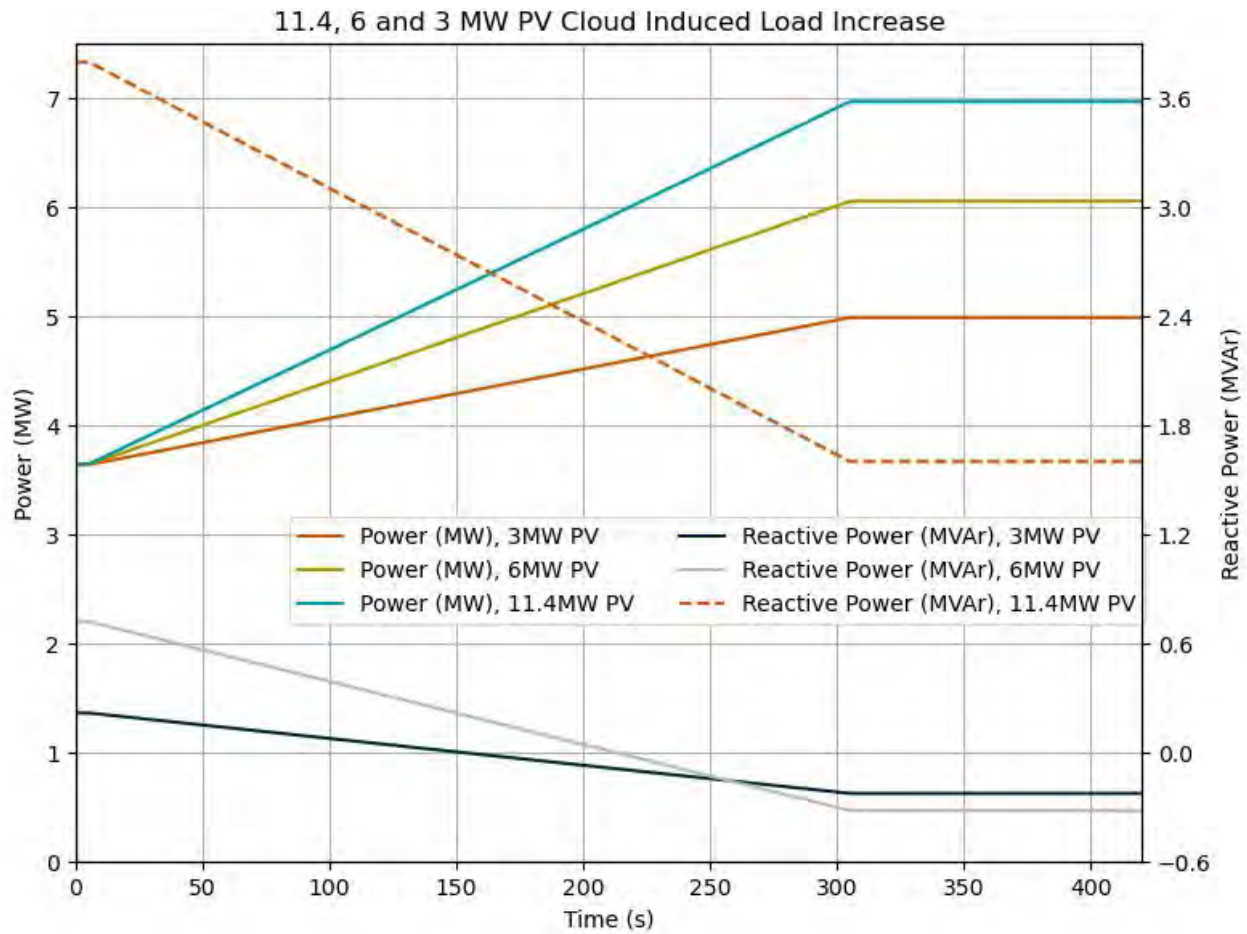


Figure 65. Real power and reactive power changes corresponding to the voltage changes shown in Figure 37. The 11.4MW PV scenario net load power increase stops at 7MW to prevent overloading of the generators.

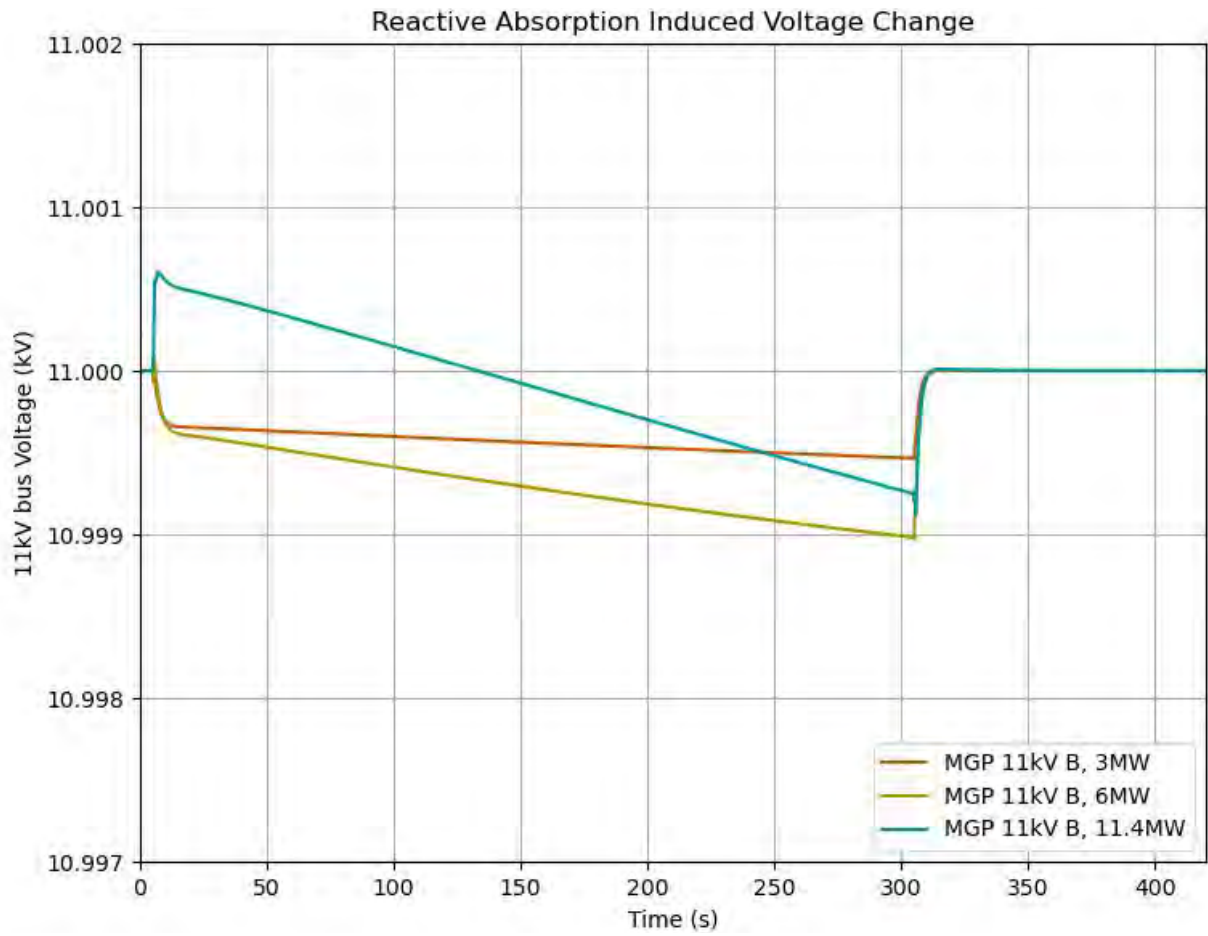


Figure 66. Voltage on the Mungullah 11kV Board B HV bus bar during the power changes.

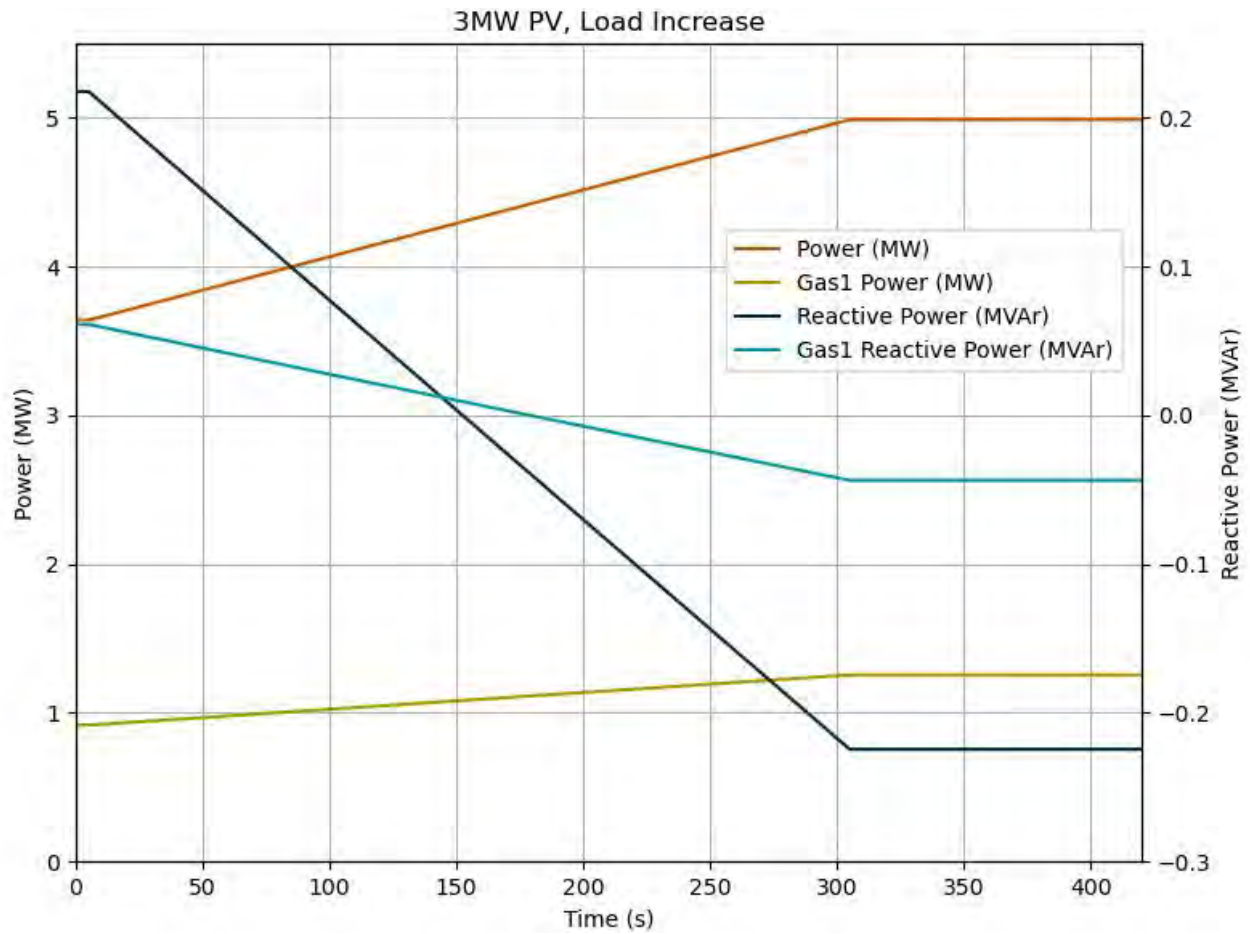


Figure 67. Load increase due to a 1.2MW decrease in PV over 300 seconds. 3MW of installed PV capacity, initial minimum load, total load and one gas generator load are shown. Reactive power decreases also.

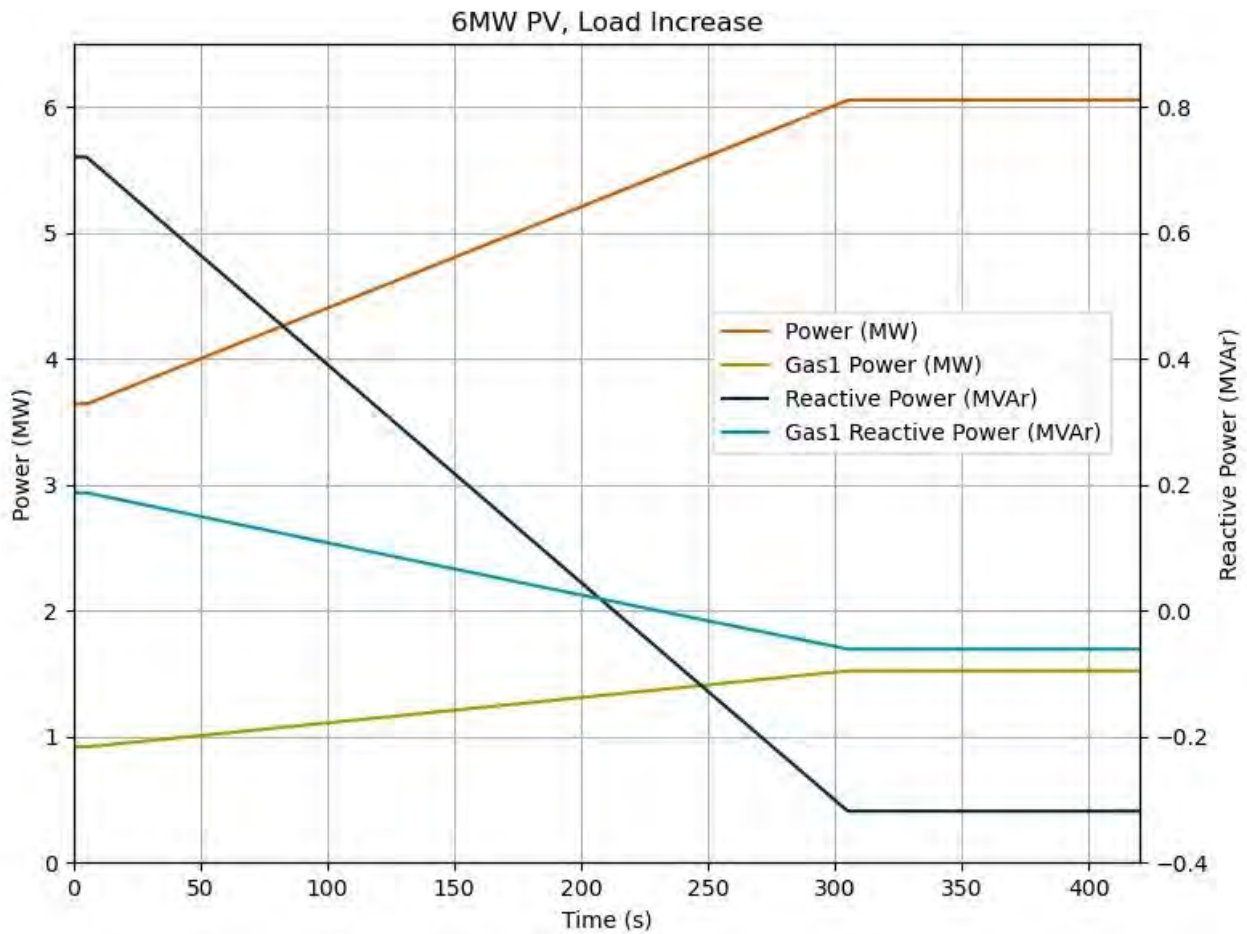


Figure 68. Load increase due to a 2.4MW decrease in PV over 300s. 6MW of installed PV capacity, initial minimum load, total load and one gas generator load are shown. Reactive power decreases also.

Table 26. HV feeder loads for the minimum load scenario in the “Carnarvon Generation Model – Nov 2017”.

Minimum Load Scenario “Carnarvon Generation Model – Nov 2017” Feeder Loads		
HV Feeder	P (MW)	Q (MVar)
Babbage Island	0.495	0.213
South Carnarvon	0.402	0.1389
Lake Macleod	0.531	-0.057
North River	0.45	0.195
South River	0.732	0.267
Town	1.02	0.387

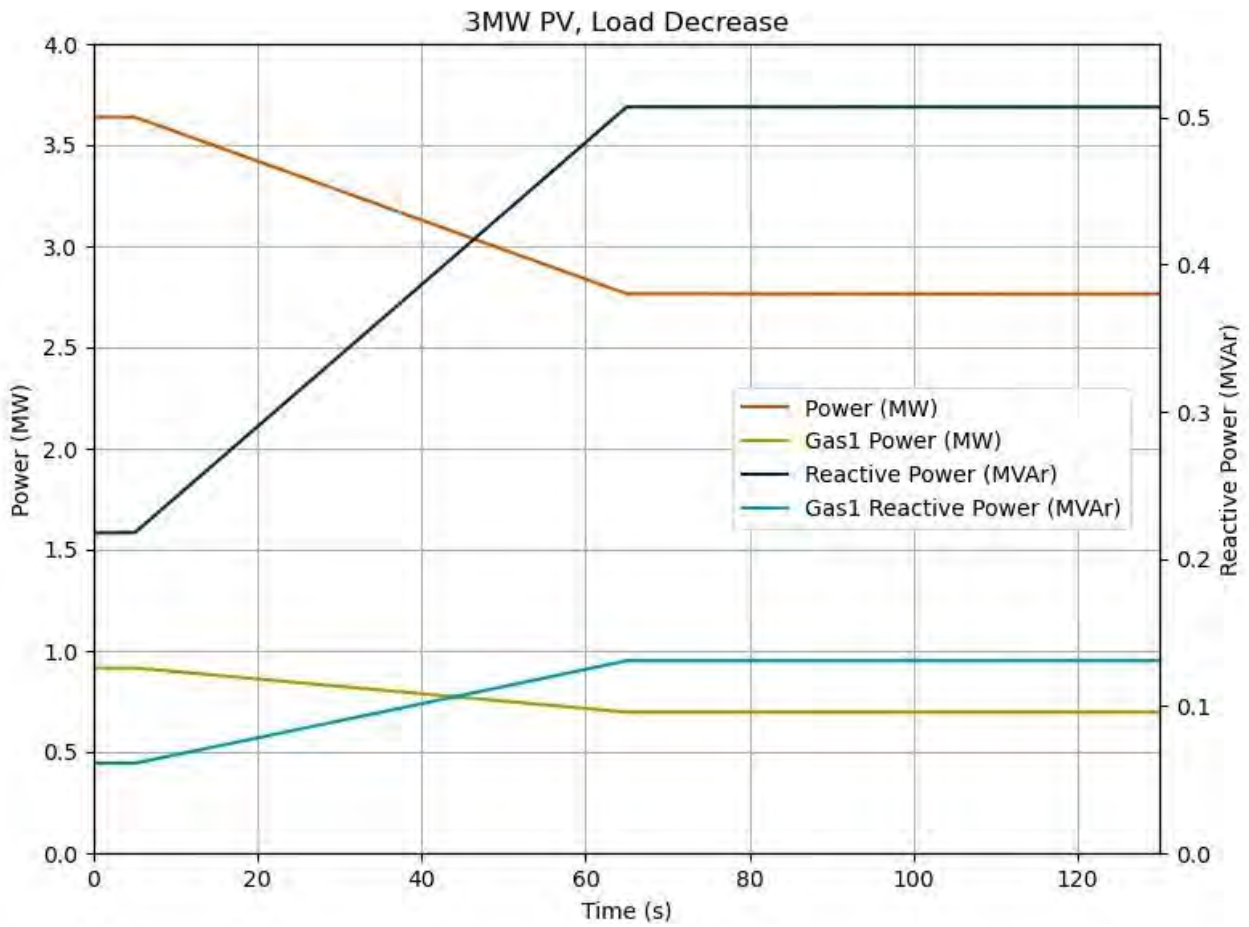


Figure 69. Load decrease due to PV output increase for 3MW of PV. 850 + j300 kVA increase in PV.

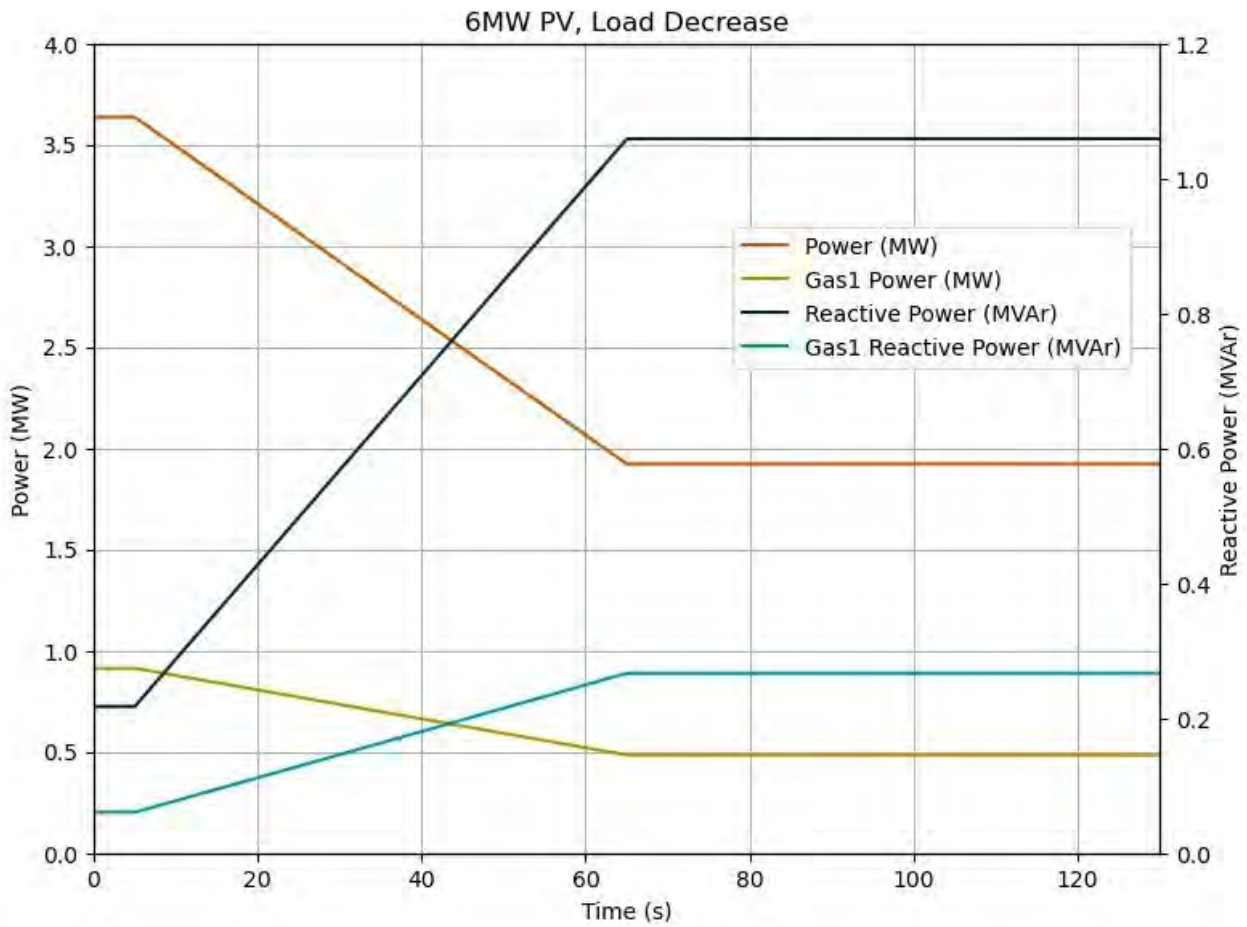


Figure 70. Load decrease due to PV output increase for 6MW of PV. 1.7 + j0.6 MVA increase in PV.

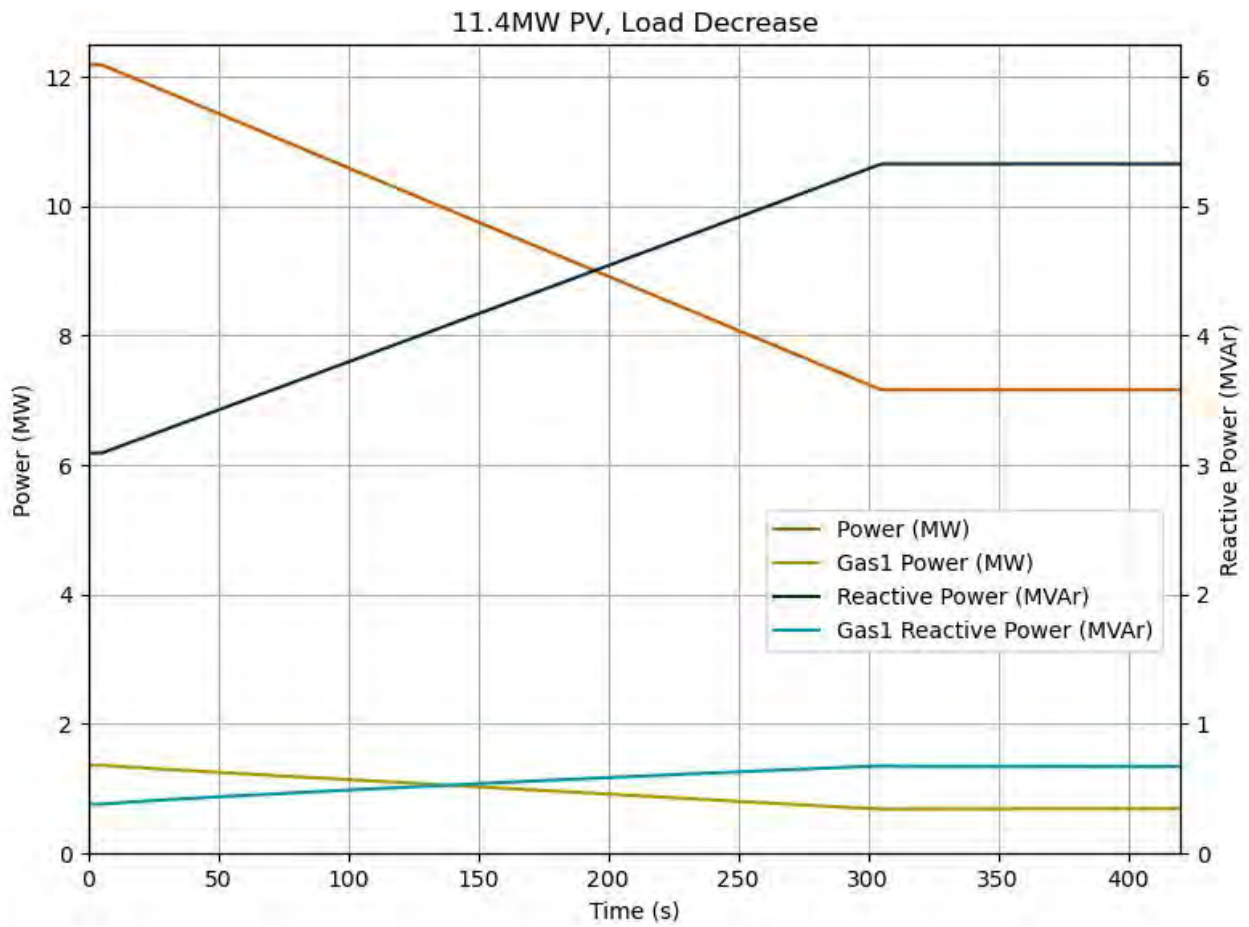


Figure 71. Load decrease due to PV increase for 11.4MW of PV. 4.7 + j2MVA increase in PV.

15.4 Appendix 4

15.4.1 Predictive Analytics Model Forecasting – Carnarvon DER Trials

In 2016, before the commencement of data gathering for the Carnarvon DER trials, Horizon Power worked with IBM to investigate the value of forecasting in the management of distributed energy resources. historical data provided by Horizon Power, IBM conducted a trial to train their Velco predictive-model and to determine if the model could reliably predict the energy demand and PV generation 24 hours in advance with 15 min resolution and at a confidence of 95%. IBM was also tasked to identify how well their model could predict energy residual demand out to 7 days.

The keys inputs were – predictive weather models from IBM Deep Thunder; Horizon Power AMI, SCADA and GIS data. For the Carnarvon substation, a Mean Absolute Percentage Error (MAPE) of 6.4% was obtained for the energy residual demand, due to the accuracy of 5.0% for the energy demand and 12.4% for PV generation.

The project sought to develop predictive models with sufficient confidence for 5 out of 6 HV feeders and for about half of the LV feeders. This covered 90% of the service connection points and 80% of the total load in Carnarvon. The remainder of the feeders (1 HV and 50% of LV) mainly serve irregular electrical loads only partially driven by weather dynamics; these include salt production operations and water pumping. Alternate methodologies will be required to understand their drivers.

Predictive models were produced for 65 of the 145 LV feeders (45%) but not for the remaining 80 (55%), since they serve particularly challenging loads which cannot be predicted with reliable confidence one day in the future. As summarised below, these feeders cover only 9% of the service connection points but about 40% of the total load in Carnarvon.

The final result of the trial indicate that it is certainly possible to provide some useful prediction:

($\leq 10\%$ error) for supply and demand for the modelled subset of LV feeders (45%).

Key drivers include the ability to classify weather correlated service points from the uncorrelated service points and to gain clearer visibility of true supply and demand through PV disaggregation. This work was undertaken by Murdoch University during their research.

More work will need to be done to better classify and predict the non-weather correlated feeders.

Table 27. Summary of the predictive models of the selected subset of LV feeders at Carnarvon.

Forecast Error (MAPE)	Service Points	Peak Demand	Peak PV Generation	Comments
$\leq 10\%$	51% (985)	30 % (2,286kW)	16% (116kW)	
(10% – 15%]	38% (730)	27% (2,065kW)	50% (362kW)	
(15% \leq 20%]	2% (47)	3% (252kW)	28% (204kW)	Large PV relatively to demand
Challenging loads	9% (183)	40% (3,066kW)	5% (37kW)	Irregular industrial customers (e.g. water corp., mining)

In terms of 7-day ahead predictions, the weather forecast and demand predictions for the period from 24th September to 1st October 2016 (Figure 72) were accurate, provided that the forecasted/predicted period of time was not affected by clouds.

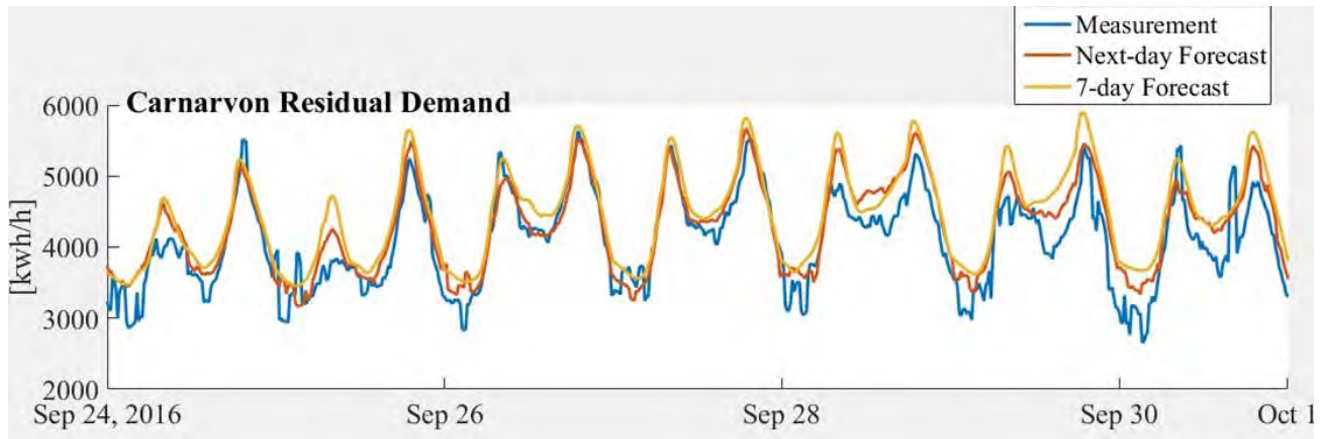


Figure 72. 7-day ahead predictions of the Carnarvon residual demand for the period 24th September – 1st October 2016.

A 7-day cloud cover prediction is much more problematic, showing significant variance between forecast and measured PV generation based on Solar Irradiance (Figure 73).

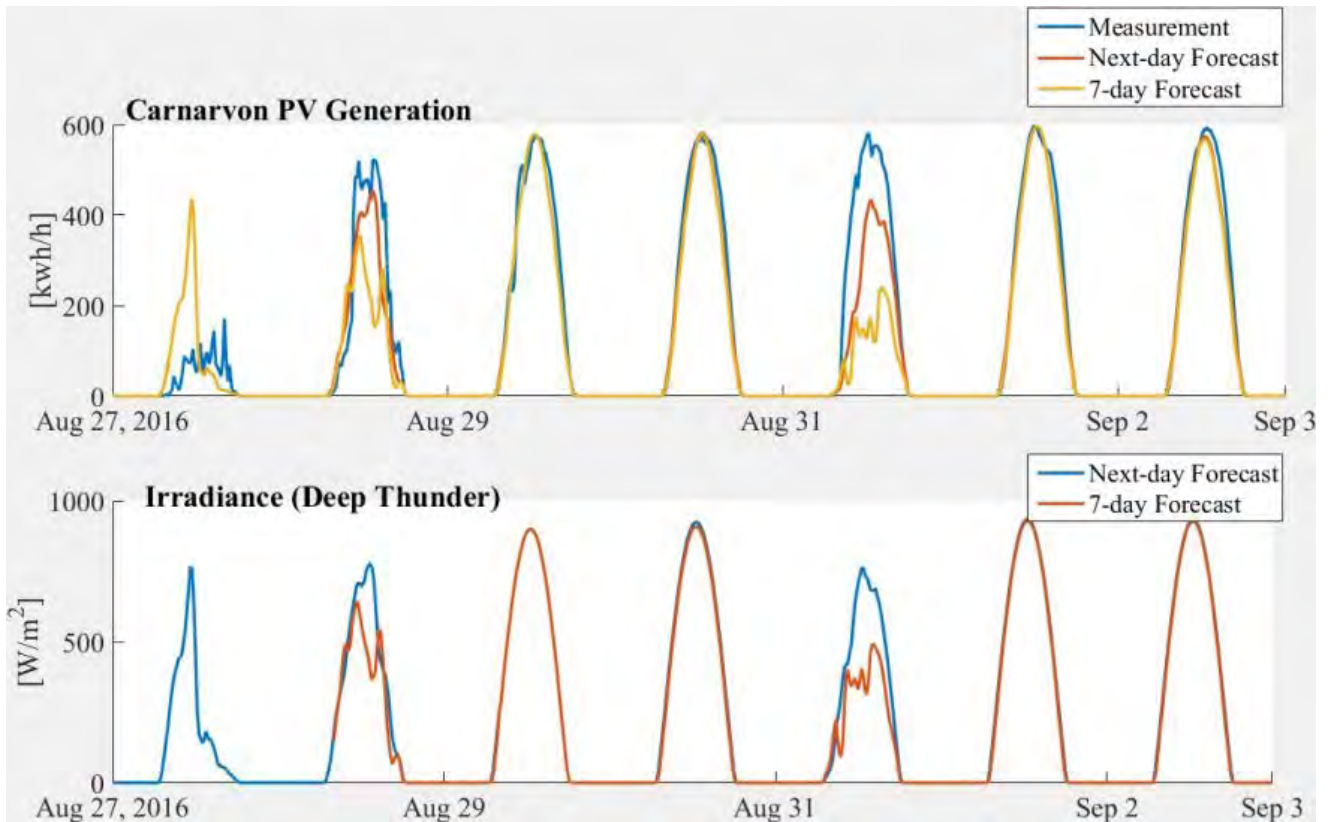


Figure 73. Carnarvon PV Generation and Irradiance based on 7-day cloud cover predictions for the period 27th August – 3rd September 2016.

15.4.2 Findings

- Some challenges were identified with the prediction of PV generation using this technique:-
 - i) on cloudy days, the timing and intensity of the clouds is not always well captured by the IBM Deep Thunder weather model, which in turn affects the accuracy of the PV generation predictive models which use irradiance as a main input. More frequent updates of the models, taking into account shorter-term predictions of cloud cover, using more recent generation measurements or sky-cameras, should be used in order to improve the accuracy in these cases;
 - ii) even on clear-sky days it is difficult for the models to capture the peak generation since the measured generation is obtained from the meter export channels, which is only a net between generation and demand. Improved disaggregation between demand and generation in the data would provide cleaner training data for the models, which would improve accuracy in capturing the actual installed PV generation.
- A few elements make a prediction of PV generation one day ahead challenging:-
 - Difficulty in the prediction of the exact timing of cloud cover on cloudy days;
 - non-stationary behaviour of large solar installations;
 - The PV-masking effect due to metering data only capturing the “net” between generation and demand. The effect of the latter is less visible at the substation and is better quantified when predictions are computed at the LV feeders.

15.4.3 Key findings/changes required to improve accuracy

- More frequent updates of the models
 - Deliver data from AMI MDR and SCADA more frequently
- Improved disaggregation between demand and generation in the data
 - Currently, all AMI Meters only provide Net Metering. Disaggregation of supply (PV/Battery) from demand (Load) will uncover the true supply and demand.
 - This disaggregation is necessary to accurately correlate the effects of external factors on supply and demand.
- For industrial sites where operational use changes the usage patterns and therefore cannot be predicted, it would be necessary to have information about these changes in advance to retrain the model accordingly.
 - The current IBM approach of correlation between weather and demand does not work for large industrial loads that are not strongly related to such factors.
 - A broader range of external factors need to be correlated to account for non-weather related impacts. (e.g. lunar cycle => tidal dates and heights, impacts salt farms; shipping schedules impact businesses that correlate with import/export commodities or services).
- Difficulties in matching the < 1 min SCADA instantaneous kW Power data with AMI 15 min energy data. Integration and comparison of the two datasets brings them more into alignment. There was a 3-10% quantisation error using raw data alone. Note: Since longer-term integration was required, this may prove a challenge for real-time predictive analysis.
- The SCADA data provides “energy residual demand” (i.e. net demand). To understand the actual demand and supply, the AMI Meter data is required along with PV Disaggregation.

- With regards to the prediction of PV generation, the predictive models can capture quite well the typical generation patterns on clear-sky days, as shown below (Figure 74).

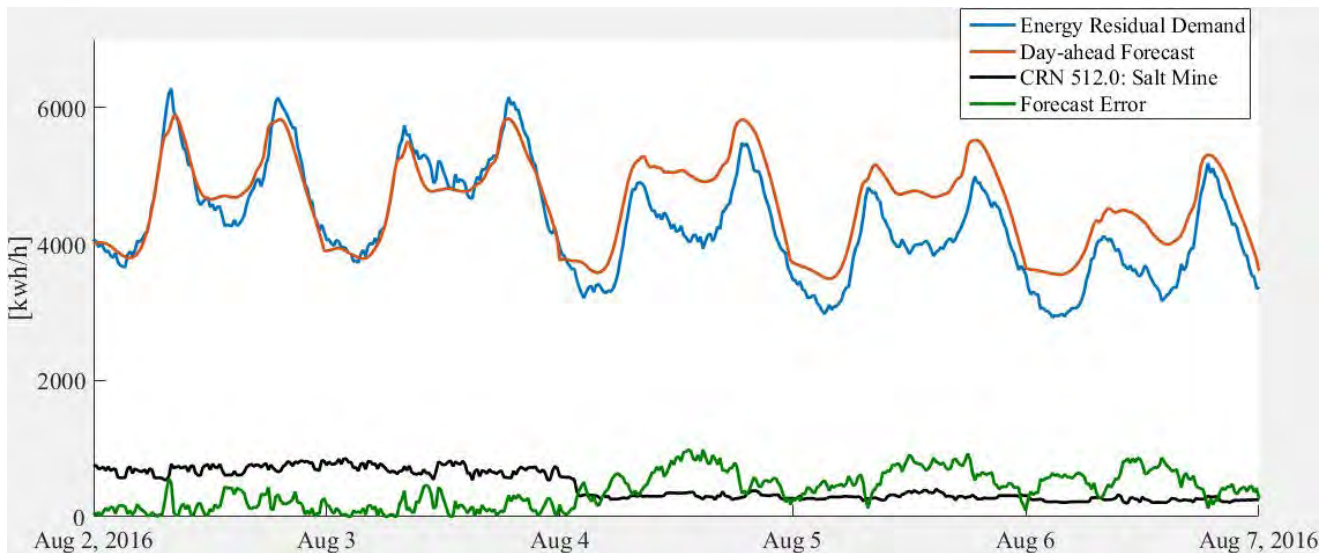


Figure 74. Prediction of PV generation from the predictive models for the period of 2nd –7th August 2016.

- However, while the average accuracy of the Velco model was approximately 12.4%, this level of accuracy dropped to 24.1% on cloudy days, most likely due to challenges in the weather forecasts of irradiance.
- From Figure 75 below, it can be seen how reliably the cloudy days are captured by the Deep Thunder forecasts, but the timing of the short-term cloud variations are more challenging, which causes significant prediction errors.

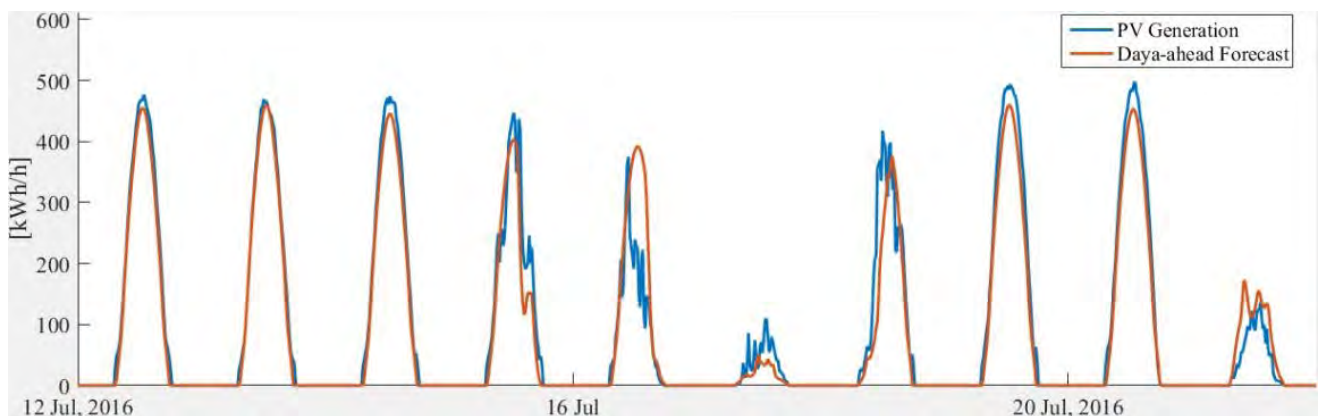


Figure 75. Day-ahead forecasts from IBM Deep Thunder and PV Generation for the period of 12th – 20th July 2016.

- Whilst training the models with 'hindcast' data, it was noted that there are other external factors that need to be considered, including cyclone events and their impact on agriculture. (e.g. Crop damage in Carnarvon in 2015)
- The IBM Deep Thunder models could not predict cloud events well, and this impacted the PV generation from irradiance.

15.4.4 Conclusions

Given the results of the work done with IBM and the cost and complexities in improving the data model for the IBM tools, Horizon Power chose to pursue alternative approaches to forecasting solar PV and load prediction in the Carnarvon DER trials.

1. Disaggregating the PV generation and load data for the participant PV systems was carried out using the Wattwatcher/Solar Analytics product which provided five second data capture and uniform synchronisation of data across the trials.
2. The adoption of a skycamera-based observation systems to provide an improved source of data for prediction of cloud events and impact.

*Owned by the
people of WA*

MU Murdoch
University

HORIZON
POWER